# CHARACTERISATION OF EPIDERMAL PRIMARY AFFERENTS INNERVATING THE HAIRY SKIN IN A *THY1.2-EGFP* TRANSGENIC MOUSE

Thesis submitted in accordance with the requirements of the

University of Liverpool for the degree of Doctor in Philosophy

by

Gareth Bruce

August 2009

# ABSTRACT


**Characterisation of epidermal primary afferents innervating the hairy skin in a *thy1.2-egfp* transgenic mouse**

**Gareth Bruce**

In a mouse which expressed enhanced green fluorescent protein (eGFP) under the control of the Thy1.2 gene promoter, a subpopulation of primary afferent fibres was selectively labelled. The peripheral terminations of these afferents were restricted to the epidermis of hairy skin and projected centrally to lamina $II_{i/o}$ of the spinal cord dorsal horn. A previous study had revealed that these neurones belonged to the "nonpeptidergic" subpopulation of small-sized DRG neurones (Belle et al., 2007). A combination of immunohistochemical and electrophysiological techniques were used to investigate the molecular and physiological characteristics of this population of neurones with a view to determining their possible function in vivo.

Antibodies against proteins implicated in pain ($TRPV_1$, $P2X_3$), itch (gastrin-releasing peptide), low threshold mechanotransduction (calbindin D-28K) and axonal guidance (glial cell line-derived neurotrophic factor family receptor α2; GFRα2) were used to determine possible roles for eGFP expressing primary afferents immunohistochemically. Neurones expressing eGFP were immunoreactive (-ir) for the $P2X_3$ ion channel subunit and GFRα2 receptor (85% and 82% respectively). They did not colocalise with the capsaicin receptor, $TRPV_1$ or gastrin-releasing peptide. This was reflected by their immunoreactivities in the dorsal horn. The expression of calbindin D-28K (calbindin) was restricted to medium- and large-sized neurones (Belle et al., 2007). In the dorsal horn, calbindin-ir cells were distributed throughtout the superficial laminae (lamina I-III) but clustered most densely in an area deemed to be lamina III. Electrophysiological responses of acutely-dissociated DRG to

depolarising and hyperpolarising current pulses identified 5 phenotypes: burst-, delayed-, phasic-, tonic- and transient-firing. Neurones expressing eGFP (eGFP+ve) were predominately (~70%) transient-firing whilst eGFP-negative neurones were largely (60%) delayed-firing. When neurones were short-term cultured (1-3 days) the proportion of eGFP+ve neurones which were transient-firing fell to 51%. This may be a consequence of the prolonged contact time with the poly-D-lysine increasing the adherence of small diameter cells or due to a redistribution in firing phenotype as a large increase in tonic-firing eGFP+ve neurones (from 6.4% to 43.4%) was observed. Transient-firing neurones often showed a hyperpolarisation-activated current ($I_h$)-like response to hyperpolarisation. Voltage-clamp investigation into the regulation of neuronal excitability in transient-firing cells revealed the presence of an M-current. This was inhibited through $P2Y_{2/4}$ activation by uridine triphosphate (UTP) but not by $P2Y_1$ activation by adenosine diphosphate (ADP). In current-clamp, UTP increased the excitability of some transient-firing cells as determined by the change in spike frequency when depolarising current was applied. ADP blocked the primary spike in a similar number of cells. Bath applied adenosine triphosphate (ATP) suggested a combined role for P2Y and P2X receptors in the sensitisation transient-firing neurones.

The work presented here describes eGFP-labelled epidermal primary afferents as ATP sensitive neurones with rapidly adapting responses influenced by an M-current. Inference from the literature suggests they are mechanosensitive, either directly or via keratinocyte signalling through ATP. Under normal conditions it is suggested that they detect novel stimuli. A mechanism for sensitisation by endogenous ligands leading to hyperalgesia is proposed.

# Contents

# LIST OF FIGURES

# Acknowledgments

The journey to a PhD is a long and often arduous process and as the saying goes "many hands make light work". So I cannot go any further without acknowledging all those who have helped me on this journey which has been far from "light work" but undoubtedly eased by their various contributions.

To start, I would like to express my deepest gratitude to my supervisors, Dr Richard Morris and Dr Richard Barrett-Jolley, without whom I would not have had such an interesting project to pursue. Through their wisdom and guidance they have helped shape the scientist I have become and their influence during these formative years will continue to shape my science for many to come. Equally, my thanks goes to the Pain Relief Foundation for providing the funding for this project.

I would also like to thank my many colleagues and friends at the University of Liverpool who have helped me along the way. Although too many to name, a particular note must be made of Dr Thippeswamy for being my PhD advisor, Dr Mino Belle for teaching me immunohistochemistry and so much more, Dr Sylvia Vasiliou for teaching me PCR, Dr Matt Womack for his guidance and Dr Siobhan Cosgrave for her help and advice throughout the course of my project.

A special thanks goes to those who have been furthest from me, my family, for without their love and support I would have never gotten here. Finally I cannot conclude this section without thanking my partner Rita:

*"Obrigado minha querida, o teu amor e apoio brilhou nas minhas horas mais negras e levantou-me quando tropeçei."*

# Abbreviations

| | |
|---|---|
| ADP | adenosine diphosphate |
| ANOVA | analysis of variance |
| AP | action potential |
| ATP | adenosine triphosphate |
| CAG | chrome-alum gelatine |
| Calbindin | calbindin D-28K |
| CHO | Chinese hamster ovaries |
| CGRP | calcitonin gene-related peptide |
| CNS | central nervous system |
| CSA | cross-sectional area |
| DAPI | 4',6-diamidino-2-phenylindole |
| DEJ | dermal-epidermal junction |
| DH | dorsal horn (of the spinal cord) |
| DRG | dorsal root ganglion |
| EDTA | ethylenediaminetetraacetic acid |
| eGFP | enhanced green fluorescent protein |
| FITC | fluorescein isothiocyanate |
| FNEs | free nerve endings |
| FRAP | fluoride-resistant acid phosphatase |
| GABA | γ-aminobutyric acid |
| $GABA_B$ | γ-aminobutyric acid receptor B |
| GDNF | glial cell line-derived neurotrophic factor |
| GFL | GDNF family ligand |
| GFRα2 | glial cell line-derived neurotrophic factor family receptor α2 |
| $G/G_{max}$ | relative conductance |
| $G_M$ | $K_v7$- (M-current) mediated conductance |
| GPCR | G-protein coupled receptor |
| GRP | gastrin-releasing peptide |
| HCN | hyperpolarisation-activated, cyclic nucleotide gated channel |
| $IB_4$ | isolectin $B_4$ (from *Griffonia simplicifolia*) |
| $I_h$ | hyperpolarisation-activated current (HCN mediated) |
| $I_{inst}$ | instantaneous current (with regard to M-current) |
| $I_{K(M)}$ | potassium M-current |
| -ir | -immunoreactivity (e.g. GFRα2-ir) |
| $I_{ss}$ | steady-state current (with regard to M-current) |
| KIF | keratin intermediate filaments |
| $L_n$ | lamina (where n = I to X) |
| MANOVA | multivariate analysis of variance |
| MARCKS | myristoylated alanine-rich C kinase substrate |
| Mrgprd | Mas-related G protein-coupled receptor D |

| | |
|---|---|
| NGF | nerve growth factor |
| PCR | polymerase chain reaction |
| PFA | paraformaldehyde |
| PGP9.5 | protein gene product 9.5 |
| $PIP_2$ | phosphatidylinositol 4,5-bisphosphate |
| PNS | peripheral nervous system |
| P2X | ionotropic ATP-sensitive channel family |
| P2Y | metabotropic ATP-sensitive receptor family |
| Ret | "rearranged during transfection" receptor tyrosine kinase |
| SB | stratum basalis |
| SC | stratum corneum |
| SEM | standard error of the mean |
| SG | stratum granulosum |
| SP | substance P |
| SS | stratum spinosum |
| TAC | transit amplifying cells |
| TEWL | transepidermal water loss |
| TJ | tight junction |
| TMC | time-matched control |
| TrkA | receptor tyrosine kinase A |
| TRP | transient receptor potential |
| TRPA | transient receptor potential ankyrin |
| TRPM | transient receptor potential melastatin |
| TRPV | transient receptor potential vanilloid |
| UTP | uridine triphosphate |
| VGIC | voltage-gated ion channel |
| XE-991 | 10,10-*bis*(4-Pyridinylmethyl)-9(10*H*)-anthracenone dihydrochloride |

# Chapter 1

## INTRODUCTION

## Plan

In introducing this work I shall start by briefly outlining the objectives of the research this thesis collates. I shall follow this by reviewing the literature relevant to my research and which gives context to the work that follows thus allowing an understanding of the contribution this work makes to the overall subject area.

## Aims of Research Project

When I started my PhD project in the laboratory of Dr Richard Morris, a transgenic mouse in which a large number of epidermal primary afferents were selectively labelled with an enhanced green fluorescent protein (eGFP) had been characterised. Such was the expression of eGFP that along with the soma in the dorsal root ganglion (DRG), both the central and peripheral projections could be clearly observed using epifluorescent microscopy in freshly cut sections without the need to amplify the signal with antibodies raised against eGFP. This presented the opportunity to study the anatomy and physiology of a tissue specific population of sensory neurones using in vitro techniques.

I shall cover the study by Belle *et al.,* (2007) later in this chapter but briefly, the small diameter cell bodies of primary afferents with peripheral projections

terminating solely in the epidermis of hairy skin were intensely labelled with eGFP. These formed a separate population to the peptidergic afferents which expressed calcitonin gene related peptide (CGRP). All small diameter eGFP expressing neurones bound the plant lectin, isolectin $B_4$ ($IB_4$) from *Griffonia simplicifolia* and belonged to a subpopulation of DRG neurones defined as "nonpeptidergic". In the dorsal horn of the spinal cord, central terminations from these neurones clearly defined the substantia gelatinosa.

The aim of this project was to establish the function of these afferents by identifying the transduction molecules they express and characterising their electrophysiological and functional properties. Initially our hypothesis was that the superficial terminations of the free nerve endings (FNEs) were ideally placed to detect all manner of stimuli. As our results and the literature guided us, our hypothesis evolved accordingly and we began focussing on the role of keratinocyte signalling through purines on the excitability of these neurones.

## Background

### Brief overview of the organisation of the peripheral nervous system (PNS)

Subconsciously we act to maintain an optimal state of being, an act referred to as homeostasis. These adjustments range from minor adjustments in our physiology to overt changes in behaviour. This requires constant feedback about

both our internal and external environments, a process called somatosensation. Sensory neurones relaying information to the central nervous system (CNS) form the afferent pathway. Primary afferents (those innervating the target tissues) of the body have their soma contained within the DRG whilst the soma of sensory neurones innervating the face are located in the trigeminal ganglia. The axon myelination varies between sensory neurones and affects their conduction velocity (Yoshida and Matsuda, 1979). Unmyelinated C-fibres conduct the slowest (Yoshida and Matsuda, 1979) and form free nerve endings in the epidermis (Navarro et al., 1995). The majority of intraepidermal innervations are from unmyelinated afferents with the few that do arise from myelinated afferents losing their Schwann cell sheath as they cross the dermal-epidermal junction (Fundin et al., 1997).

Sensory neurones possess a pseudounipolar morphology and project centrally to the dorsal horn (DH) of the spinal cord (Figure 1.1.A). The grey matter of the spinal cord comprises of laminae (Rexed, 1952) of which lamina I-VI form the dorsal horn (Millan, 1999). Rexed (1952) described lamina II as having an inner and outer zone ($LII_i$ and $LII_o$ respectively). Nociceptive afferents terminate in the superficial laminae (lamina I & $II_o$), and along with the deeper laminae V, VI and X, these laminae are implicated in the reception, processing and transmission of nociceptive information (Millan, 1999). Afferents entering the dorsal horn grey matter branch, synapsing with interneurones to form a local circuit, and projection neurones which transmit the information to supraspinal

centres or ascend themselves to the dorsal column nuclei at the junction of the spinal cord and the medulla (Amaral, 2001; Millan, 1999). Supraspinal targets include the spinothalamic tract to the thalamus and the spinomesencephalic tract to the periaqueductal grey (Millan, 1999).

In contrast to the sensory, afferent pathway is the efferent pathway by which the body stimulates the skeletal muscles. Motor neurones located in the ventral horn receive synaptic input from both descending efferent pathways and DH interneurones. Input from DH interneurones forms a polysynaptic pathway responsible for spinal reflexes such as the stretch reflex (Pearson and Gordon, 2001). Monosynaptic pathways also occur when an afferent branch projects directly on to a ventral horn motor neurone (Pearson and Gordon, 2001).

**Figure 1.1. Organisation of the peripheral nervous system with regard to cutaneous innervations.**

A) The somas of primary afferents are located in the dorsal root ganglia and project centrally to the dorsal horn. Motor neurones of the ventral horn project peripherally along the ventral root which joins with the dorsal root to form the spinal nerve. The grey matter of the spinal cord is part of the central nervous system and is organised into laminae of which LI-VI form the dorsal horn.

B) The skin possesses many specialised sensory structures almost all of which are located within the dermis. The most superficial of these sensory structures are the Merkel cells located in the basal layer of the epidermis. The epidermis is densely innervated by the free nerve endings of unmyelinated C-fibres.

C) Neuronal innervation of the epidermis can be observed using antibody staining for the pan-neuronal marker, protein gene product 9.5 (PGP9.5; green). The nuclei of the keratinocytes are counterstained with DAPI (blue).

Figure taken from Patapoutian *et al.*, (2003)

**Figure 1.1.**

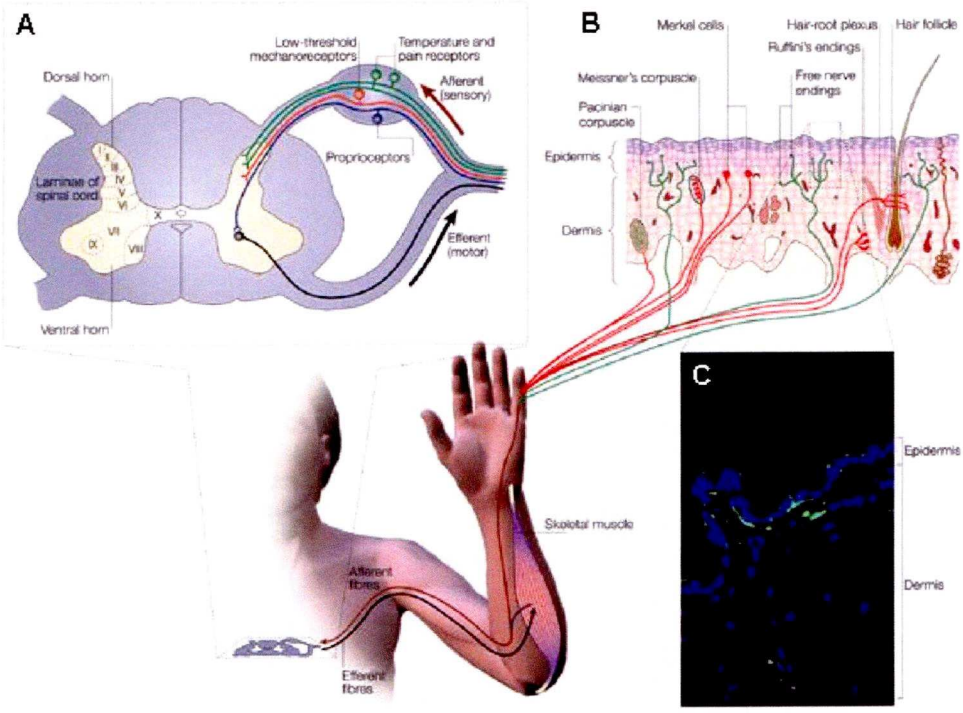
A
Low-threshold mechanoreceptors
Temperature and pain receptors
Dorsal horn
Afferent (sensory)
Proprioceptors
Laminae of spinal cord
I
II
III
IV
V
VI
VII
VIII
IX
X
Efferent (motor)
Ventral horn
B
Merkel cells
Hair-root plexus
Hair follicle
Ruffini's endings
Meissner's corpuscle
Free nerve endings
Pacinian corpuscle
Epidermis
Dermis
Skeletal muscle
Afferent fibres
Efferent fibres
C
Epidermis
Dermis

**Structure of the epidermis**

Three layers; the hypodermis, the dermis and the epidermis form the skin, an organ that covers the body almost in its entirety (Haake et al., 2001). The epidermis, a continually self-renewing layer of squamous epithelium, is the most superficial layer of the skin (Fuchs and Raghavan, 2002; Haake et al., 2001). A non-vascularised tissue, the epidermis is dependent on nutrients from the capillaries of the underlying dermis (Fuchs and Raghavan, 2002).

Stem cells within the bulge of the hair follicle give rise to transit amplifying cells (TAC) which are then distributed throughout the basal layer of the epidermis (Fuchs and Raghavan, 2002; Jones and Watt, 1993). The daughters of these rapidly dividing TAC undergo progressive differentiation as they migrate suprabasally, giving rise to the stratification of the epidermis (Fig. 1.2A) (Houben et al., 2007). As the migrating keratinocytes differentiate, they express distinct pairs of keratin intermediate filaments (KIF) allowing each strata to be identified by the keratins present (Haake et al., 2001; Smack et al., 1994). The morphology of the keratinocyte is also altered by the changes in protein expression and intercellular environment that occur during its migration and differentiation (Haake et al., 2001).

Keratinocytes of the basal layer (stratum basalis) are attached to the basement membrane that forms the dermal-epidermal junction (DEJ) and contributes to its

formation (Fuchs and Raghavan, 2002). The majority of interfollicular basal keratinocytes are epidermal stem cells and TAC (Barrandon and Green, 1987; Strachan and Ghadially, 2008). These are mitotically active cells which supply new keratinocytes for terminal differentiation to replace those lost from the more superficial layers (Fuchs and Raghavan, 2002; Houben et al., 2007). The newly formed keratinocytes begin their migration, forming the stratum spinosum, by changing their keratin expression and synthesising new organelles, the lamellar bodies. Although initially polyhedral, the keratinocytes become larger and flattened as they reach the upper stratum spinosum (Haake et al., 2001). The production of profilaggrin and its assembly into keratohyalin granules along with KIF is the defining feature of the epidermis' final nucleated layer, the stratum granulosum (Haake et al., 2001; Houben et al., 2007).

The cells of the granular layer synthesize and process the proteins responsible for the cornification of the keratinocyte (Haake et al., 2001). Protein aggregates beneath the plasma membrane cross link to form the cornified cell envelope as the cell enters the final stages of a process known as "epidermal programmed cell death" (Houben et al., 2007). Penultimately, the plasma membrane is broken down and replaced by a lipid envelope (Proksch et al., 2008) whilst intracellularly, the organelles and DNA are digested (Houben et al., 2007). The resulting anucleated, protein-enriched cell is called a corneocyte (Houben et al., 2007; Proksch et al., 2008). The most superficial layer of the epidermis, the stratum corneum, is a "brick and mortar" arrangement of corneocytes within a

lipid intercellular matrix (Heisig et al., 1996; Proksch et al., 2008). Partially formed by the extruded organelles of the cell, the lipid matrix is comprised of ceramides, cholesterol and free fatty acids (Houben et al., 2007). At this point the corneocytes are still bound tightly together by cell-cell adhesive structures which undergo controlled destruction leading to desquamation (Houben et al., 2007).

**Figure 1.2. Structure of the epidermis.**

A) Haematoxylin & eosin stain of rat plantar hind paw epidermis showing its stratification. sc, stratum corneum; sg, stratum granulosum; ss, stratum spinosum; sb, stratum basalis; derm, dermis. Scale bar = 50μm.

Figure taken from Khodorova et al., (2002).

B) Schematic of the structural organisation of dermis and epidermis. Although corneocytes and their lipid enriched intercellular matrix are important in the barrier function of the epidermis, the tight and adheren junctions formed by the keratinocytes of the nucleated epidermal strata (basal, spinous & granular layers) also have a vital role in barrier function.

Figure taken from Fuchs & Raghavan, (2002).

**Figure 1.2.**

A

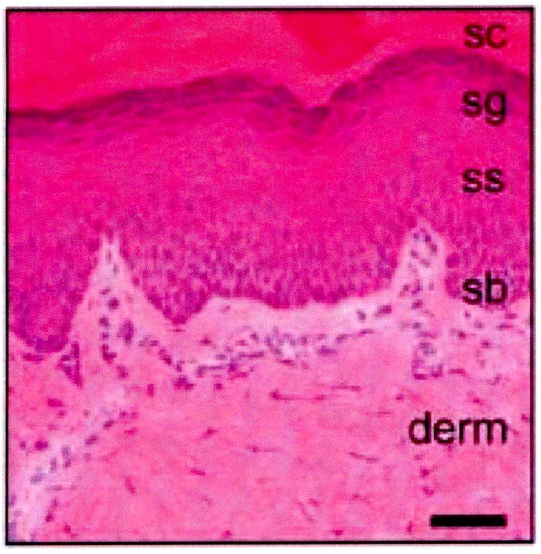
sc
sg
ss
sb
derm

B

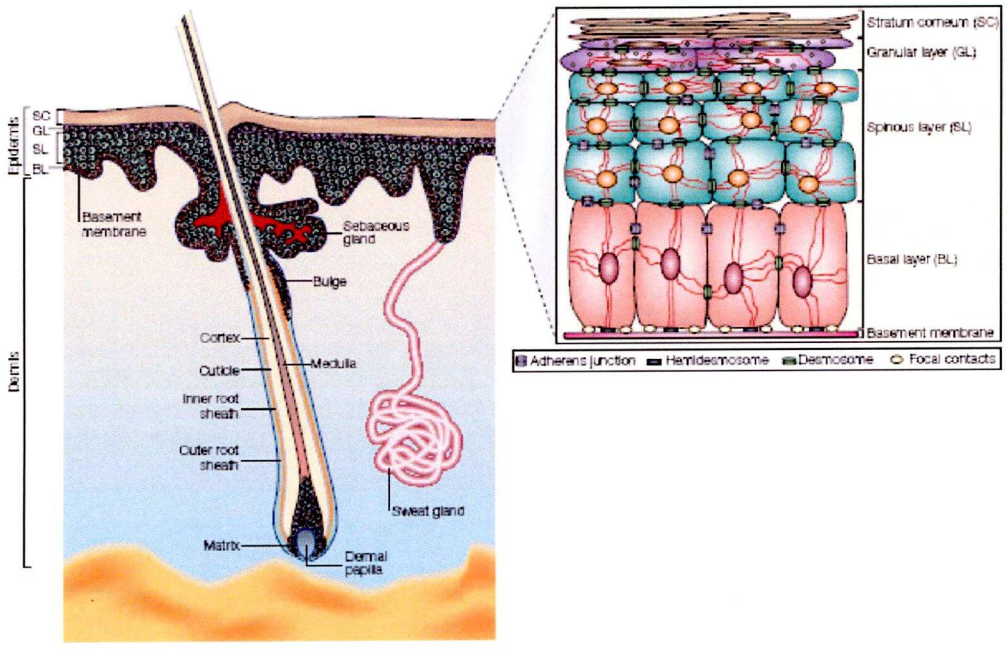
Epidermis
SC
GL
SL
BL
Dermis
Basement membrane
Sebaceous gland
Bulge
Cortex
Medulla
Cuticle
Inner root sheath
Outer root sheath
Sweat gland
Matrix
Dermal papilla
Stratum corneum (SC)
Granular layer (GL)
Spinous layer (SL)
Basal layer (BL)
Basement membrane
Adherens junction
Hemidesmosome
Desmosome
Focal contacts

**Functions of the skin with particular reference to the epidermis**

The skin is one of the body's largest organs and serves many important roles in sensation, protection, communication, thermoregulation, hydration, storage and synthesis. Such broad functions are beyond the scope of this work and so I shall focus upon the role of the epidermis within those as a barrier and sensory organ.

The barrier function of the epidermis is bidirectional (Proksch et al., 2008) and vital to an organisms survival. Prevention of transepidermal permeation from external (outside-in barrier) and internal (inside-out barrier) environments can be considered separately as whilst their respective functions are often correlated, this is not always the case (Tunggal et al., 2005). The "outside-in" barrier protects the organism from physical, chemical and microbial assaults whilst the "inside-out" greatly limits dehydration through transepidermal water loss (TEWL) (Proksch et al., 2008).

The SC, with its "brick and mortar" arrangement, is the principal barrier of the epidermis (Madison, 2003). The lipids which comprise the intercellular matrix are responsible for much of the permeability barrier (Madison, 2003). They are organised in the intercellular space of the SC as tightly packed sheets of lamellae (Madison et al., 1987). Excessive (TEWL) leads to dessication of the skin as seen in skin diseases where "inside-out" barrier function is compromised. Removal of the SC using tape-stripping gives rise to a moderate increase in

TEWL but is not detrimental to barrier function (Proksch et al., 2008). The tight junctions (TJ) formed by cell-cell adhesion molecules within the SG seem to have a more crucial role in preventing TEWL. In mice with compromised TJ due to direct (Furuse et al., 2002) and indirect (Tunggal et al., 2005) knock out of claudin-1, TEWL is greatly increased and proves fatal within 12 hours of birth. This apparent loss of "inside-out" barrier function is not associated with structural changes in the epidermis (Furuse et al., 2002) and is not mirrored by the "outside-in" barrier which remains functional (Tunggal et al., 2005).

The importance of epidermal "outside-in" barrier function in the prevention of microbial infection is clearly demonstrated in burn victims. A critical component of care for patients suffering thermal and chemical burns is wound sterility and closure (Church et al., 2006). Sepsis from burn wound infection, other infection complications and/or inhalation injuries account for 75% of all deaths in patients with burns to 40% or more of their total body surface area (Church et al., 2006). In uninjured epidermis, increased paracellular permeation of microbes such as Staphylococcus *aureus*, is associated with dislocalisation of epidermal TJ (Ohnemus et al., 2008). Langherans cells represent 3-5% of all nucleated cells within the epidermis and are epidermal antigen-presenting dendritic cells (Merad et al., 2008). They form the first active component of the skins immune system, detecting the presence of foreign antigens through extended dendrites which form a continuous network throughout the epidermis (Merad et al., 2008).

**Epidermal innervations: Possible roles for nonpeptidergic C-fibre free nerve endings in the epidermis**

The epidermis is densely innervated with several types of FNEs, only a minority of which is clearly peptidergic (Fundin et al., 1997; Lindfors et al., 2006). These mostly arise from unmyelinated and occasionally Aδ fibres (Fundin et al., 1997). Cluster endings surround the mouths of hair follicles as bush, radiating and pencillate endings are spread throughout the interfollicular epidermis (Fundin et al., 1997). Neurotrophic factors are crucial to the survival, maturation and targeting of peripheral terminations (Albers and Davis, 2007).

Small sensory neurones can be differentiated by their expression of neuropeptides and ability to bind $IB_4$ (Nagy and Hunt, 1982; Silverman and Kruger, 1990). These groups of DRG neurone have been termed peptidergic and nonpeptidergic respectively (Hunt and Rossi, 1985), and represent functionally distinct populations of neurones (Stucky and Lewin, 1999). Selective ablation of nonpeptidergic sensory neurones in adult rats using a lectin conjugated cytotoxin ($IB_4$-saporin) revealed a role for C-fibres in the transduction of acute nociceptive stimuli (Tarpley et al., 2004; Vulchanova et al., 2001).

Chateau & Misery (2004) proposed that neuro-epidermal junctions should be considered as true synapses. It has been shown that cultured keratinocytes can induce propagating $Ca^{2+}$ waves in other keratinocytes over distances up to 100

μm through the release and diffusion of ATP (Koizumi et al., 2004). This ATP release also increased $[Ca^{2+}]_i$ in co-cultured mouse DRG neurones (Koizumi et al., 2004). A population of nonpeptidergic primary afferents innervating the epidermis express the $P2X_3$ subunit (Zylka et al., 2005) and are selectively sensitive to ATP (Dussor et al., 2008). The aforementioned evidence would suggest that these neurones play an important role in transducing signals from surrounding keratinocytes (Dussor et al., 2009). When the glial cell line-derived neurotrophic factor (GDNF) family receptor α2 (GFRα2) is genetically deleted there is no loss of nonpeptidergic DRG neurones but a 70% reduction in nonpeptidergic FNEs terminating in the epidermis (Lindfors et al., 2006). Behavioural manifestations of this hypoinnervation included a deficit in persistent inflammatory pain response and hypersensitivity to noxious heat and cold but only when the tail was immersed in water (Lindfors et al., 2006).

Unmyelinated fibres in the skin can possess low or high thresholds of activation to mechanical stimulation (Bessou and Perl, 1969; Iggo, 1960). A population of C-fibres with epidermal FNEs bind $IB_4$ but do not express the $P2X_3$ subunit (Liu et al., 2007). Their peripheral projections innervate the hair follicles and the surrounding epidermis whilst their receptive fields are discontinuously distributed (Liu et al., 2007). The authors postulated a potential role for them in gentle, innocuous touch (Liu et al., 2007). Experiments in humans have identified a population of C-fibres that are responsive to pleasurable touch (Loken et al., 2009).

Itch (pruritus) is a phenomenon that is almost exclusive to the epidermis with the exception of a few epithelial surfaces such as the mouth, eyes and genitalia. Histamine is a well known pruritogen and antihistamines are commonly used in the treatment of acute itch but are of limited use for many chronic pruritic diseases (Ikoma et al., 2006). Indeed, both histaminergic (Schmelz et al., 1997) and non-histaminergic (Sun and Chen, 2007) itch pathways have been identified in C-fibres (Ikoma et al., 2006). Pain is antagonistic to itch, which can be exacerbated (Atanassoff et al., 1999) and induced (Ko et al., 2004) by analgesia. Schmelz et al., (Schmelz et al., 2003) concluded that itch sensation was a product of both "itch-pathway" activity and an absence of "pain-pathway" activity.

**Transduction molecules**

The skin forms the largest sensory organ of the body and, through various structures contained within it, is capable of transducing many different types of stimulus (Lumpkin and Caterina, 2007) . These energy types transduced are of three types; thermal, chemical and mechanical. Transduction is carried out by a range of ion channels and G-protein coupled receptors. The "law of specific nerve energies" formulated by Johannes Müller in 1826 stated that regardless of the method of stimulation, the sensation felt would always be of the type appropriate to that system (Norrsell et al., 1999). This is supported by the fact that chemical agonists of thermosensitive ion channels often illicit a similar sensation to the thermal stimulus but tells us more about the perception and central processing of the information transduced than the actual transduction process.

The transductive properties of sensory neurones are thought to be determined by their ion channel expression (Hjerling-Leffler et al., 2007) but it is also becoming increasingly clear that the cellular environment that these transduction molecules are expressed within also exerts great influence on their function and thus modality (Belmonte and Viana, 2008). Adding further complexity is the often polymodal nature of many ion channels implicated in somatosensory transduction (Bandell et al., 2007; Belmonte and Viana, 2008; Lumpkin and Caterina, 2007).

## Thermoreception

Thermoreception has been largely attributed to several members of the transient receptor potential (TRP) ion channel superfamily (Schepers and Ringkamp, 2009). Some TRP channels belonging to the vanilloid (TRPV) and melastatin (TRPM) subfamilies are selectively activated at temperatures spanning the warm to noxious heat ranges (Bandell et al., 2007; Schepers and Ringkamp, 2009; Talavera et al., 2008b). The first channel to be identified was $TRPV_1$ which is activated at noxious temperatures (>43°C) and by the pungent chemical responsible for the sensation of heat in chillies, capsaicin (Caterina et al., 1997). Three of the remaining 5 members of the TRPV subfamily ($TRPV_{2-4}$) are thermosensitive (Figure 1.3A) and are expressed in sensory neurones or keratinocytes (Bandell et al., 2007). So far none of the warm-activated TRPM channels ($TRPM_2$, $TRPM_{4-5}$) have been located in sensory neurones or keratinocytes (Talavera et al., 2008a).

Meanwhile the transduction of cooling and noxious cold stimuli by $TRPM_8$ and TRP Ankyrin 1($TRPA_1$) has been reported (McKemy et al., 2002; Peier et al., 2002a; Story et al., 2003). Genetic deletion studies support a role for $TRPM_8$ in cold pain but evidence for $TRPA_1$ involvement is less clear (Bandell et al., 2007; Bautista et al., 2006; Dhaka et al., 2007; Kwan et al., 2006). The colocalisation of $TRPA_1$ with $TRPV_1$ in peptidergic small sensory neurones may explain the burning sensation elicited by very cold stimuli (Bandell et al., 2004).

When cold sensitive neurones are identified by their functional response to cooling, two populations can be identified, those that are menthol-sensitive and those that are menthol insensitive (Babes et al., 2004). It was observed that the pharmacology of the menthol-insensitive population did not correspond with the known pharmacology of TRPA1 channels (Babes et al., 2004). Other work has described cold sensitivity as a result of a "favourable blend" of ion channels rather than the product of a single transduction molecule (Viana et al., 2002). All neurones determined to be cold-sensitive were activated or sensitised by menthol (Viana et al., 2002). Neurones previously identified as cold-insensitive responded to cooling when a 4-aminopyridine-sensitive K+ current was blocked (Viana et al., 2002). Inhibition of a background potassium channel resistant to 4-aminopyridine (4-AP) and tetraethylammonium (TEA) has also been suggested as a mechanism of cold transduction (Reid and Flonta, 2001). A couple of members of the two pore domains ($K_{2P}$) potassium channel family mediate a background current and have been implicated in this effect (Noel et al., 2009). Genetic deletion of both TRAAK and TREK-1 (both $K_{2P}$) resulted in a significant increase in the proportion of small DRG neurones displaying cold-sensitivity (Noel et al., 2009). Whilst TRP channels have an important role in thermotransduction it is clear that they are not the sole transducers of thermal stimuli (Figure 1.3B).

**Figure 1.3. TRP channels are activated by a range of temperatures.**

A) Six thermosensitive transient receptor potential (TRP) channels have so far been identified in sensory neurones and keratinocytes. The C-terminal also seems to play an important role in the thermal selectivity of some channels. Chimeric channels created by exchanging the C-terminals of TRPV1 and TRPM8 channels also exchanged their thermal sensitivity whilst leaving their ligand selectivity unaffected (Brauchi et al., 2006).

Figure taken from Jordt et al., (2003).

B) Whilst strong emphasis is placed on the role of TRP channels in thermosensation in the literature, there is evidence to support a place for non-TRP ion channels in thermotransduction.

Table adapted from Patapoutian et al., (2003).

**Figure 1.3.**

A

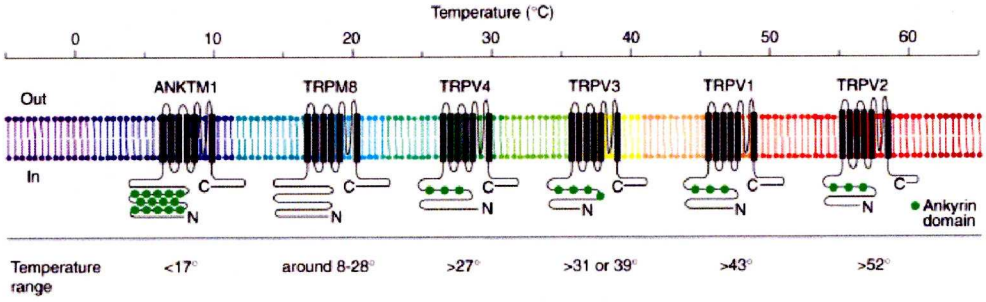


B

| Nomenclature | Other names | Temperature sensitivity | Non-thermal agonists | Blockers | Tissue distribution |
|---|---|---|---|---|---|
| ***Non-TRP proteins that might be involved in thermosensation*** | | | | | |
| TREK-1 | Kcnk2 | Cold | Membrane stretch, polyunsaturated fatty acids intracellular pH | | PNS, brain |
| P2X3 | | Warmth | ATP | | PNS |
| Na/K ATPase | ? | Cold? | | Ouabain | PNS? |
| BNC1, ASIC, DRASIC | | Cold | Acidic pH (potentiated) | Amiloride | PNS |

## Chemoreception

As already described, many TRP channels are expressed in sensory neurones conferring them with thermotransductive properties. TRP channels are also activated by a wide variety of organic compounds found in herbs and spices (Table 1.1) (Macpherson et al., 2007; Macpherson et al., 2006; Voets et al., 2005; Xu et al., 2006). Whilst the capsaicin receptor (VR1, TRPV1) and the menthol receptor (CMR1, TRPM8) were defined by their ligand specific activation, even before their molecular identity was deduced (Calixto et al., 2005), several TRPs are gated by ligands with cross channel activity (Macpherson et al., 2006). Along with plant-derived compounds, TRPs can be opened by changes in external pH (Dhaka et al., 2009) and modulated by endogenous signalling molecules (Ramsey et al., 2006). Changes in extracellular proton ($H^+$) concentration is not solely transduced by TRP channels but also by a group of acid-sensing ion channels (ASIC) which belong to the degenerin/epithelial $Na^+$ channel (DEG/ENaC) family (Lumpkin and Caterina, 2007).

Chemoreception extends beyond external sources as in some cases the primary transducer is not the nerve ending itself but the surrounding cells such as the keratinocytes of the epidermis or epithelial cells (Boulais and Misery, 2008; Denda et al., 2007; Dussor et al., 2009; Koizumi et al., 2004). Once thought of as passive and nonexcitable (Wohlrab et al., 2000), keratinoytes are capable of

releasing a variety of chemical messengers which are detectable by the free nerve endings innervating them (Khodorova et al., 2002; Khodorova et al., 2003; Koizumi et al., 2004; Wilmer et al., 1994). Keratinocytes express several ion channels commonly found in sensory neurones and some channels are more abundant in keratinocytes than the nerve fibres innervating them (Boulais and Misery, 2008; Peier et al., 2002b; Xu et al., 2002). Upon stimulation keratinocytes have been shown to release inflammatory mediators (PGE2, interlukin-8) (Huang et al., 2008; Southall et al., 2003), excitatory (ATP, endothelin-1) (Khodorova et al., 2002; Koizumi et al., 2004) and inhibitory (β-endorphin) (Ibrahim et al., 2005; Khodorova et al., 2003) transmitters. The antagonistic nature of these transmitters is suggestive of a capacity to filter signals prior to reaching the nervous system (Lumpkin and Caterina, 2007).

Chemoreception is not restricted to ion channels; G-protein coupled receptors (GPCRs) have an important role in chemoreception in sensory neurones. Gentle mechanical stimulation evokes ATP release from cultured keratinocytes (Koizumi et al., 2004). Extracellular ATP activates ionotropic P2X channels and metabotropic P2Y receptors, both of which are expressed in epidermal keratinocytes and the neurones innervating them (Dixon et al., 1999; Greig et al., 2003; Gu and MacDermott, 1997; Ruan and Burnstock, 2003; Volonte et al., 2006; Zylka et al., 2005). The transduction of itch is one role in which at least two families of GPCR are known to be involved, the gastrin-releasing peptide receptor (GRPR) (Sun and Chen, 2007) and the histamine receptor (Ikoma et al.,

2006). Primary afferents also express a family of GPCRs, subsets of which are exclusive to sensory neurones, the Mas-related gene (Mrg) family (Dong et al., 2001). The expression of several members of this family delineates specific subpopulations of c-fibres (Liu et al., 2007; Liu et al., 2008; Zylka et al., 2005). The GABA analogue, β-alanine, activates the Mas-related G protein-coupled receptor D (Mrgprd) at physiological concentrations and inhibits a taurine transporter (TAUT) important in the maintenance of keratinocyte hydration (Janeke et al., 2003; Shinohara et al., 2004).

**Table 1.1. Thermosensitive TRP ion channels are activated by a range of plant-derived and endogenous ligands.**

Thermosensitive TRP ion channels are activated by a diverse collection of pungent, plant-derived chemicals and endogenous ligands. Many of the sensations associated with the herbs and spices we enjoy in our diets are the result of TRP activation.

Figure taken from Voets et al., (2005).

# Table 1.1

**Chemical agonists for thermoTRPs**

| Name | Structure | Occurrance | Target | Concentration |
|---|---|---|---|---|
| Capsaicin | 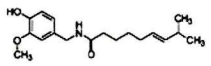 | Plant-derived | TRPV1 | $10^{-8}$–$10^{-6}$ |
| Resiniferatoxin | 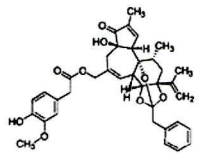 | Plant-derived | TRPV1 | $10^{-10}$–$10^{-8}$ |
| Piperine | 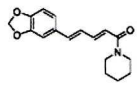 | Plant-derived | TRPV1 | $10^{-5}$–$10^{-4}$ |
| Olvanil | 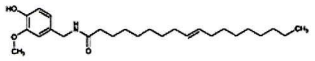 | Synthetic | TRPV1 | $10^{-8}$–$10^{-6}$ |
| Anandamide | 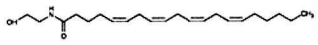 | Endogenous | TRPV1 | $10^{-6}$–$10^{-4}$ |
| 2-APB | 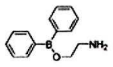 | Synthetic | TRPV3 > TRPV1 > TRPV2 | $10^{-5}$–$10^{-3}$ |
| Camphor |  | Plant-derived | TRPV3 | $10^{-4}$–$10^{-2}$ |
| 4α-PDD | 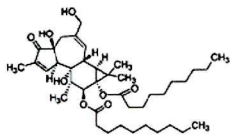 | Synthetic | TRPV4 | $10^{-7}$–$10^{-5}$ |
| 5',6'-EET | 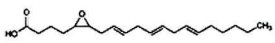 | Endogenous | TRPV4 | $10^{-8}$–$10^{-6}$ |
| Menthol |  | Plant-derived | TRPM8 | $10^{-5}$–$10^{-3}$ |
| Eucalyptol |  | Plant-derived | TRPM8 | $10^{-4}$–$10^{-2}$ |
| Icilin | 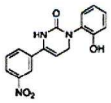 | Synthetic | TRPM8 > TRPA1 | $10^{-7}$–$10^{-4}$ |
| Cinnamaldehyde |  | Plant-derived | TRPA1 | $10^{-5}$–$10^{-4}$ |
| Allylisothiocyanate |  | Plant-derived | TRPA1 | $10^{-5}$–$10^{-4}$ |
| $\Delta^9$-Tetrahydrocannabinol | 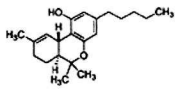 | Plant-derived | TRPA1 | $10^{-5}$–$10^{-4}$ |
| Allicin | 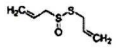 | Plant-derived | TRPA1 > TRPV1 | $10^{-7}$–$10^{-4}$ |

**Mechanotransduction**

Innervation of the skin by mechanoreceptors varies across the body surface with the greatest density found in glabrous skin (Gardner et al., 2000). Afferents terminate in the epidermis as FNEs (Wang et al., 1990), in association with Merkel disc receptors (Reinisch and Tschachler, 2005) and in association with hairs (Fundin et al., 1997). Those afferents terminating in the dermis are associated with encapsulated, corpuscular endings consisting of neural and non-neural structures (Gardner et al., 2000; Metze, 2001). Cutaneous mechanoreceptors have been described both morphologically and functionally (Hamann, 1995; Munger and Ide, 1988).

Functional classification of mechanoreceptive afferents innervating the skin has distinguished between neurones on the basis of conduction velocity (Brown and Iggo, 1967; Koerber et al., 1988; Koltzenburg et al., 1997), electrical properties (Koerber et al., 1988), threshold of activation (Brown and Iggo, 1967; Koltzenburg et al., 1997), innervation target (Brown and Iggo, 1967; Koerber et al., 1988)and adaptation to sustained stimuli (Brown and Iggo, 1967; Koltzenburg et al., 1997). Histological observations identified specialised end organs associated with afferent fibres (Munger and Ide, 1988). Several submodalities of touch are associated with these structures (Table 1.2) (Hamann, 1995; Johnson, 2001; Lewin and Moshourab, 2004). Unmyelinated C-fibres terminating as FNEs are also mechanosensitive, with both low and high

thresholds of activation (Bessou and Perl, 1969; Iggo, 1960).

**Table 1.2. Summary of the mechanoreceptors present in hairy skin.**

Many qualities of touch are associated with specialised sensory structures in the skin. As well as these sensory specific structures the epidermis is richly innervated by unmyelinated C-fibres. Some of these unmyelinated afferents are mechanosensitive, others are also thermosensitive and thus considered polymodal.

Figure taken from Lewin & Moshourab, (2004).

**Table 1.2**

| Mechanoreceptors Types | Structure Innervated | Vertebrate Species | Mechanosensitive Property |
|---|---|---|---|
| SA-I | Merkel discs | Mouse, rat, cat, human, monkey | Movement and static indentation stretch |
| SA-II | Ruffini, Haarscheibe | Mouse, rat, cat human, monkey | |
| FA-I | Pacinian Corpuscles. | Mouse, rat, cat human, monkey | Vibration-flutter |
| FA-II | Meissner corpuscles | Mouse, rat, cat, human, monkey | Movement |
| G1 Hair | Hair-lanceolate | Cat, rabbit, rat, human | Rapid hair movement, low velocity distort |
| G2 hair | | | |
| Field 1/2 | | Cat, rabbit, rat | Skin movement |
| D-hair | Sinus Hair ? | Mouse, rat, cat, human, monkey | Down/sinus hair movement, very sensitive |
| AM | Aδ-HTMR. "Free nerve endings" | Mouse, rat, cat, human, monkey | High threshold, noxious stimulus |
| AMH-AMC Type I and II | "Free nerve endings" | Monkey, human, rodents | Two types with different thermal thresholds |
| AMi-H | "Free nerve endings" | Monkey, human | Very high threshold |
| C-LT | "Free nerve endings" | Mouse, rat, cat, human, monkey | Low mechanical threshold |
| C-M | "Free nerve endings" | Mouse, rat, cat human, monkey | High mechanical threshold |
| C-MH/C-MC/C-MHC | "Free nerve endings" | Mouse, rat, cat, human, monkey | High mechanical threshold |
| C-MiHi | "Free nerve endings" | Mouse, rat, monkey, human | Very high threshold, nonmechanosensitive |

SA - slowly adapting; FA - fast (rapidly) adapting; G - guard hair; D – down hair; AM – A-fiber mechanoreceptors; Aδ-HTMR – Aδ-fiber high threshold mechanoreceptors; AMH - A-fiber mechanoheat receptors; AMC – A-fiber mechanocold receptors; AMiH – A-fiber mechanoinsensitive heat receptor; C-LT – C-fiber low threshold mechanoreceptor; C-M – C-fiber mechanonociceptors; C-MH – C-fiber mechanonociceptors heat; C-MC – C-fiber mechanonociceptors cold; C-MHC – C-fiber mechanonociceptors heat cold; C-MiHi – C-Mechano insensitive, heat insensitive.

**Transduction to action potential**

Activation of a transduction molecule does not equate to an action potential. The resting membrane potential of a neurone is a dynamic equilibrium between passive excitatory (inward) and inhibitory (outward) currents. Action potential firing is an all-or-nothing event, requiring sufficient depolarisation of the nerve ending to activate enough voltage-gated ion channels (VGIC) to create a self propagating wave of depolarisation. This point, called the threshold of activation, is determined by the sensitivity of the voltage-gates of the ion channels in the nerve ending. Subthreshold activation causes a transient disturbance in the local membrane potential which is quickly restored to a resting value. Membrane depolarisation by transduction molecules (generator potentials) can be effected by two processes. The permeability of the nerve ending membrane to either $Na^+$ and/or $Ca^{2+}$ influx can be increased or the permeability to $K^+$ efflux can be decreased. Many transductive ion channels have pores permeable to $Na^+$, $Ca^{2+}$ or both. Conversley GPCRs, through second messenger signalling, can decrease membrane $K^+$ permeability, hyperpolarise the activation-gates of VGICs and in some cases directly activate some ion channels via an internal ligand-binding site.

Primary afferent neurones express many VGICs that influence the initiation and conduction of an action potential. Generator potentials can activate the subthreshold currents mediated by the voltage-gated sodium channel (VGNaC),

$Na_v1.9$ (Herzog et al., 2001) or the voltage-gated calcium channel (VGCaC), $Ca_v3.2$(Huguenard, 1996; Scroggs and Fox, 1992). The voltage-gated potassium channel (VGKC) family, $K_v7$, conducts a slowly developing, non-inactivating current which reduces cellular excitability (Brown and Adams, 1980). Hyperpolarisation, an ordinarily inhibitory action, can lead to depolarisation and increased excitability through the activation of hyperpolariastion-activated, cyclic nucleotide-gated (HCN) channels (Bobker and Williams, 1989; Scroggs et al., 1994). In small, C-type DRG neurones the tetrodotoxin resistant (TTX-R) VGNaC, Nav1.8, make a substantial contribution to action potential electrogenesis (Renganathan et al., 2001). Although not a transducer of cold stimuli, expression of $Na_v1.8$ is important for conduction in neurones activated in cold conditions (Zimmermann et al., 2007). Whilst cooling increases the slow inactivation of tetrodotoxin (TTX) sensitive VGSCs, the inactivation properties of $Na_v1.8$ remain unaffected (Zimmermann et al., 2007).

**Modification of transduction leading to sensitization**

Most sensory systems adapt to sustained or repeated stimulation. As most innocuous stimuli pose little threat of harm, their continued presence is gradually ignored in a process of habituation. If we were to habituate to noxious stimuli then we would potentially ignore injurious or disabling afflictions leading to exacerbation of the problem with ultimately grave results. The detection of potentially damaging stimuli, nociception, serves a protective role by drawing our attention to damage and influencing our behaviour in a self-preserving manner. The nociceptive pathway unlike other sensory systems does not adapt but rather sensitises to sustained or repeated stimulation. This sensitization leads to increased pain from a noxious stimulus (hyperalgesia) and the perception of ordinarily innocuous stimuli as painful (allodynia) (Ji et al., 2003). Sensitization has both central and peripheral components to it. Central sensitization can occur within the DH, as well as supraspinally, and can arise from several mechanisms including reversible early-onset plasticity (windup), prolonged synaptic plasticity (classical central sensitization) and a late-onset transcription-dependent form of plasticity that shares a similar mechanism to the long-term potentiation observed in the hippocampus(see Ji et al., 2003 for review).

Peripheral mechanisms of sensitization are the result of either changes in the sensitivity of pre-existing ion channels or changes in the expression of ion channels in the neurone (Ji et al., 2003). Modulation of the activation gate by

inflammatory mediators such as prostaglandin $E_2$ ($PGE_2$) increases the open probability of VGICs at membrane potentials that they would usually be largely inactive at (Gold et al., 1998; Momin and McNaughton, 2009). Bradykinin acting through the B2 receptor leads to the phosphorylation of TRPV1 channels which potentiates their gating by noxious stimuli (Huang et al., 2006). Alternatively, trafficking of TRPV1 to the membrane is increased when tyrosine receptor kinase A (TrkA) is activated by the endogenous ligand nerve growth factor (NGF) (Zhang et al., 2005).

**Transgenic mice in which epidermal afferents are selectively labelled with marker genes**

A group of GPCRs that belong to the Mas-related G protein-coupled receptor (Mrgpr) family are expressed in the $IB_4$-binding population of DRG neurones (Dong et al., 2001). The transcription factor, Runx1, has a critical role in the determination of sensory neurone phenotype during the postnatal maturation of DRG neurones (Chen et al., 2006). Persistent expression of Runx1 represses the expression of some Mrgprs resulting in non-overlapping subsets within the $IB_4$-binding population (Liu et al., 2008). The selective expression of Mrgprs in the PNS has allowed the innervations of distinct populations of nonpeptidergic sensory neurones to be examined (Liu et al., 2007; Zylka et al., 2005). I shall describe the anatomical and immunohistochemical features of two transgenic mice which express reporter genes in specific Mrgpr-expressing primary afferents before describing a study by Belle et al., (2007) on the *thy1.2-eGFP* mouse the work in this thesis centres on.

Work by David Anderson's group on a transgenic mouse which co-expressed a farnesylated enhanced green fluorescent protein (EGFP*f*) alongside the Mrgprd receptor (Mrgprd$\Delta^{EGFPf}$) revealed a population of unmyelinated, nonpeptidergic sensory neurones with peripheral innervations restricted to the epidermis (Zylka et al., 2005). These neurones were characterised as Runx1+ve (Liu et al., 2008), c-RET+ve and $P2X_3$+ve (Zylka et al., 2005). Mrgprd$\Delta^{EGFPf}$ primary afferent

fibres terminated as FNEs in the epidermis of both hairy and glabrous skin as superficially as the stratum granulosum (Zylka et al., 2005). The central terminations of Mrgprd$\Delta^{EGFPf}$ neurones clearly marked a region of LII which extensively overlapped with $IB_4$-binding (Zylka et al., 2005). This labelling showed little overlap with CGRP (LI & $LII_o$ marker) or protein kinase Cγ (PKCγ; LIIi & LIII marker) leading the authors to postulate whether lamina $II_i$ should be further subdivided (Zylka et al., 2005). A comparison of PKCγ-immunoreactivity in the dorsal horn of rodents observed that whilst there was some overlap with $IB_4$-binding in rats none was seen in mice and the authors concurred with the further division of lamina $II_i$ (Neumann et al., 2008).

Using placental alkaline phosphatase (PLAP) as the reporter gene, a mouse with selective labelling of MrgprB4-expressing (MrgprB4$\Delta^{PLAP}$) primary afferents was also investigated by Anderson's group (Liu et al., 2007). MrgprB4$\Delta^{PLAP}$ neurones marked a small population of unmyelinated afferents which exclusively innervated the epidermis of hairy skin (Liu et al., 2007). These neurones were characterised as Runx1-ve (Liu et al., 2008), c-RET+ve and $P2X_3$-ve (Liu et al., 2007). Although only accounting for 2% of the neuronal population in thoracic DRG, MrgprB4 neurones branched extensively, covering ~50-60% of the skin surface area in large, discontinuous patches (Liu et al., 2007). Their peripheral terminations encircled and penetrated the necks of hair follicles and the surrounding epidermis (Liu et al., 2007). In the dorsal horn, MrgprB4$\Delta^{PLAP}$ neurones terminated in lamina $II_o$, colocalising with $IB_4$-bound terminals (Liu et

al., 2007). Crossbreeding with MrgprdΔ$^{EGFPf}$ mice revealed the central terminations of MrgprB4 and Mrgprd overlapped but remained distinct (Liu et al., 2007).

Neither of these mice showed significant colocalisation with CGRP or neurofilament 200kD supporting their characterisation as unmyelinated, nonpeptidergic afferents (Liu et al., 2007; Zylka et al., 2005). Only Mrgprd colocalised with TRPV1 in a small (9%) subpopulation which does not vary remarkably from previously reported values for mice (Woodbury et al., 2004).

In the study by Belle et al. (2007), a transgenic mouse expressing a membrane-linked enhanced green fluorescent protein (eGFP) under the control of the *thy1.2* gene promoter was characterised. Despite abundant eGFP expression within the brain this transgene was found to have highly restricted expression outside of the central nervous system. eGFP was observed in a heterogeneous population of DRG neurones which innervated a single tissue, the epidermis. This mouse was one of several produced by Silvia Arber (Belle et al., 2007) and this particular strain was labelled SA36. Contrary to another transgenic animal in which neurones innervating the epidermis of both glabrous and hairy skin were labelled (Zylka et al., 2005), only those terminating in the epidermis of hairy skin expressed the thy1.2-eGFP transgene.

In the SA36 strain, 74.2% of the DRG neurones positive for eGFP had soma diameters under 450 $\mu m^2$ and were considered small diameter, which are known to give rise to unmyelinated C-fibres (Lawson, 1979). All these small diameter DRG neurones bound $IB_4$, a marker of nonpeptidergic DRG neurones whilst conversely 87.3% of $IB_4$-positive neurones contained eGFP. Two populations of eGFP expressing neurone did not bind $IB_4$. These neurones could be considered medium (450-850 $\mu m^2$) and large (>850 $\mu m^2$) on the basis of soma diameter (Lawson, 1979). Approximately half (52%) of these were positive for calbindin D-28K, a calcium binding protein frequently found in low-threshold mechanoreceptive sensory neurones (Ichikawa et al., 1997; Ichikawa and Sugimoto, 1997). There was no colocalisation of eGFP with the peptidergic sensory neurone markers, calcitonin gene-related peptide (CGRP) and substance P.

Peripheral projections from eGFP DRG neurones traverse the dermis in bundles with little branching prior to the dermal-epidermal junction. Upon entering the basal layer of the epidermis (SB) these nerve bundles ramify into a dense network of free nerve endings terminating as superficially as the granular layer (SG). Epidermal hair follicles were also innervated by a group of eGFP- positive afferents which terminated in club endings at the bases of hairs or lanceolate endings at the neck of vibrissae hairs. Central terminations from eGFP DRG neurones delineated $LII_i$ and $LII_o$ of the dorsal horn, colocalising extensively with $IB_4$ but not CGRP or substance P (SP).

# Chapter 2

## MATERIALS AND METHODS

## Methods

### Animal welfare and housing conditions

All procedures were approved by The University of Liverpool Animal Ethics committee and were carried out under the provisions of the UK Animal (Scientific Procedures) Act 1986. Animals were housed on a 12-hour light/dark cycle beginning at 8:00 am with free access to food and water. Temperature was maintained at 22±2°C.

### Animals

Transgenic mice from the SA36 strain of *thy1.2-eGFP*/C57/BL6 line were used. The founder animals for the colony were kindly supplied by Professor Silvia Arber. Mice expressing membrane-bound enhanced green fluorescent protein (eGFP) were produced using pronuclear injection of mouse blastocysts from C57/BL6 mice with a Thy1.2 expression cassette containing the transgene (Belle, 2007). The transgene was a combination of the initial 40 amino acids of the human myristoylated alanine-rich C kinase substrate (MARCKS) protein and eGFP (Clonetech) (Belle et al., 2007; De Paola et al., 2003; Harlan et al., 1991; Livet et al., 2002; Wiederkehr et al., 1997). This fusion transgene was inserted into the Thy1.2 expression cassette using the Xho1 site (Caroni, 1997). This excises intron 3 which is required for transcription outside of the nervous system

thus limiting expression to neuronal tissues (Caroni, 1997; Vidal et al., 1990). Animals were inbred to maintain a homozygous line and out bred with wild type C57/BL6 mice when necessary.

**Genotyping of transgenic offspring**

To produce a homozygous line, breeding trials were conducted to identify homozygous individuals. Trial pairs were set up and all offspring were tested for the eGFP transgene using polymerase chain reaction (PCR). To confirm homozygosity, suspected individuals were out bred with C57/BL6 mice and the offspring tested for eGFP by polymerase chain reaction.

Transgenic mice (P10-21) were lightly anaesthetised in an induction chamber with halothane prior to the removal of the tail tip (approximately 5mm). Collected tail tips were stored in individually labelled 1.5ml Eppendorf tubes and stored at -20°C. Using a water bath, tail tips were incubated overnight at 55°C in an extraction buffer (500µl/tube) containing: 1% sodium dodecyl sulphate (SDS), 0.3M sodium acetate, 10mM Tris-HCl (pH 7.9), 1mM ethylenediaminetetraacetic acid (EDTA) and 200µg/ml Proteinase K (Helena Biosciences, UK). Tail tips were then frozen for 30 min (-20°C) and spun for 15 min at 13,000rpm and 4°C. The supernatant was removed and placed in fresh tube. Tissue pellets were frozen for later use. Added to the supernatant was 40µl 3M sodium acetate (pH 7) and 400µl isopropanol (BDH, UK). Tubes were

inverted several times and spun for 30s (13,000rpm) to precipitate the DNA before removing the supernatant. The DNA pellets were allowed to air dry for 10 min and resuspended in 200µl/tube Tris/EDTA buffer (1mM EDTA, 10mM Tris, pH 7.4) prior to storage at -20°C. Unless otherwise stated all chemicals and reagents came from Sigma, UK.

**Polymerase Chain Reaction**

Mice were tested for the inheritance of the transgene, enhanced green fluorescent protein (EGFP), using the primers, EGFP for: 5'-GAG GGC GAT GCC ACC TAC GGC AAG-3' and EGFP rev: 5'-CTC AGG GCG GAC TGG GTG CTC AGG-3'. A reaction mixture containing: 2.5µl reaction buffer (10x), 1.5µl $MgCl_2$ (25mM), 0.5µl dNTP's (10mM), 0.25µl forward primer (20µM), 0.25µl reverse primer (20µM), 18.5µl $H_2O$, 0.5µl Taq Polymerase and 1µl DNA sample was added to each 200µl dome-capped microtube. Sample DNA was replaced with equivalent sterile water to provide a control, whilst wild-type mouse DNA was used as a negative control and for EGFP, plasmid containing the EGFP gene was used as a positive control. Microtubes were loaded into a thermocycler (Mastercycler gradient, Eppendorf, Germany) and set with the following program:

| | Temperature (°C) | Duration |
|---|---|---|
| 1 | 95 | 5 min |
| 2 | 95 | 30 s |
| 3 | 60 | 30 s |
| 4 | 72 | 50 s |

| | | |
|---|---|---|
| 5 | Go to step 2 34x | |
| 6 | 72 | 10 min |
| 7 | 4 | 15+ min |

A loading dye (6µl) was added to samples which were run in a 1% agarose/Tris-Borate-EDTA buffer (TBE) gel containing 4µl ethidium bromide (10mg/ml) per 100ml alongside a 1Kb ladder. The agarose gel was immersed in a TBE containing gel runner prior to sample loading. Gels were run for 30-40 minutes at 130V and visualised using a UV transilluminator. Images were captured using a camera equipped PC.

**Electrophysiology**

Electrophysiological studies were conducted on DRG which were either acutely dissociated or maintained in short term culture for one–three days.

**Dissection and recovery of DRG neurones**

Adapted from Rau et al., (2005), adult mouse DRG neurones were dissociated to provide a monolayer for electrophysiological study using the following method. Adult *thy1.2-eGFP* mice (SA36 strain) were deeply anaesthetised with halothane and rapidly decapitated.

**Acute dissociation protocol**

The physiological properties of DRG neurones from Thy1.2-mGFP (SA36 strain) mice were investigated using the whole cell patch clamp technique. Adult DRG neurones were acutely dissociated to provide a monolayer of cells suitable for whole cell patch-clamping whilst limiting changes in their phenotype induced by culturing. Schoenen (1989) showed adult DRG neurones can change their expression of neurotransmitters when cultured. Acutely dissociated neurones were patched 2-9 hours post plating.

The vertebral column was dissected from the animal and placed in to a beaker of ice cold extracellular solution containing (in mM): 142 NaCl, 2.5 KCl, 2 $CaCl_2$, 1 $MgCl_2.6H_2O$, 5 HEPES, 10 D-glucose and pH 7.4 with 1M NaOH. The vertebral column was then transferred to a bath where the DRGs from all levels were removed underflow (extracellular solution) with the aid of a dissecting microscope. DRG were collected into a glass vial containing 5mls chilled extracellular solution. Collagenase (2mg/ml) and dispase (5mg/ml) were added prior to 70 min incubation at 35°C in a water bath. The enzymes were aspirated off and DRGs washed 3 times in extracellular solution before resuspending in 1ml extracellular solution. A fire polished Pasteur pipette was used to dissociate DRGs through open end trituration and the cell suspension was plated onto poly-D-lysine coated 35mm glass bottom microwell dish (MaTech, USA). Cells were left for two hours at room temperature to adhere before use.

**Cultured DRG neurones protocol**

The soma diameters of acutely dissociated mGFP-expressing DRG neurones were found to be larger than expected when measured using a calibrated eyepiece graticule. A possible bias towards larger cells due to loss of unadhered small neurones was considered. Neurones were short term cultured (<72 hours) to verify that small diameter neuronal bodies were not being lost due to the shorter time cells had to settle when acutely dissociated. A defined, NGF free culture protocol was used (Brewer et al., 1993). Most neonatal DRG neurones express the tyrosine kinase receptor, Trk A and are dependent on nerve growth factor for their survival (Molliver et al., 1997). During postnatal maturation, approximately half of this NGF-dependent population stops expressing Trk A and switches dependence for survival to glial cell derived neurotrophic factor (GDNF) through the expression of the c-RET receptor and associated GFRα coreceptors (Luo et al., 2007; Molliver et al., 1997; Zhu et al., 2004). Adult sensory neurones are not dependent on NGF for survival but are sensitised by it following postnatal period P4-10 (Zhu et al., 2004).

The vertebral column was blunt dissected from the animal and placed in to a beaker of ice cold artificial cerebrospinal fluid (aCSF) solution containing (in mM): 120 NaCl, 2.1 KCl, 2.4 $CaCl_2$, 1.3 $MgSO_4.7H_2O$, 0.1 $KH_2PO_4$, 25 $NaHCO_3$, 10 D-glucose, 0.028 phenol red and gassed with 95% $O_2$/5% $CO_2$. The vertebral column was then transferred to a bath continuously perfused with

ice cold aCSF where the DRGs from all levels were removed with the aid of a dissecting microscope. DRGs were collected into a glass vial containing 5ml chilled, sterile HBSS-HEPES solution (HBSS containing 10mM HEPES, the pH of which was adjusted to7.4 with 1M NaOH). Collagenase (2mg/ml) and dispase (5mg/ml) were added prior to 70 min incubation at 35°C in a water bath. DRG were then washed 3x with sterile HBSS-HEPES solution to remove the enzymes and once with plating media (PM; 15ml Neurobasal-A, 150µl Glutamax-1, 250µl B27 supplement, 100µl penicillin/streptomycin/amphotericin B) before the DRG were dissociated in 1ml PM by open end trituration. The cell suspension was made up to 10ml with PM and 2ml was added to each 35mm tissue culture dish containing poly-D-lysine (100µg/ml) coated glass shards. The cells were then incubated at 37°C & 5% $CO_2$. Cells were used 20-72 hours post plating.

**Electrophysiological configurations**

The electrophysiological properties of DRG neurones were examined using the whole cell patch clamp technique (Hamill et al., 1981). Cells were identified as eGFP positive or negative depending on the presence of fluorescence when observed using an epifluorescence equipped inverted Nikon Diaphot microscope (Nikon, Japan). A calibrated eyepiece graticule was used to measure soma diameter. Pipettes pulled from thick walled borosilicate glass capillaries (GC150F-10, Harvard Apparatus, UK) using a micropipette puller

(Flaming/Brown P-87, Sutter; Narishige PP-83, Narishige, Japan) were filled with an intracellular solution containing (mM): 142 potassium gluconate, 1 $CaCl_2$, 2 $MgCl_2.6H_2O$, 10 HEPES, 11 EGTA and pH 7.4 using 1M KOH. Pipette resistances were 4-7MΩ. Acutely dissociated DRG neurones adhered to poly-D-lysine coated glass bottom microwell dishes (35mm, MaTech, USA) or poly-D-lysine coated (100μg/ml) glass shards were superfused with a standard extracellular solution (in mM: 142 NaCl, 2.5 KCl, 2 $CaCl_2$, 1 $MgCl_2.6H_2O$, 5 HEPES, 10 D-glucose and pH 7.4 with 1M NaOH) under gravity. Whole cell patched, acutely dissociated DRG neurones were current clamped under flow and held at -60mV using the DC current command on an Axoclamp 2A (Axon Instruments, USA) amplifier. Current pulses (0.01-1.5nA) of varying duration (0.002-2s) were generated using Spike2.5.14 (CED, UK) software. Pulse magnitude and polarity were controlled with the "step command" setting on the amplifier. Recordings were acquired at 5 KHz and filtered at 30 KHz (approximately equivalent to sampling at 3.5 KHz). Data was logged to a PC via a Micro1401 A/D converter using Spike2.5.14. To repeat these experiments in cultured DRG neurones, cells were current clamped and stimulated as described. To allow more detailed measurements, recordings were acquired at 10 KHz and filtered at 3 KHz. Data was logged to a PC via a Micro1401 A/D converter using Spike2.5.14.

**Voltage clamp protocol for M-current investigation in cultured DRG neurones**

Tissue culture dishes (35mm) containing 6-8 glass shards were rinsed with extracellular solution to remove unbound debris prior to electrophysiological investigation. A single glass shard was placed in the bath and superfused with extracellular solution. Extracellular solution contained 1mM CsCl to prevent contamination of records by the hyperpolarisation-activated current, $I_h$ (Passmore et al., 2003). Where drugs were used, shards were disposed of after a single exposure and the bath was rinsed before another shard was placed in it. Pipettes pulled from thick walled borosilicate glass capillaries (GC150F-10, Harvard Apparatus, UK) using a micropipette puller (Narishige PP-83, Narishige, Japan) were filled with an intracellular solution containing (mM): 142 potassium gluconate, 1 $CaCl_2$, 2 $MgCl_2.6H_2O$, 10 HEPES, 11 EGTA and pH 7.4 using 1M KOH. Pipette resistances were 4-7MΩ. A standard deactivation protocol was used to isolate the M-current from other voltage-activated currents (Brown and Adams, 1980; Passmore et al., 2003). Whole cell patched DRG neurones were voltage clamped at -20mV and hyperpolarised in 10mV steps for 1s before returning to -20mV. This was repeated every 10s to give a range of -30mV to -110mV. Series resistance was compensated 60-90% using a Cairn Optopatch amplifier (Cairn Research, UK). Drugs from solenoid controlled reservoirs were bath applied for 5mins before repeating the protocol. Data was acquired at 20 KHz and filtered at 5 KHz. Data was logged to PC via a

micro1401 using WCPv3.9.5 software (John Dempster, University of Strathclyde).

For current clamp recordings CsCl was omitted from the extracellular solution. Current pulses (230ms; 0.1-1nA) were generated using Spike2.5.14 software. Data was digitised at 10 KHz and filtered at 5 KHz. The Cairn Optopatch amplifier was used for this series of experiments because it was better suited for voltage clamping than the Axoclamp 2A.

**Data Acquisition and analysis**

Digitised recordings were analysed offline using Spike2.5.14 and WCPv3.9.5. Data values were inputted in to Microsoft Excel spreadsheets and analysed using the statistical tools it contains or exported to either Prism Graphpad 3 (Prism Software) or SPSS.

**Immunohistochemistry**

**Perfusion of animals**

Adult transgenic mice (Thy1.2-EGFP; SA36 strain) were anaesthetised with halothane prior to euthanizing by an intra peritoneal injection of a lethal dose (80mg/kg) of sodium pentobarbitone. The superior vena cava was transected and an ACSF perfusate was introduced into the left ventricle through a

hypodermic needle under gravity to remove the blood from the cardiovascular system. This was followed by a 4% paraformaldehyde solution (PFA) to "fix" the animal before the removal of the vertebral column.

**Tissue preparation for sectioning**

The tissue was post-fixed in 4% PFA solution for 1 hour then placed in 30% sucrose solution for cryoprotection and storage. Dorsal root ganglia were micro-surgically removed under a dissecting microscope. The dissected tissue was placed in to 30% sucrose (30% sucrose in 0.1M PBS) for storage. DRG were mounted in Optimal cutting temperature (OCT, RA Lamb, USA) embedding agent and frozen using liquid nitrogen cooled isopentane then stored at -20°C.

**Immunohistochemical staining of tissue sections and cell culture**

Tissues for sectioning were dried of excess sucrose solution and frozen into blocks with OCT embedding media. Sections were cut at appropriate thicknesses on a cryostat (DRG 12μm, spinal cord and skin 30μm) or freezing knife microtome (spinal cord and skin 40μm). Cryostat sections were collected onto chrome-alum gelatine (CAG) coated slides and stored at -20°C (Appendix I). Freezing knife microtome sections were collected into tubes containing 0.1M PBS for processing as free floating sections. Sections were washed with PBS then permeabilised with Triton X solution (10min, 0.4% for DRG, 2% for spinal

cord and skin). After further washes tissue was incubated for 1 hour with 5% NDS before addition of the primary antibody (dilutions given in Appendix II) and incubated at 4°C overnight. This incubation period was extended to 36 hours for some antibodies to optimise specific binding. Tissue sections were washed repeatedly to remove unbound primary antibody before overnight incubation in Cy3-conjugated secondary antibody at 4°C. Unbound secondary antibody was washed off sections prior to mounting slides. DAPI (300nM, 5min) was used to mark the nuclei in some sections. Free floating sections were mounted onto CAG-coated slides and all slides rinsed with distilled water to remove salt residues prior to coverslipping with Vectashield mounting medium (Vector Laboratories, CA, USA).

Cultured DRG neurones were grown on poly-D-lysine coated eight-well culture slides for 48 hours (37°C, 5% $CO_2$). Cells were fixed with 4% PFA for 10 min then rinsed with 0.1M PBS. Immunohistochemistry was performed as described for other tissues with minor adaptations to accommodate for the wells (Appendix III). After the final antibody incubation and washes the wells were removed. The excess adhesive was carefully scraped away and a coverslip mounted using Vectashield mounting medium (Vector Laboratories, CA, USA).

Sections were visualised using epifluorescent microscopy (see Appendix V for excitation-emission spectra for fluophores) and images were captured to PC using Metavue software via a monochrome digital camera. Images were

calibrated using a stage micrometer imaged at the same magnification. Tiff files were analysed using the Metamorph software. DRG cells showing clear, specific staining with intact unstained nuclei were selected from sections taken at 60μm intervals. The diameter and surface area measurements of manually thresholded cells were calculated by the software. Cell measurements were logged to Microsoft Excel and statistical analysis was performed with Prism 3 Graphpad.

# Chapter 3

## IMMUNOHISTOCHEMICAL INVESTIGATION OF CHANNELS AND RECEPTORS EXPRESSED BY LABELLED DRG NEURONES FROM THE *THY1.2-EGFP* (SA36) MOUSE

## Introduction

The DRGs contain a heterogeneous population of neurones which vary in diameter and express a diverse collection of proteins in the form of ion channels, receptors and enzymes. They can be preferentially identified by immunohistochemistry and subpopulations identified by their selective expression of a specific ion channel, receptor or surface antigen (Jessell and Dodd, 1985). Using antibodies raised against amino acid sequences specific to a given peptide, labelling of that peptide within sections of tissue can be achieved with high specificity (Cuello et al., 1983). Separation of neurones from other cell types within DRG such as glia is possible using pan-neuronal markers which bind to moieties common to neurones but not found elsewhere (Mullen et al., 1992; Schmechel et al., 1978; Thompson et al., 1983). Protein gene product 9.5 (PGP9.5; Thompson et al., 1983) and neuron nuclei (NeuN; Mullen et al., 1992) are two commonly used marker proteins. Neurones within the DRG vary in their degree of myelination and can be differentiated accordingly (Yoshida & Matsuda, 1979). Antibodies against neurofilament and peripherin label "large light" and "small dark" DRG neurones respectively (Goldstein et al., 1991; Lawson, 1979). Peripherin-labelled DRG neurones have unmyelinated axons whilst large, neurofilament-labelled cells have thickly myelinated axons (Goldstein et al., 1991). The degree of axonal myelination is positively correlated to axonal conduction velocity (Gallego & Eyzaguirre, 1978).

Studies have revealed great diversity in the proteins expressed in small-diameter DRG neurones. Many synthesise and secrete neuropeptides such as CGRP, substance P and somatostatin (reviewed by Hunt & Rossi, 1985). A population of DRG neurones does not express these neuropeptides but are identifiable by their selective expression of a fluoride-resistant acid phosphatase (FRAP) (Nagy & Hunt, 1982). A plant lectin from *Griffonia simplicifolia* ($IB_4$) binds to the α-D-galactose in some glycoproteins and glycolipids present in the FRAP-population of unmyelinated neurones (Streit et al., 1985). Hunt and Rossi (1985) described those neurones expressing substance P, CGRP and somatostatin as "peptidergic" and those expressing FRAP as "non-peptidergic". Expression of ion channels and receptors within these divisions of DRG neurone varies posing the complication of subdivisions defined by their ion channel/receptor expression partially overlapping with multiple subpopulations of DRG neurone. Further complication arises from potential interspecies differences in the expression of recently identified populations thus far described in a single animal. One example is the localisation of $TRPV_1$ in both "peptidergic" and "non-peptidergic" DRG neurones in rats (Guo et al., 1999) but almost complete absence from the "non-peptidergic" DRG neurones in mice (Zwick et al., 2002).

This difference between the two species has yet to be explained but Price and Flores (2007) postulated that the overlap may be due to an increase in $IB_4$-binding capacity in rat sensory neurones. A possible explanation may lie in the developmental regulation of DRG neurones. Almost all DRG neurones express

receptor tyrosine kinase A (TrkA) and are dependent on nerve growth factor (NGF) for survival during embryonic development (Johnson et al., 1980). Starting at embryonic day 15.5 some of the TrkA population begins expressing the "rearranged during transfection" (Ret) receptor tyrosine kinase (Molliver et al., 1997). Approximately half the embryonic TrkA population has ceased expressing TrkA and switched to Ret expression by postnatal day 21 (Molliver and Snider, 1997; Molliver et al., 1997). Neurotrophic factors have numerous important roles in the survival and axonal targeting of afferents and serve defined populations of neurone (Albers and Davis, 2007).

Two ion channels implicated in somatotransduction and nociception are $TRPV_1$ and the $P2X_3$ subunit (Lumpkin and Caterina, 2007). The $P2X_3$ subunit belongs to a family of ATP-gated ion channels (Chen et al., 1995) and is highly expressed in a population of epidermal primary afferent fibres (Zylka et al., 2005). Immunohistochemical staining for this subunit has been described in "peptidergic" and "non-peptidergic" DRG neurones in rats (Bradbury et al., 1998) where it is largely colocalised with $TRPV_1$ (Guo et al., 1999). Glial cell line-derived neurotrophic factor (GDNF) signals through Ret (Durbec et al., 1996; Trupp et al., 1996) by binding to a coreceptor (Jing et al., 1996). The coreceptor belongs to a family called GDNF family receptor-α (GFRα) receptors which determine ligand specificity (Airaksinen and Saarma, 2002). The GDNF family ligand (GFL) neurturin binds to GFRα2 (Buj-Bello et al., 1997; Klein et

al., 1997) and is necessary for the termination of "non-peptidergic" afferents in the epidermis (Lindfors et al., 2006).

The purpose of this part of the study was to investigate the channels and receptors expressed by the transgene labelled (eGFP+ve) population of DRG neurones in the thy1.2-egfp (SA36) mouse using immunohistochemistry. Observations on the anatomical localisation of immunoreactivity (-ir) for antibody markers in relation to eGFP expression were also made. Profiles were classified by cross-sectional area as small- (<450 $\mu m^2$), medium- (450-850 $\mu m^2$) and large-sized (>850 $\mu m^2$) in accordance with the study by Lawson (1979) on DRG postnatal development (Belle et al., 2007).

## Results

*Localisation and quantification of $P2X_3$-ir in relation to eGFP in the DRG and DH of the thy1.2-egfp (SA36) mouse*

Measurements of eGFP+ve profiles (n=737) gave a mean cross-sectional area (CSA) of 509.9 ± 7.3 $\mu m^2$ (mean ± SEM). Whilst eGFP was observed in neurones of all sizes (range 174.9-1864.3 $\mu m^2$, median 472.9 $\mu m^2$), most profiles were within the small- and medium-sized populations (Fig.. 3.1). Slightly more $P2X_3$-ir profiles were observed (n=800) which were on average smaller (CSA 444 ± 4.4$\mu m^2$) ranging in CSA from 174.9 $\mu m^2$ to 1116.3 $\mu m^2$ (median 437.8 $\mu m^2$) (Fig. 3.1). Extensive colocalisation of $P2X_3$-ir was observed in eGFP +ve DRG neurones (85.1%, n=627/737 cells) (Fig. 3.2 & Fig. 3.3C). Of the $P2X_3$-ir population, 78.4% expressed eGFP. Colocalised profiles were of small- to medium-size (CSA 463 ± 4.5 $\mu m^2$) with few possessing a CSA larger than 850 $\mu m^2$ (Fig. 3.2). The eGFP+ve population in which $P2X_3$-ir was absent ($P2X_3$-ve) were on average larger in CSA (772 ± 32 $\mu m^2$, n=110) and widely distributed (median 720.4 $\mu m^2$, 25th-75th percentile 507.6-909.5 $\mu m^2$) (Fig. 3.2). Those $P2X_3$-ir profiles which were not colocalised with eGFP (eGFP-ve) formed a population consisting mostly of small-sized neurones (median 352.5 $\mu m^2$, 25th-75th percentile 277.5-431.5 $\mu m^2$) with a CSA of 373.1 ± 10.9 $\mu m^2$ (n=173) (Fig. 3.2). In DRG sections, intense P2X3-ir was observed in many small- and

medium-sized profiles and extensively colocalised with eGFP+ve cells (Fig. 3.3B, C). Weak $P2X_3$-ir was detected in the superficial laminae of the DH and predominately colocalised with eGFP terminals in lamina $II_i$ (Vulchanova et al., 1998) (Fig. 3.4B,C).

**Figure 3.1. Distribution of eGFP+ve and $P2X_3$-ir single label profiles by size**

Frequency distribution graph of eGFP+ve (white bars, n=737) and $P2X_3$-ir (black bars, n=800) by size. Single label profiles for eGFP+ve (median 472.9 $\mu m^2$, 25th-75th percentile 397.9-560.4 $\mu m^2$) and $P2X_3$-ir (median 437.8 $\mu m^2$, 25th-75th percentile 362.2-514.4 $\mu m^2$) displayed similar size distributions. Neurones expressing eGFP (509.9 ± 7.3 $\mu m^2$) were on average larger than those with $P2X_3$-ir (444 ± 4.4 $\mu m^2$). Most profiles were small to medium in diameter (CSA <850 $\mu m^2$).

**Figure 3.1.**

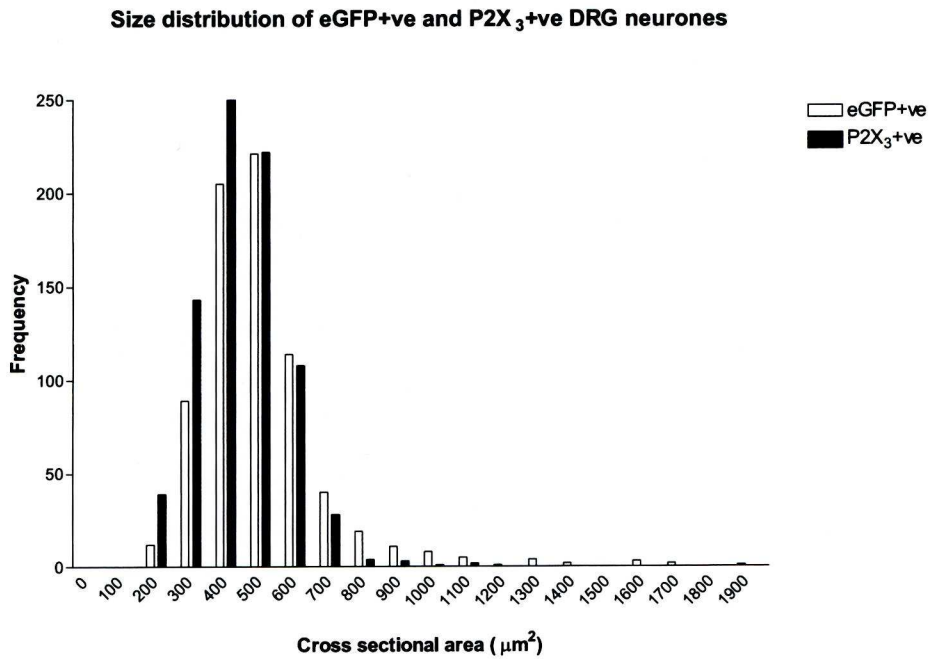
Size distribution of eGFP+ve and P2X3+ve DRG neurones
eGFP+ve
P2X3+ve
Frequency
250
200
150
100
50
0
0
100
200
300
400
500
600
700
800
900
1000
1100
1200
1300
1400
1500
1600
1700
1800
1900
Cross sectional area (μm2)

**Figure 3.2. Distribution of eGFP+ve and $P2X_3$-ir single and double label profiles by size**

This graph shows the frequency distribution of colocalised (double labelled) and single labelled profiles for $P2X_3$-ir in the *thy1.2-egfp* (SA36) mouse. Colocalised profiles (grey bars, n=627) were mostly small- and medium-sized cells (CSA <850 $\mu m^2$). Those neurones expressing eGFP only were predominantly medium- and large-sized cells (CSA >450 $\mu m^2$) whilst profiles solely $P2X_3$-ir formed a population of small-sized cells (CSA <450 $\mu m^2$).

**Figure 3.2.**

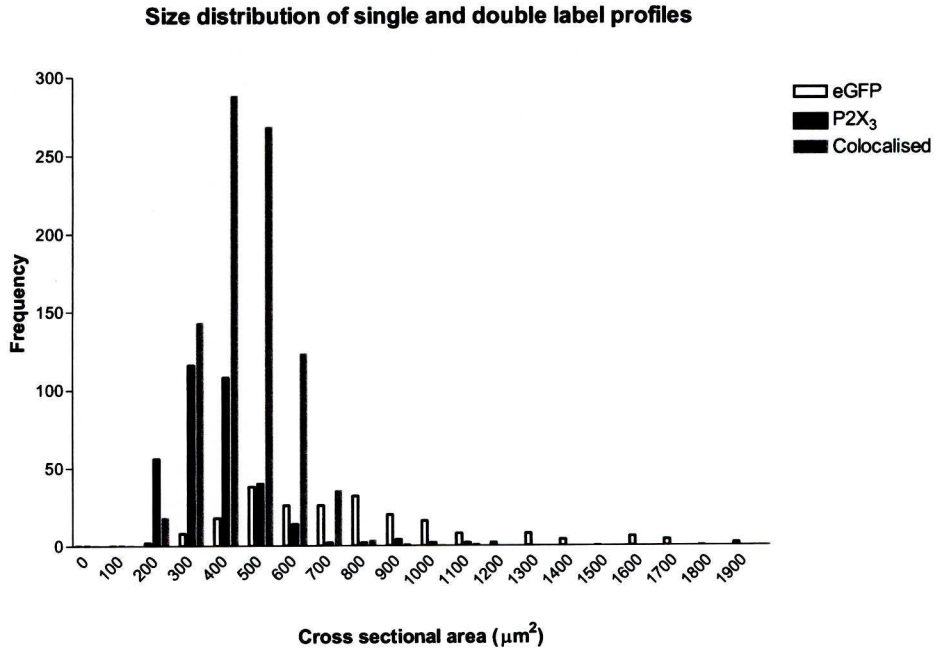
Size distribution of single and double label profiles
eGFP
P2X3
Colocalised
Frequency
300
250
200
150
100
50
0
0
100
200
300
400
500
600
700
800
900
1000
1100
1200
1300
1400
1500
1600
1700
1800
1900
Cross sectional area (μm2)

**Figure 3.3. Localisation of $P2X_3$-ir in DRG neurones from the *thy1.2-egfp* (SA36) mouse**

A) Fluoresence from eGFP+ve neurones was sufficiently robust enough to allow direct visualisation the soma using epifluorescent microscopy. Small- and medium-sized profiles were more intensely labelled than large-sized profiles.

B) $P2X_3$-ir was observed in small- and medium-sized profiles and rarely in the large-sized population. Cells were labelled using a Cy3-conjugated secondary antibody.

C) Of the eGFP+ve (green) population, 85.1% were also $P2X_3$-ir (long arrowhead). Colocalised profiles appear yellow. A subpopulation of $P2X_3$-ir (red) neurones lacking eGFP was also present (thick arrow). Some medium-sized and most large-sized eGFP+ve profiles lacked immunoreactivity for $P2X_3$ (short arrowhead). Section thickness 12 μm, magnification x200, scale bar 100 μm.

**Figure 3.3**

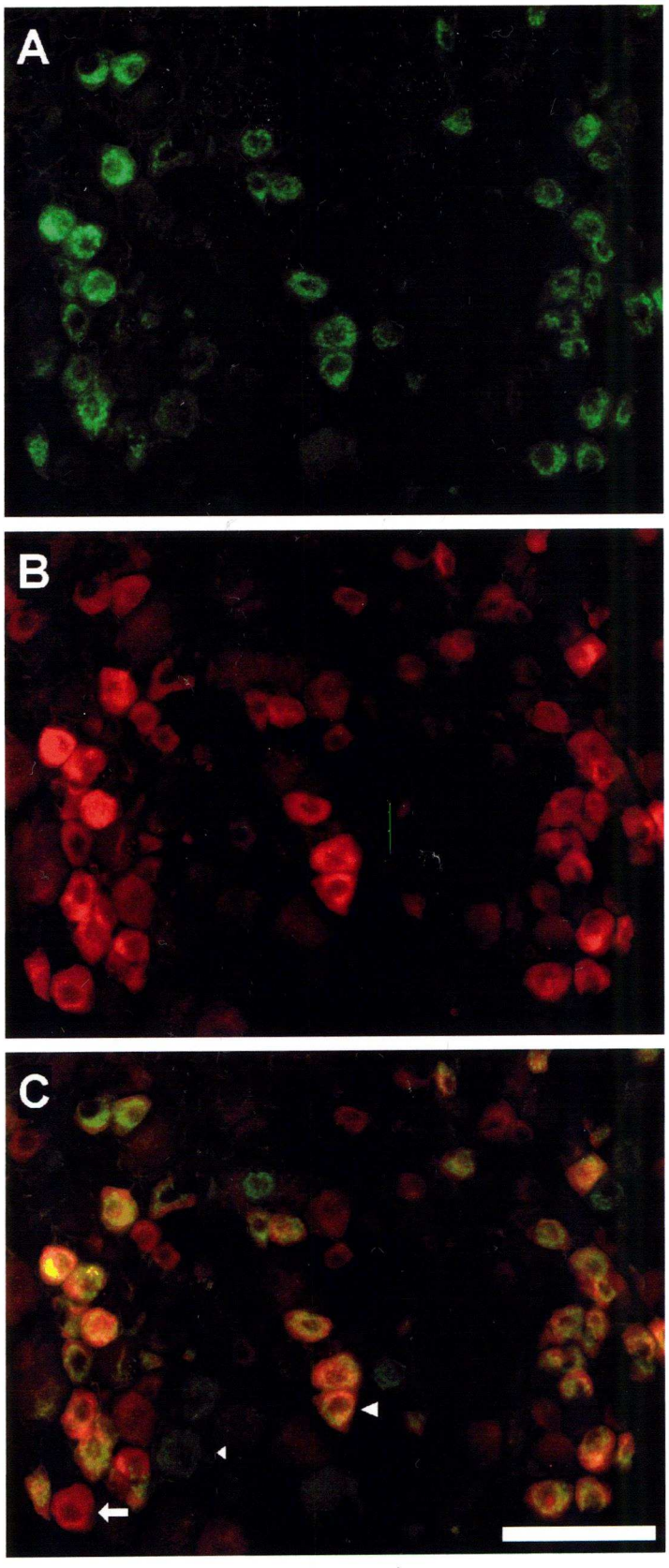

**Figure 3.4. Localisation of P2X3-ir in the dorsal horn of the thy1.2-egfp (SA36) mouse**

A) The central terminations eGFP+ve afferents clearly delineate $LII_{i/o}$ of the dorsal horn.

B) Weak P2X3-ir was observed throughout $LII_{i/o}$ and in the medial part of LI. Arrowheads denote the LII/LIII boundary. A Cy3-conjugated secondary antibody was used.

C) The central terminations of eGFP neurones (green) and P2X3-ir neurones (red/arrowheads) colocalise in $LII_i$ (yellow). There is no colocalisation of P2X3-ir with eGFP terminals in LI. Section thickness 40 μm, magnification x200, scale bar 100 μm.

**Figure 3.4.**

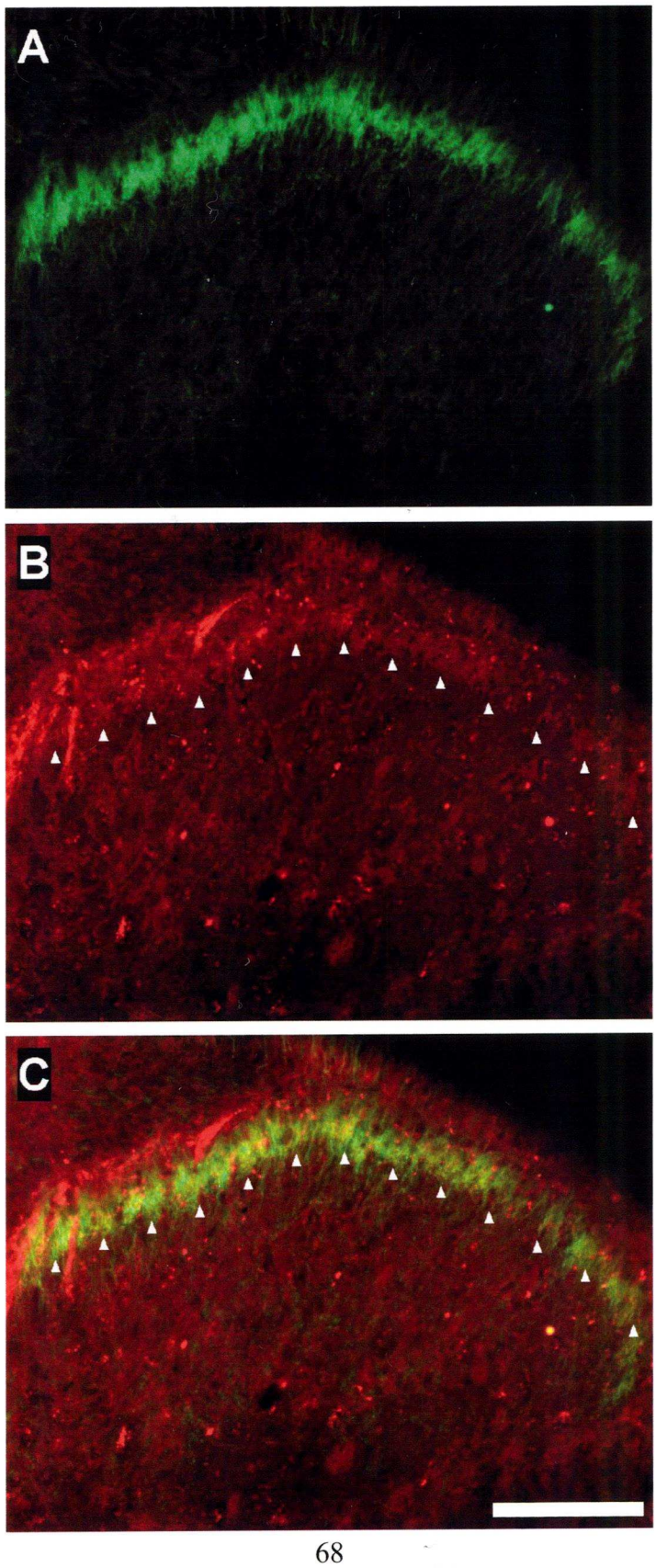

*Localisation and quantification of $TRPV_1$-ir in relation to eGFP in the DRG and DH of the thy1.2-egfp (SA36) mouse*

$TRPV_1$ immunoreactivity ($TRPV_1$-ir) and eGFP expression marked two distinct and separate populations of DRG neurone (Fig. 3.6 & Fig. 3.7C). Profiles showing $TRPV_1$-ir belonged to a population smaller (CSA 358.1 ± 15.7 $\mu m^2$, n=179) than the eGFP+ve population (CSA 543.6 ± 8 $\mu m^2$, n=557) and were less abundant (Fig. 3.5 & Fig. 3.6). Only 1.62% of eGFP+ve profiles colocalised with $TRPV_1$-ir which formed a subpopulation of medium- and large-sized neurones (CSA 734.7 ± 114.4 $\mu m^2$, n=9). Single-labelled eGFP+ve profiles (n=548) were comprised of mostly small- and medium-sized cells (median 518.9 $\mu m^2$, 25th-75th percentile 425.7-622.3 $\mu m^2$) (Fig. 3.6). The $TRPV_1$-ir single-labelled population contained mainly small-sized cells (median 292.2 $\mu m^2$, 25th-75th percentile 204.1-434 $\mu m^2$) with a mean CSA of 338.2 $\mu m^2$ (Fig. 3.6). In the DRG, $TRPV_1$-ir was confined to a subpopulation of small-sized neurones which did not colocalise with eGFP+ve profiles (Fig. 3.7B, C). This segregation of eGFP+ve and $TRPV_1$-ir populations was reflected by the distribution of $TRPV_1$-ir in the DH which was clearly present in LI (Fig. 3.8B, C).

**Figure 3.5. Distribution of eGFP+ve and $TRPV_1$-ir single label profiles by size**

Frequency distribution graph of eGFP+ve (white bars, n=557) and TRPV1-ir (black bars, n=179) by cross-sectional area. Single label profiles with TRPV1-ir formed a population of small- and medium-sized neurones (median 304.4 $\mu m^2$, 25th-75th percentile 206.7-461.4 $\mu m^2$) with a distribution which overlapped that of eGFP+ve profiles. eGFP+ve profiles were on average larger (eGFP+ve CSA 543.6 $\mu m^2$, $TRPV_1$-ir CSA 358.1 $\mu m^2$) with a distribution indicating a greater prevalence of medium-sized profiles (median 521.1 $\mu m^2$, 25th-75th percentile 425.9-625.3 $\mu m^2$).

**Figure 3.5.**

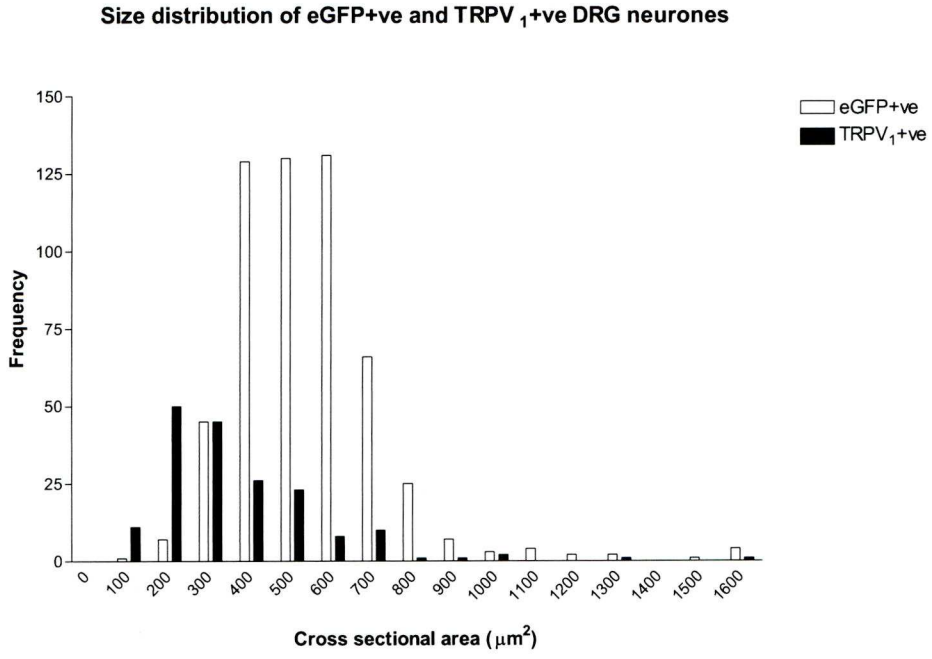
Size distribution of eGFP+ve and TRPV 1+ve DRG neurones
eGFP+ve
TRPV1+ve
Frequency
150
125
100
75
50
25
0
0
100
200
300
400
500
600
700
800
900
1000
1100
1200
1300
1400
1500
1600
Cross sectional area (μm2)

**Figure 3.6. Distribution of eGFP+ve and $TRPV_1$-ir single and double label profiles by size**

This graph shows the frequency distribution of colocalised (double labelled) and single labelled profiles for $TRPV_1$-ir in the *thy1.2-egfp* (SA36) mouse. Profiles labelled with eGFP only (white bars, n=548) were mostly small- and medium-sized with an average CSA of 540.4 ± 7.8 $\mu m^2$. The population labelled with $TRPV_1$-ir only (black bars, n=170) formed a distinct, separate population of predominantly small-sized neurones (CSA 338.2 ± 13.9 $\mu m^2$). The few profiles in which eGFP and $TRPV_1$-ir were colocalised (grey bars, n=9) were mostly medium- and large-sized cells (CSA >450 $\mu m^2$).

**Figure 3.6.**

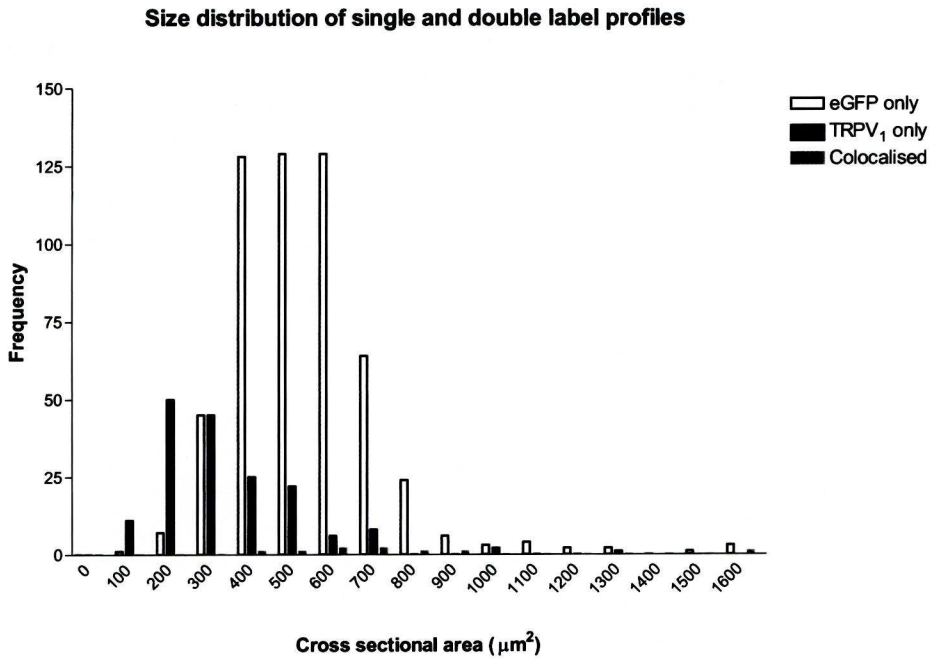
Size distribution of single and double label profiles
eGFP only
TRPV1 only
Colocalised
Frequency
150
125
100
75
50
25
0
0
100
200
300
400
500
600
700
800
900
1000
1100
1200
1300
1400
1500
1600
Cross sectional area (μm2)

**Figure 3.7. Localisation of $TRPV_1$-ir in DRG neurones from the *thy1.2-egfp* (SA36) mouse**

A) Neurones expressing eGFP in the DRG were small- and medium-sized cells.

B) A small population of DRG neurones were labelled $TRPV_1$-ir and had predominately small-sized soma. Cells were labelled using a Cy3-conjugated secondary antibody.

C) There was little (1.62%) colocalisation between TRPV1-ir (red; arrowheads) and eGFP+ve (green; thick arrow) profiles. Section thickness 12 μm, magnification x200, scale bar 100 μm.

**Figure 3.7.**

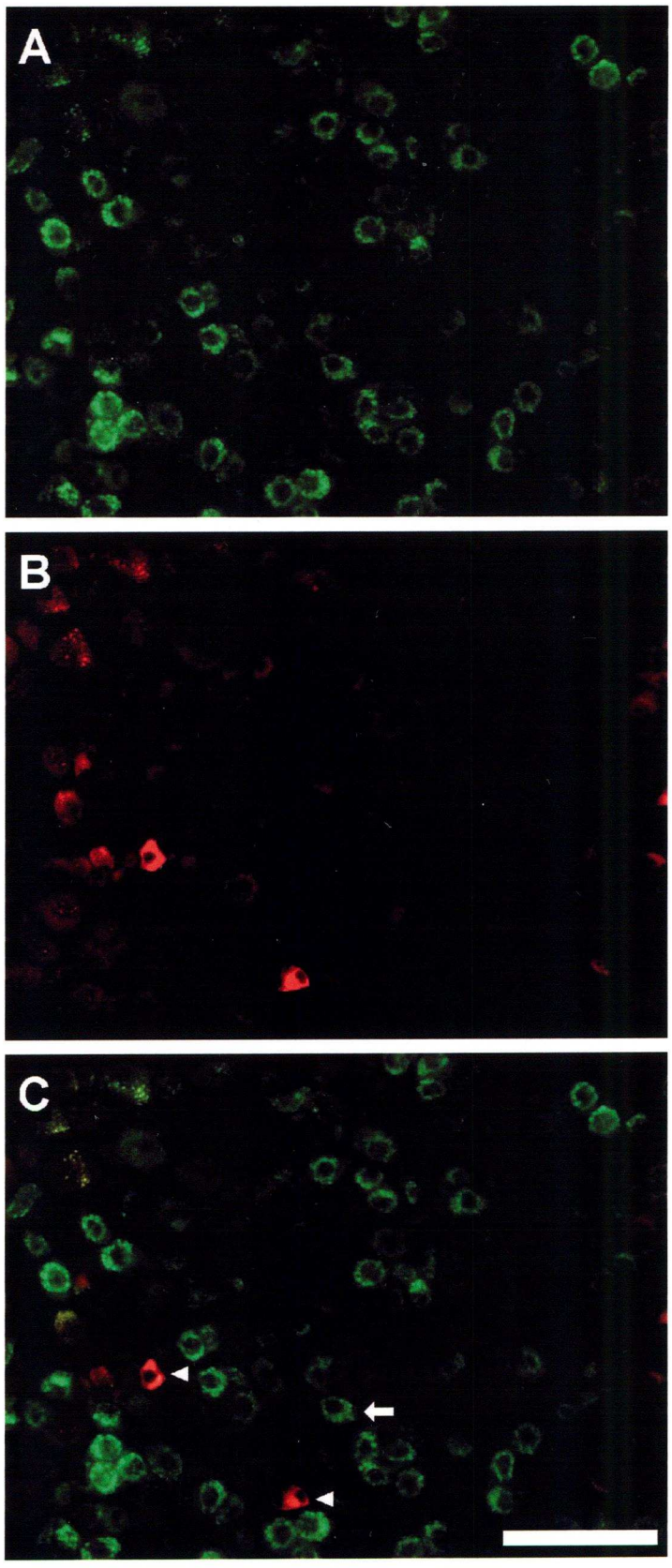

**Figure 3.8. Localisation of $TRPV_1$-ir in the dorsal horn of the *thy1.2-egfp* (SA36) mouse**

A) The central terminations eGFP+ve afferents clearly delineate $LII_{i/o}$ of the dorsal horn.

B) $TRPV_1$-ir was observed in lamina I. A Cy3-conjugated secondary antibody was used.

C) $TRPV_1$-ir (red) and eGFP+ve (green) afferents terminate in LI and $LII_{i/o}$ respectively. Section thickness 40 μm, magnification x200, scale bar 100 μm.

**Figure 3.8.**

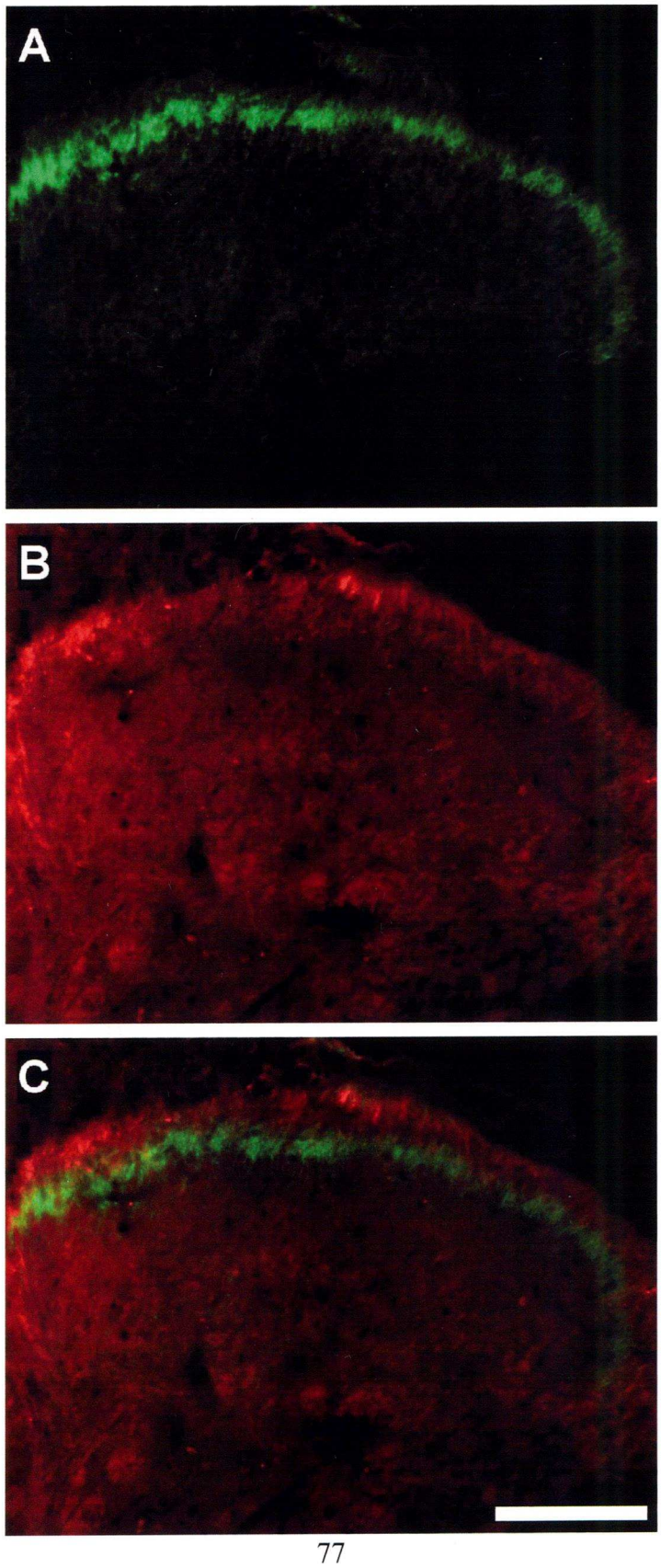

*Localisation and quantification of GFRα2-ir in relation to eGFP in the DRG, DH and skin of the thy1.2-egfp (SA36) mouse*

Profiles expressing eGFP (n=777) had a mean CSA of 559.1 ± 7.4 $\mu m^2$ and consisted of small- and medium-sized cells (median 524.6 $\mu m^2$, 25th-75th percentile 436.3-638.7 $\mu m^2$) with few large-sized cells (Fig. 3.9 & Fig. 3.11A). Forming a larger population, GFRα2-ir profiles (n=982) had a smaller CSA (485.3 ± 5.5 $\mu m^2$) reflecting a higher incidence of small-sized soma (median 464.3 $\mu m^2$, $25^{th}$-$75^{th}$ percentile 379.7-559 $\mu m^2$) (Fig. 3.9 & Fig. 3.11B). Most eGFP+ve cells were also GFRα2-ir (81.9%, n=636/777) (Fig. 3.10 & Fig. 3.11C). Colocalised profiles (CSA 528. 8 ± 6.9 $\mu m^2$) were small- to medium-sized cells (median 511.2 $\mu m^2$, $25^{th}$-$75^{th}$ percentile 425.4-602.3 $\mu m^2$) (Fig3.10). A separate population of small- and medium-sized soma were GFRα2-ir but did not express eGFP (median 399.7 $\mu m^2$, $25^{th}$-$75^{th}$ percentile 329.2-467.1 $\mu m^2$) (Fig. 3.10). These were mostly small-sized cells with a mean CSA of 405.3 ± 7.2 $\mu m^2$ (n=346). The eGFP+ve neurones lacking GFRα2-ir were a small population (n=141) of medium-sized cells (median 641.8 $\mu m^2$, $25^{th}$-$75^{th}$ percentile 487.1-839 $\mu m^2$) (Fig. 3.10).

Sections of DRG showed intense GFRα2-ir in the membranes and fibres of most neurones which clearly demarcated the boundaries of other cells (Fig. 3.11B). Profiles were judged to be GFRα2-ir if they showed staining throughout the soma cytoplasm and were counted if they had a complete nucleus. In large-cells,

soma staining was often less intense than in small- and medium-sized cells but could be distinguished from profiles negative for GFRα2-ir as their soma lacked any staining (Fig. 3.11B). The superficial laminae (LI-III) of the DH showed clear GFRα2-ir with the greatest intensity observed in $LII_{i/o}$ (Fig. 3.12B). This region of intense GFRα2-ir colocalised with the central terminals of eGFP+ve afferents (Fig. 3.12A, C). Immunoreactivity for GFRα2 could also be detected colocalised with the peripheral terminals of eGFP+ve primary afferents in the epidermis (Fig. 3.13A, B, D).

**Figure 3.9. Distribution of eGFP+ve and GFRα2-ir single label profiles by size**

Frequency distribution graph of eGFP+ve (white bars, n=777) and GFRα2-ir (black bars, n=982) by cross-sectional area. Profiles labelled with GFRα2-ir constituted a population of small- and medium-sized cells (median 464.3 $\mu m^2$, $25^{th}$-$75^{th}$ percentile 379.7-559 $\mu m^2$) whose distribution overlapped extensively with that of eGFP+ve profiles (median 524.6 $\mu m^2$, 25th-75th percentile 436.3-638.7 $\mu m^2$) but was shifted leftward indicating a greater prevalence of small-sized cells.

**Figure 3.9.**

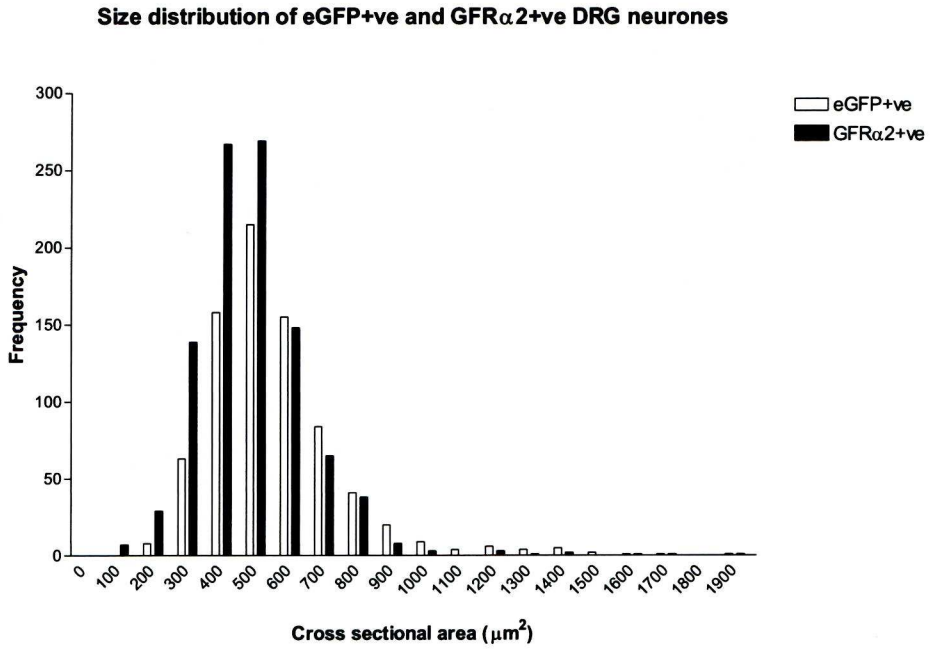
Size distribution of eGFP+ve and GFRα2+ve DRG neurones
eGFP+ve
GFRα2+ve
Frequency
300
250
200
150
100
50
0
0
100
200
300
400
500
600
700
800
900
1000
1100
1200
1300
1400
1500
1600
1700
1800
1900
Cross sectional area (μm²)

**Figure 3.10. Distribution of eGFP+ve and GFRα2-ir single and double label profiles by size**

This graph shows the frequency distribution of colocalised (double labelled) and single labelled profiles for GFRα2-ir in the *thy1.2-egfp* (SA36) mouse. The extensive overlap in the distribution of GFRα2-ir and eGFP+ve profiles seen in Fig. 3.9 was due to the large degree of colocalisation between the markers. When the incidence of double labelling was looked at it was revealed that 81.9% of the eGFP+ve population were also GFRα2-ir (n=636/777). Colocalised profiles (grey bars) were mostly from small- and medium-sized cells (median 511.2 $\mu m^2$, $25^{th}$-$75^{th}$ percentile 425.4-602.3 $\mu m^2$). The remaining eGFP+ve profiles (white bars, n=141) consisted of mainly medium-cells (median 641.8 $\mu m^2$, $25^{th}$-$75^{th}$ percentile 487.1-839 $\mu m^2$). Profiles labelled by GFRα2-ir alone (black bars, n=346) were predominately small-sized with some medium-sized cells (median 399.7 $\mu m^2$, $25^{th}$-$75^{th}$ percentile 329.2-467.1 $\mu m^2$).

**Figure 3.10.**

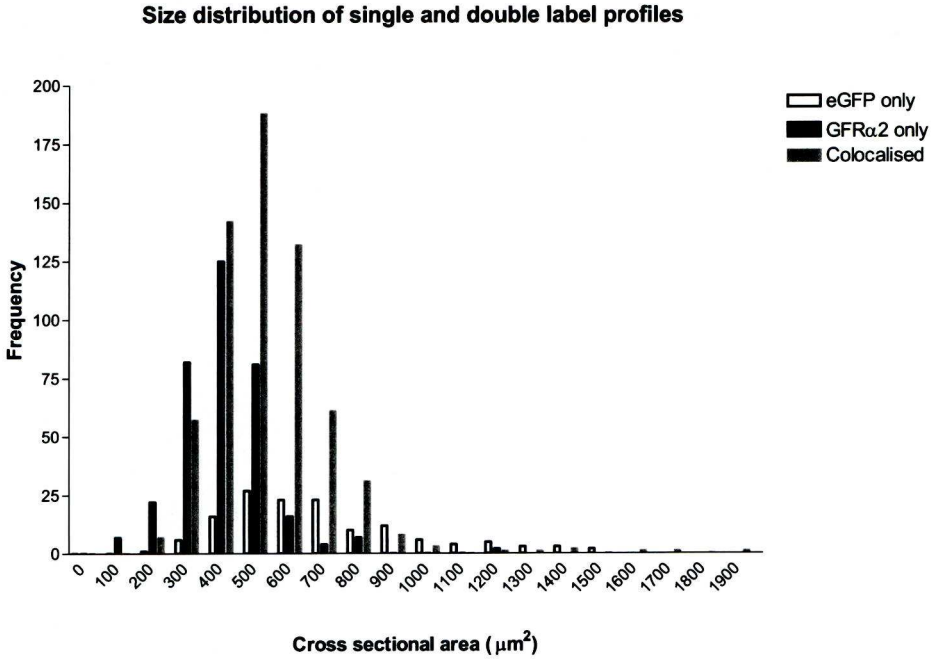
Size distribution of single and double label profiles
eGFP only
GFRα2 only
Colocalised
Frequency
200
175
150
125
100
75
50
25
0
0
100
200
300
400
500
600
700
800
900
1000
1100
1200
1300
1400
1500
1600
1700
1800
1900
Cross sectional area (μm²)

**Figure 3.11. Localisation of GFRα2-ir in DRG neurones from the thy1.2-egfp (SA36) mouse**

A) Direct visualisation of eGFP expressing DRG neurones.

B) GFRα2-ir strongly labelled the membranes and processes of positive cells and consequently marked the boundaries with unlabelled cells. Cells were labelled using a Cy3-conjugated secondary antibody.

C) Most eGFP+ve profiles (green) were also GFRα2-ir (red). Colocalisation appears yellow (short arrowheads). A population of small- and medium-sized GFRα2-ir neurones did not express eGFP (long arrowheads). Neurones expressing eGFP but not GFRα2-ir belonged to a population of mostly medium-sized neurones although some small- (thick arrow) and large-sized neurones also belonged to this group. Section thickness 12 μm, magnification x200, scale bar 100 μm.

**Figure 3.11.**

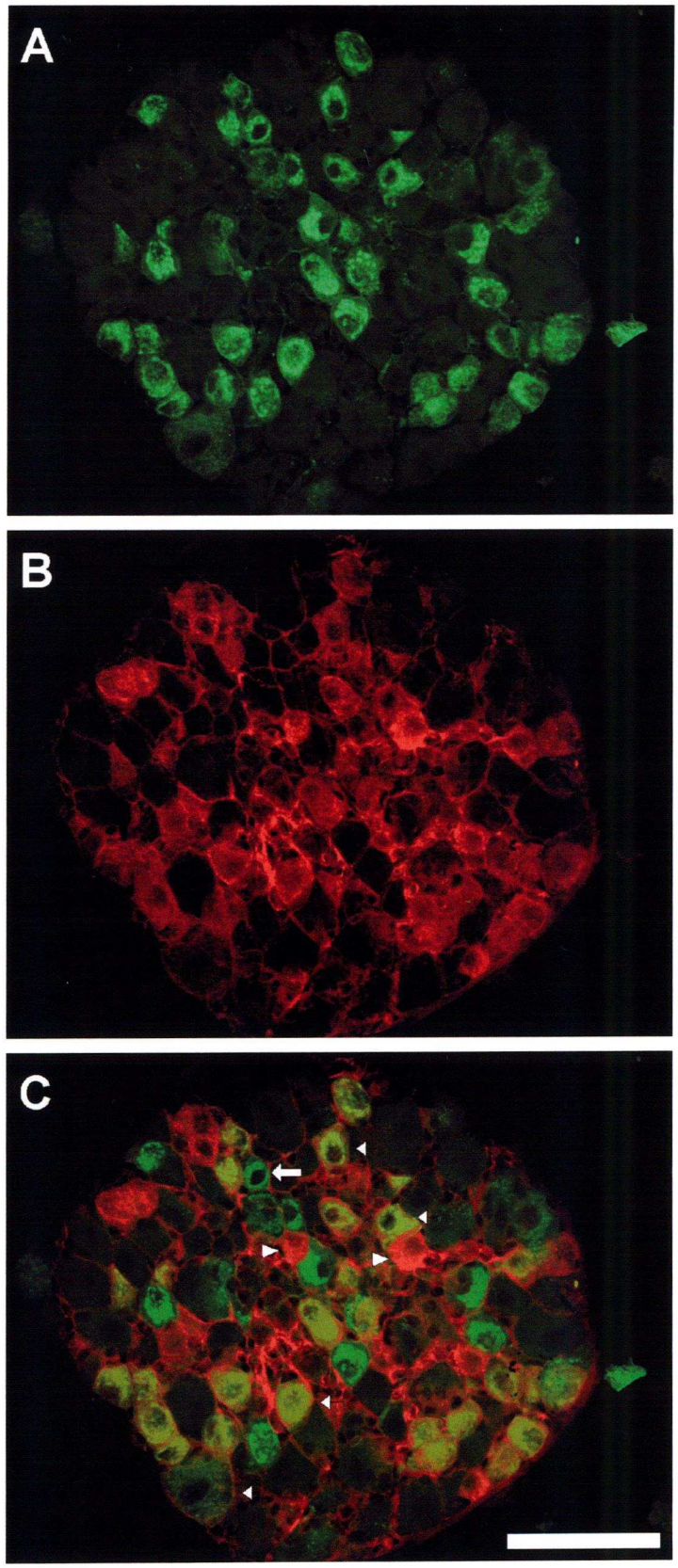

**Figure 3.12. Localisation of GFRα2-ir in the dorsal horn of the *thy1.2-egfp* (SA36) mouse**

A) Lamina $II_{i/o}$ is clearly defined by the central terminals of eGFP expressing primary afferents.

B) GFRα2-ir was observed throughout the superficial laminae (LI-III). Labelling was most intense in $LII_{i/o}$ and LIII. A Cy3-conjugated secondary antibody was used.

C) Fluorescence from eGFP colocalised in lamina $II_{i/o}$ where GFRα2-ir staining was most intense. Lamina III was identified by its ventral proximity to eGFP fluorescence and "lateral bend in the apex" as defined by Rexed (1952). Section thickness 30 μm, magnification x100, scale bar 200 μm.

**Figure 3.12.**

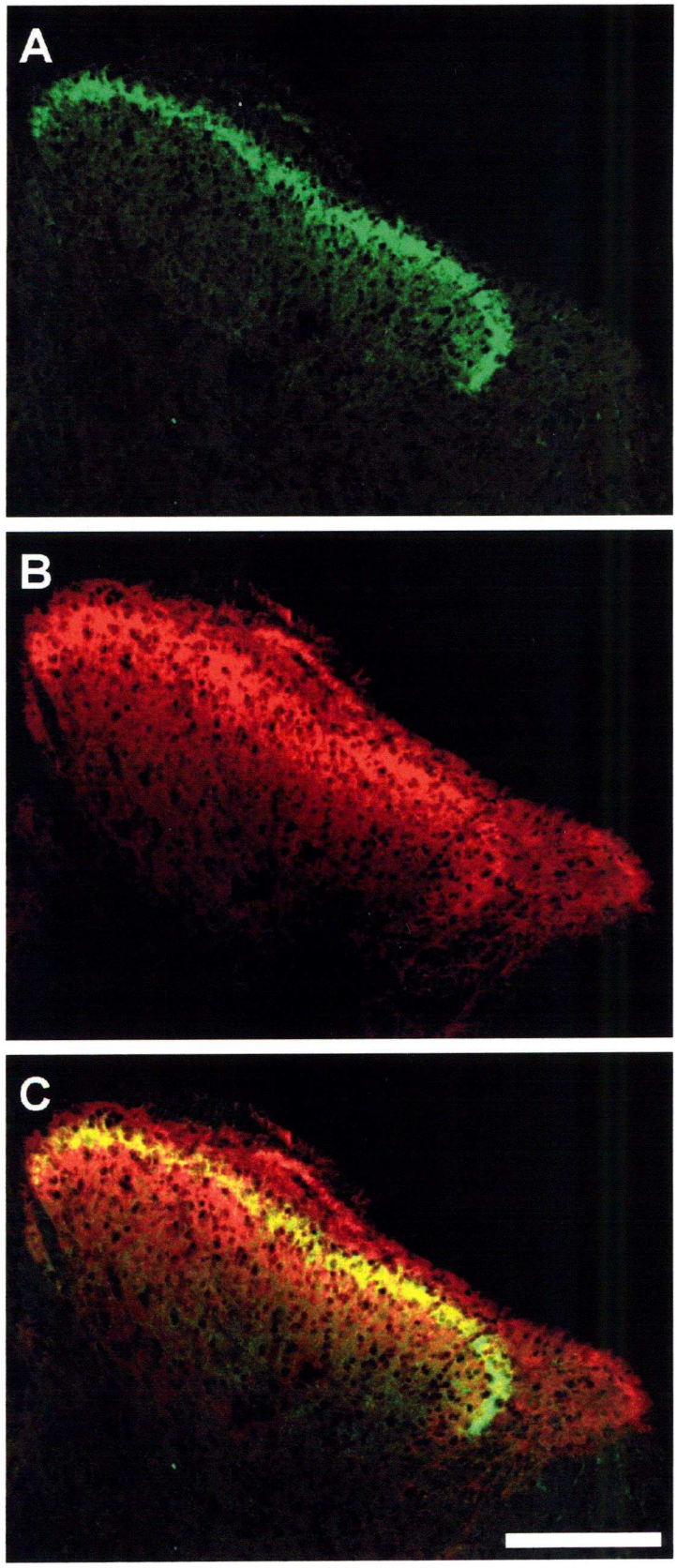

**Figure 3.13. Localisation of GFRα2-ir in the epidermis of the *thy1.2-egfp* (SA36) mouse**

A) Primary afferent fibres expressing eGFP are readily observed innervating the epidermis. Dermal side of the epidermis is to the right of the fluorescence with the external side in the lower left corner of the image.

B) GFRα2-ir can be seen in some epidermal afferents. A Cy3-conjugated secondary antibody was used.

C) The nuclei of epidermal keratinocytes can be visualised using DAPI. Only the stratum basalis, stratum spinosum and stratum granulosum have nucleated cells. A defining feature of corneocytes (fully differentiated keratinocytes of the stratum corneum) is their lack of a nucleus.

D) Colocalisation of GFRα2-ir (red) in eGFP+ve afferents (red) (thick arrow) innervating epidermal keratinocytes (blue). Section thickness 30 μm, magnification x400, scale bar 50 μm.

**Figure 3.13.**

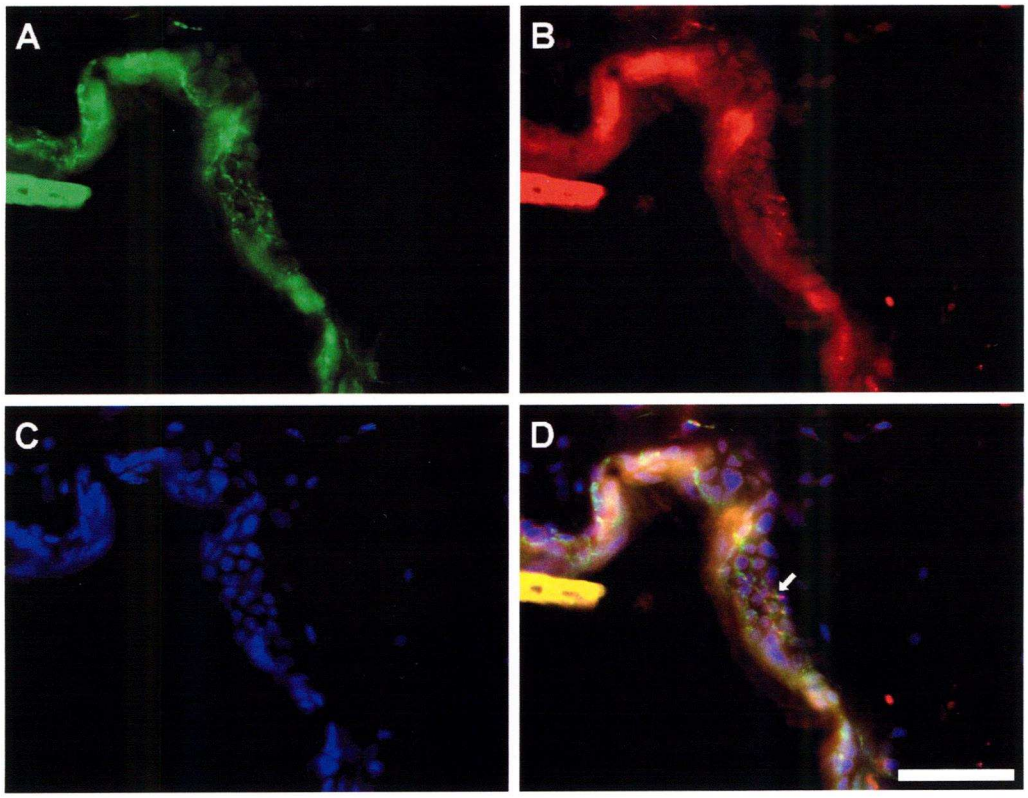

*Localisation of calbindin D-28K and GFRα2 in relation to eGFP in the DRG and DH of the thy1.2-egfp (SA36) mouse*

Consistent with the study by Belle et al., (2007), which found 52% of medium- and large-sized eGFP+ve profiles colocalised with calbindin D-28K (calbindin) in the DRG of *thy1.2-egfp* (SA36) mice, calbindin D-28K-immunoreactivity (calbindin-ir) was observed in mostly medium- and large-sized profiles some of which were eGFP+ve. (Fig. 3.14). Localisation of calbindin-ir in the spinal cord revealed a band of cells in the DH (Fig. 3.15B, E). This band was mostly ventral to eGFP+ve terminals in $LII_{i/o}$ with occasional overlap with $LII_i$ (Fig. 3.15C, F). To investigate whether the ventral proximity of calbindin-ir to eGFP in the dorsal horn was related to GFRα2-ir we looked at their distributions in DRG and DH using double-immunofluorescence staining.

Calbindin-ir colocalised with GFRα2-ir in medium- and large-sized neurones, of which some also expressed eGFP (Fig. 3.16). In the DH, calbindin-ir was distributed throughout the superficial laminae with a band of particularly strong labelling located ventrally within this region (Fig. 3.17C). When calbindin-ir was compared to eGFP fluorescence and GFRα2-ir it was apparent that the area of greatest calbindin-ir corresponded well with the region of GFRα2-ir located ventrally to the eGFP in $LII_{i/o}$ (Fig. 3.17D). Neurones with calbindin-ir were observed scattered within LI and $LII_{i/o}$ but clustered most densely within the

region earlier described as LIII with regard to GFRα2-ir (Fig. 3.12C and Fig. 3.17D).

*Localisation of gastrin-releasing peptide in relation to eGFP in the DRG of the thy1.2-egfp (SA36) mouse*

Gastrin-releasing peptide (GRP) is a mediator of itch which is expressed in a subpopulation of "peptidergic" primary afferents (Sun & Chen, 2007). In agreement with this we found GRP-immunoreactivity (GRP-ir) was not colocalised with eGFP expression in DRG neurones. GRP-ir was observed profiles of comparable size to the small- and medium-sized cells which express eGFP intensely (Fig. 3.18).

**Figure 3.14. Localisation of calbindin D-28K-ir in DRG neurones from the *thy1.2-egfp* (SA36) mouse**

A) DRG neurones expressing eGFP are a heterogeneous population of small-, medium- and large-sized cells.

B) Calbindin-ir was observed in medium- and large-sized DRG neurones. Cells were labelled using a Cy5-conjugated secondary antibody

C) Colocalisation of calbindin-ir (blue) was seen in some medium- and large-sized profiles (arrowhead). Approximately half (Belle et al., 2007) of the calbindin-ir population does not colocalise with eGFP in medium- and large-sized neurones (thick arrow). Section thickness 12 μm, magnification x200, scale bar 100 μm.

**Figure 3.14.**

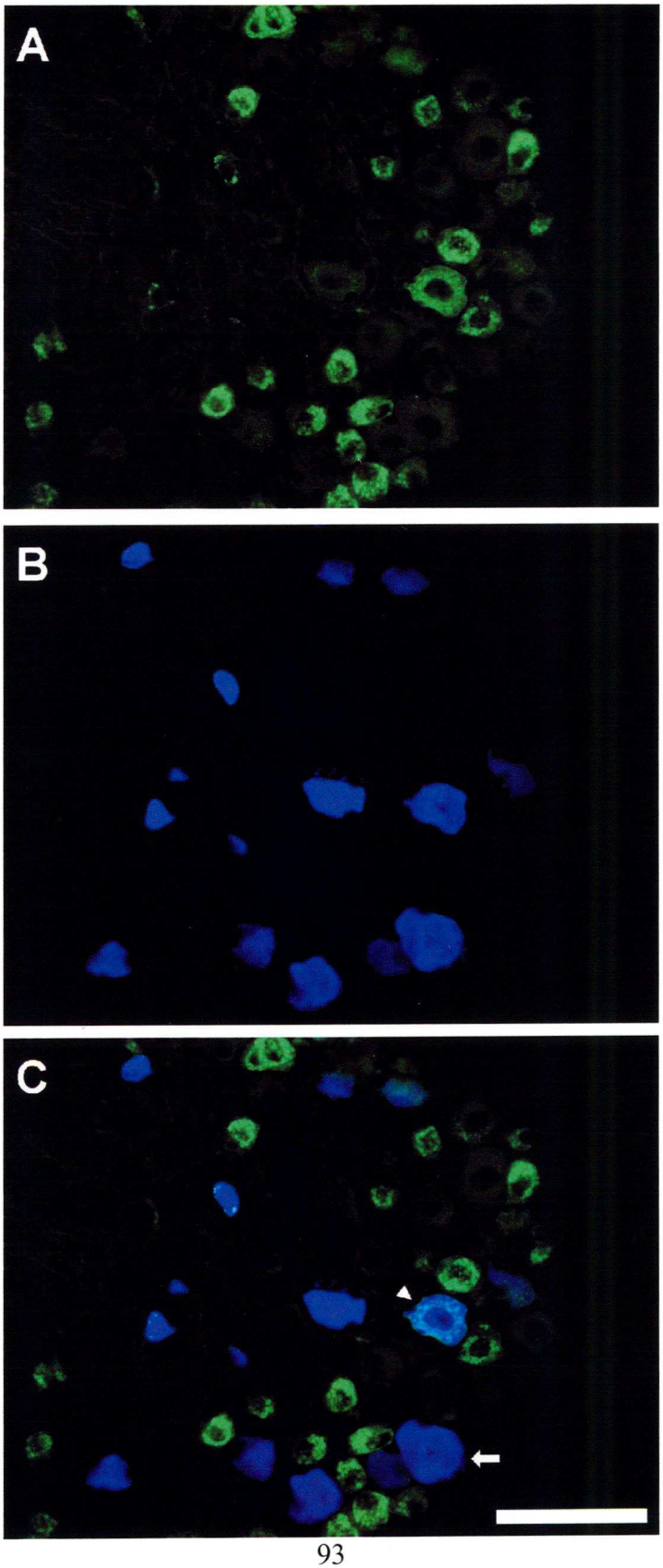

**Figure 3.15. Localisation of calbindin D-28K-ir in the DH of the *thy1.2-egfp* (SA36) mouse**

A & D) In the spinal cord, eGFP fluorescence from the central terminations of labelled primary afferents clearly demarcated $LII_{i/o}$ of the dorsal horn.

B & E) Calbindin-ir was detected in the superficial laminae of the dorsal horn with a band of intensely stained cells in the ventral portion of this region. A Cy5-conjugated secondary antibody was used.

C & F) The band of calbindin-ir cells was located ventrally to $LII_{i/o}$ (as defined by eGFP fluorescence). Some overlap with $LII_i$ was seen.

A-C) Section thickness 30 μm, magnification x100, scale bar 200 μm.

D-F) Same section, magnification x200, scale bar 100 μm.

**Figure 3.15.**

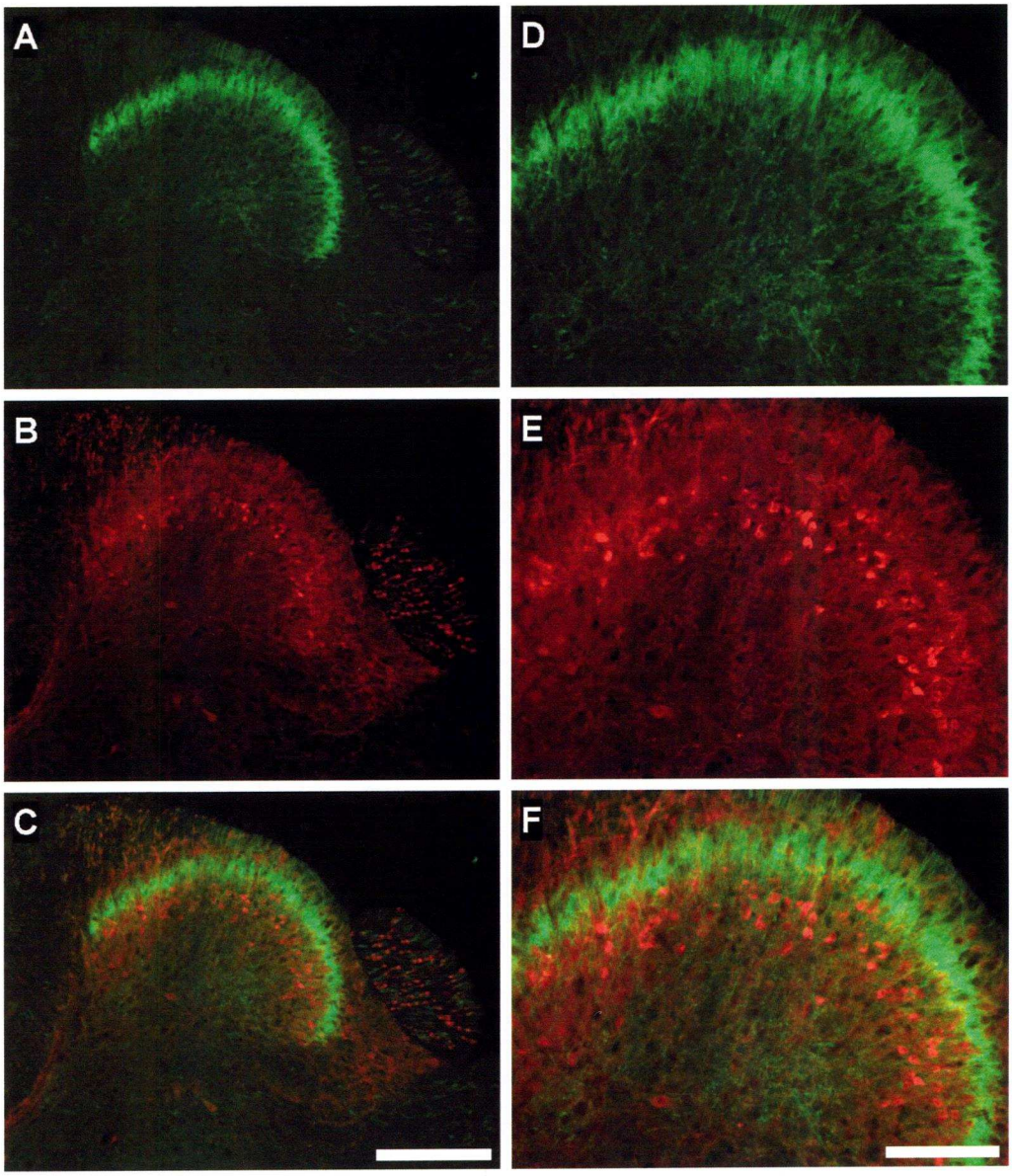

**Figure 3.16. Localisation of calbindin D-28K-ir and GFRα2-ir in DRG neurones from the *thy1.2-egfp* (SA36) mouse**

A) Neurones expressing eGFP in the DRG.

B) GFRα2-ir neurones in the DRG labelled with Cy3. Small- and medium-sized neurones show more intensive staining of the soma than large-sized neurones.

C) Calbindin-ir labels a subpopulation of medium- and large-sized neurones. A Cy5-conjugated secondary antibody was used.

D) Colocalisation of eGFP (green) with the GFRα2-ir (red) and calbindin-ir (blue) reveals diverse populations. Some small-sized neurones are GFRα2-ir/eGFP-ve/calbindin-ve. Most small- and medium-sized neurones are GFRα2-ir/eGFP+ve/calbindin-ve (yellow, arrowhead). Medium- and large-sized colocalised formed populations with (GFRα2-ir/eGFP+ve/calbindin-ir, thick arrow) and without eGFP expression (GFRα2-ir/eGFP-ve/calbindin-ir, thin arrow). Section thickness 12 μm, magnification x200, scale bar 100 μm.

**Figure 3.16.**

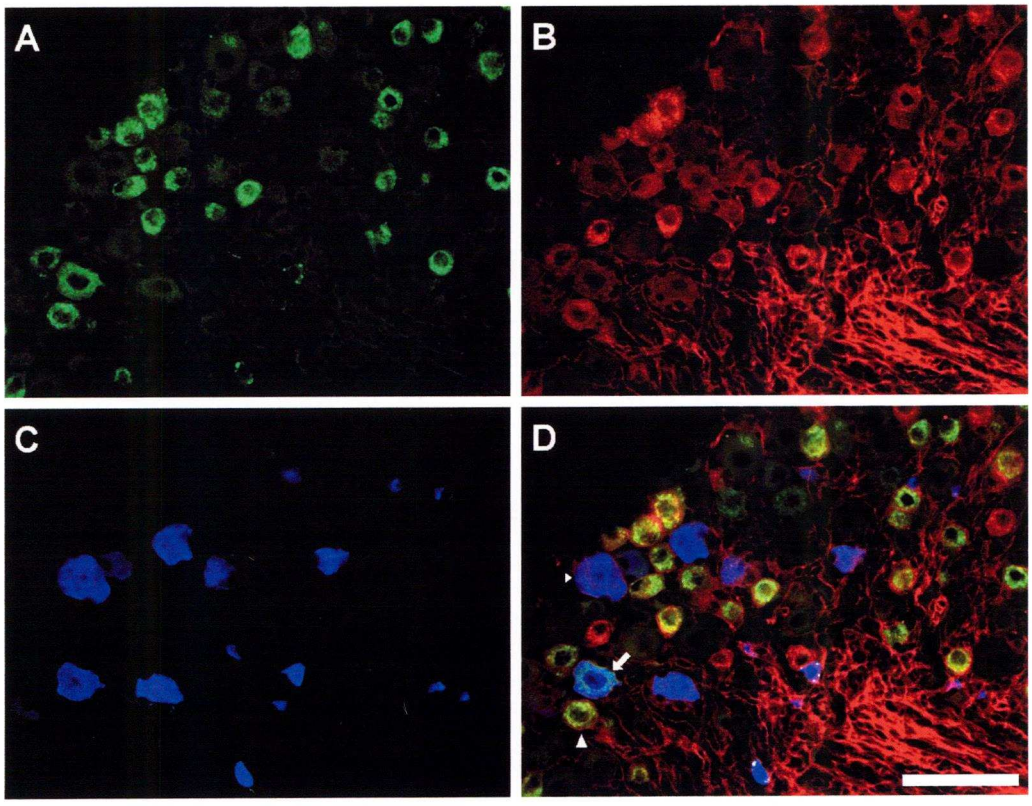

**Figure 3.17. Localisation of calbindin D-28K-ir and GFRα2-ir in the DH of the *thy1.2-egfp* (SA36) mouse**

A) Lamina $II_{i/o}$ is clearly defined by the central terminals of eGFP-expressing epidermal primary afferents.

B) GFRα2-ir is present in the superficial laminae of the dorsal horn. Secondary antibody labelled with Cy3.

C) Calbindin-ir is distributed throughout the superficial laminae with a band of densely clustered neurones located in the ventral portion of this region. Secondary antibody labelled with Cy5.

D) The differences in the distribution of eGFP (green), GFRα2-ir (red), and calbindin-ir (blue) delineates the superficial laminae of the dorsal horn. Dorsal to ventral (top to bottom), LI has weak GFRα2-ir, eGFP-ve and little calbindin-ir thus appearing red. $LII_{i/o}$ is strongly eGFP+ve, strongly GFRα2-ir, weakly calbindin-ir and appears yellow. LIII is strongly GFRα2-ir, eGFP-ve, strongly calbindin-ir and appears pink/purple densely punctuated by blue calbindin-ir soma. Calbindin-ir soma are more sparsely distributed in LI and $LII_{i/o}$. Section thickness 30 μm, magnification x200, scale bar 100 μm.

**Figure 3.17.**

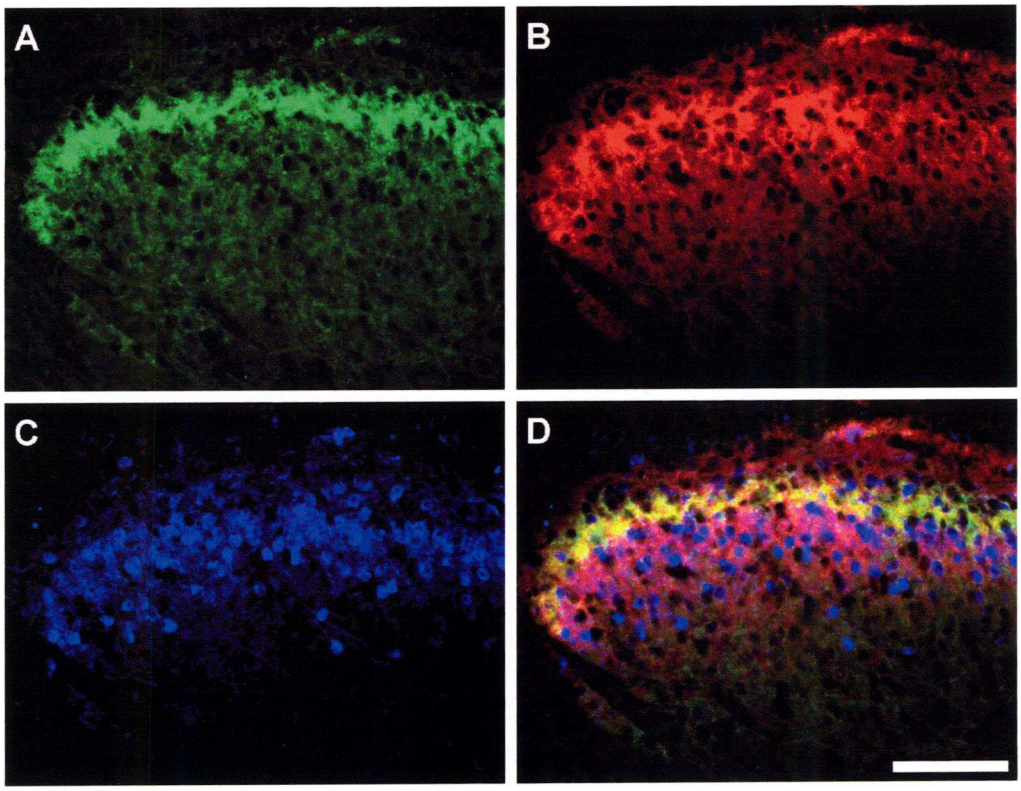

**Figure 3.18. Localisation of GRP in DRG neurones from the *thy1.2-egfp* (SA36) mouse**

A) Small- and medium-sized "nonpeptidergic" DRG neurones express eGFP.

B) Cells of comparable size are GRP-ir in their soma and processes. Secondary antibody used was Cy3-conjugated.

C) Profiles expressing eGFP (green) and GRP-ir (red) did not colocalise.

Section thickness 12 μm, magnification x200, scale bar 100 μm.

**Figure 3.18.**

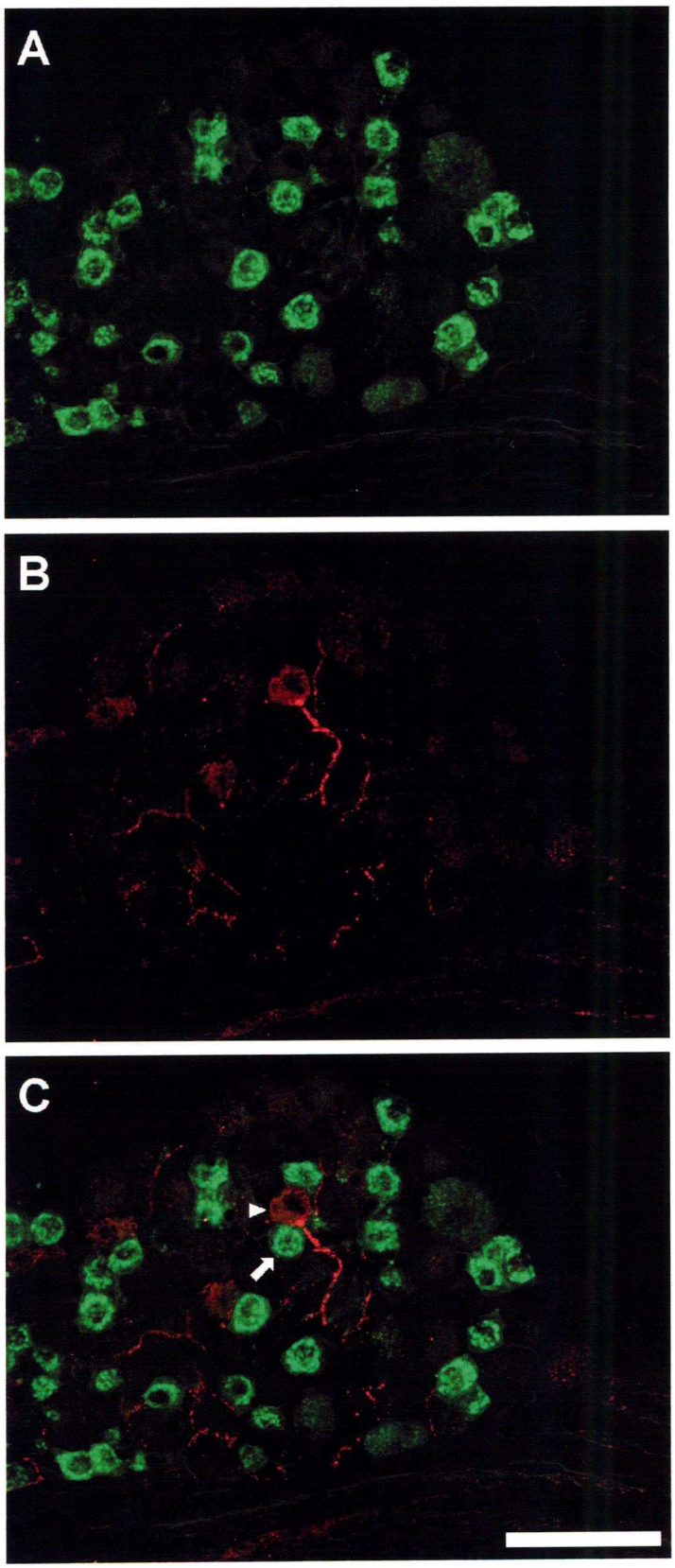

*Determination of small-, medium- and large-sized neuronal population diameter*

The classification of neuronal population by soma cross-sectional area was used to characterise profiles from DRG sections as small-, medium- and large-sized cells. The values used to define the populations were derived from a study in to the postnatal maturation of mouse DRG neurones (Lawson, 1979; Belle et al., 2007). To determine the size, and thus estimate the population a cell is likely to belong to during electrophysiological experiments, soma diameter is a more practical measure than cross-sectional area. Mathematically derived values using the equation, area = $\pi r^2$, gives boundaries of <23.9 μm for small-sized cells and >32.9 μm for large-sized cells (Fig.3.19.A). The flaw with this method is that it assumes the cell is perfectly spherical and the average cross section in any plane is therefore a perfect circle. Using measurements of the diameter taken along two perpendicular axes from eGFP+ve neurones whose cross-sectional area was measured for the analysis of GFRα2-ir, an average diameter for each profile was calculated. Average diameter was plotted against corresponding cross-sectional area and simple linear regression was used to produce a line of best fit (Fig. 3.19.B). Using this model, population sizes were estimated to be <25.1 μm for small-sized cells and >34.9 μm for large sized cells ($r^2$=0.92, n=777).

**Figure 3.19. Linear and nonlinear regression plots of average diameter against cross-sectional area for eGFP+ve profiles**

A) This graph shows a nonlinear regression model of the relationship between average cell diameter and cross-sectional area using the equation, area = $\pi r^2$. Diameter measurements taken along two perpendicular axes for each cell were averaged to give a mean diameter for that cell. The model predicted the diameter of small- (CSA <450 $\mu m^2$) and large-sized (CSA <850 $\mu m^2$) to be <23.9 μm and >32.9 μm respectively ($r^2$=0.8, n=777).

B) This graph shows a simple linear regression model of the relationship between average cell diameter and cross-sectional area. Diameter measurements taken along two perpendicular axes for each cell were averaged to give a mean diameter for that cell. Cross-sectional area measurements were calculated using Metamorph software. Mean diameter was plotted against cross-sectional area and a line of best fit modelled. The resultant best-fit regression line predicted the diameter of small- (CSA <450 $\mu m^2$) and large-sized (CSA <850 $\mu m^2$) to be <25.1 μm and >34.9 μm respectively ($r^2$=0.92, n=777). Cells whose diameter fell within these two values would be classed as medium-sized.

**Figure 3.19.**

**A**

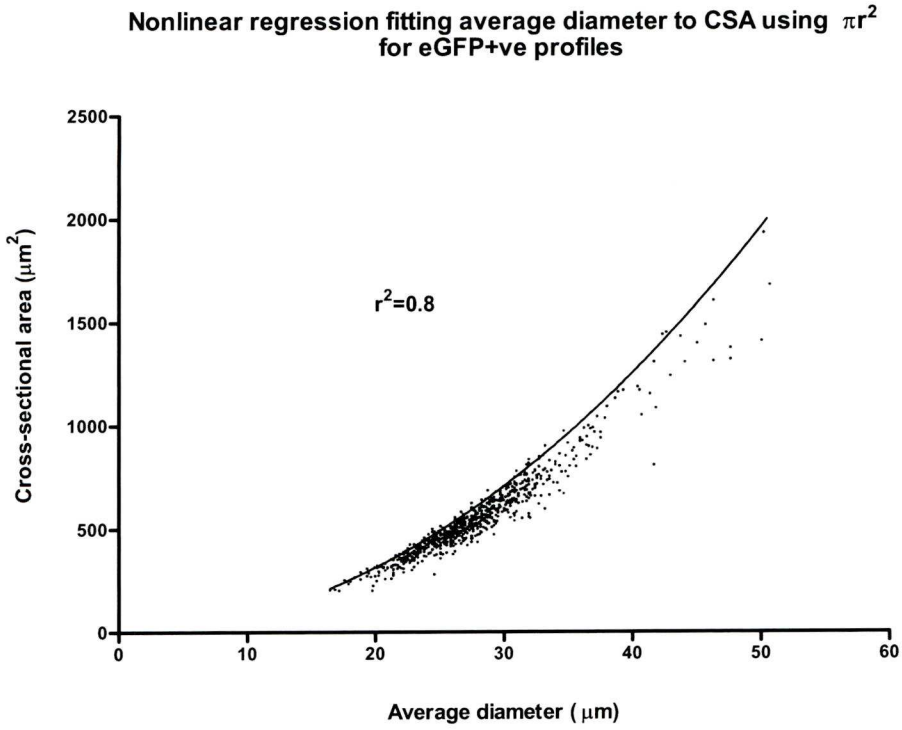


**B**

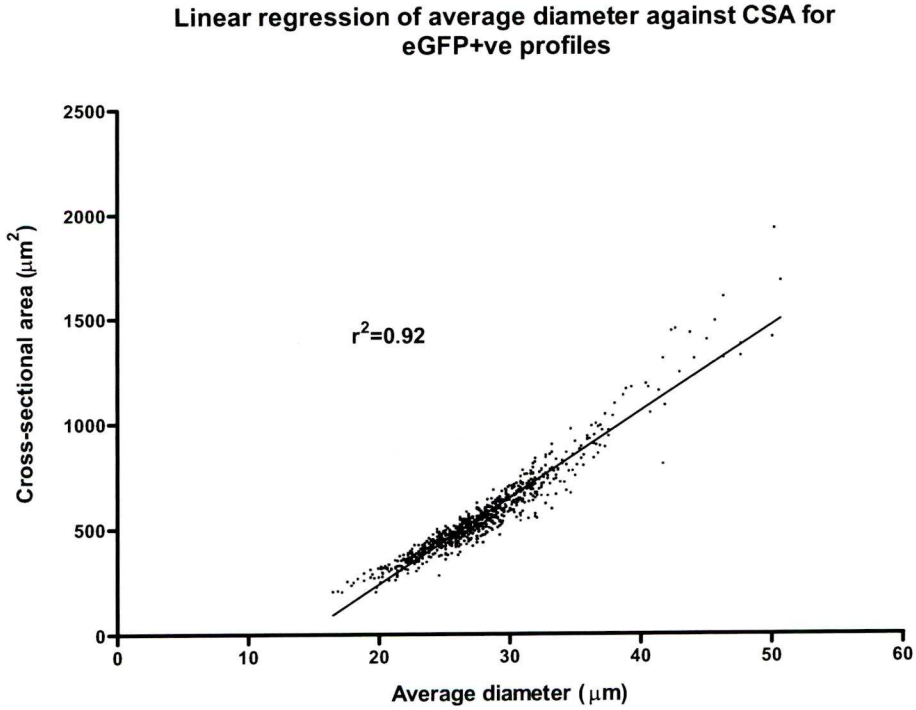

**Table 3.1. Summary of the colocalisation of quantified markers with eGFP in DRG neurones from the thy1.2-egfp (SA36) mouse.**

This table summarises the colocalisation of antibody immunoreactivity with eGFP in DRG neurones. Colocalisation for each marker is expressed as a percentage of the eGFP population showing immunoreactivity and as a percentage of the immunoreactive population which contained eGFP. High colocalisation of P2X3-ir and GFR2-ir was observed within the eGFP expressing population. $TRPV_1$-ir did not colocalise with eGFP in DRG neurones.

**Table 3.1.**

| Label | eGFP+ve neurones expressing other label | Other label neurones expressing eGFP |
|---|---|---|
| $P2X_3$-ir | 85.1% (627/737) | 78.4% (627/800) |
| $TRPV_1$-ir | 1.6% (9/557) | 5% (9/179) |
| GFRα2-ir | 81.9% (636/777) | 64.8% (636/982) |

## Chapter summary

Profiles from eGFP-expressing DRG neurones showed they were predominately small- and medium-sized cells. Most of these cells were immunoreactive for the $P2X_3$ subunit and GFRα2 receptor (Fig. 3.20). They did not colocalise with $TRPV_1$ or GRP, which have been identified as belonging to "peptidergic" populations of small, unmyelinated DRG (Zwick et al., 2002; Sun & Chen, 2007) (Fig. 3.20). As previously reported by Belle et al., (2007), calbindin D-28K immunoreactivity was observed in some medium- and large-sized DRG profiles.

In the spinal cord eGFP fluorescence, which delineates $LII_{i/o}$ of the dorsal horn, colocalised with P2X3-ir. Lamina I was labelled with $TRPV_1$-ir which did not colocalise with the terminals of eGFP-labelled afferents. GFRα2-ir was observed in the superficial laminae where intense staining was colocalised with eGFP in $LII_{i/o}$. Neurones in the dorsal horn labelled with calbindin-ir were distributed unevenly throughout the superficial laminae. A region ventral to that marked by eGFP fluorescence contained the greatest density of calbindin-ir soma and fibres. This was identified as LIII on the basis of its ventral proximity to eGFP in $LII_{i/o}$ and morphology (Rexed, 1952) defined by GFRα2-ir. Processes from primary afferent fibres labelled with eGFP terminated in the epidermis and showed some GFRα2-ir.

Cross-sectional area was used in conjunction with a simple linear regression model to estimate the corresponding cell diameter boundaries for classification of cells used in electrophysiology experiments.

# Chapter 4

## ELECTROPHYSIOLOGICAL CHARACTERISATION OF DRG NEURONES FROM THE *THY1.2-EGFP* (SA36) MOUSE

## Introduction

A study by Stucky and Lewin (1999) demonstrated that the action potentials of $IB_4$-binding DRG neurones differed from those of belonging to "peptidergic" neurones. It was the first study to show that $IB_4$-binding neurones were functionally distinct from $IB_4$-ve neurones (Stucky and Lewin, 1999). The purpose of this part of the study was to functionally characterise eGFP+ve and eGFP-ve acutely dissociated neurones. Following this, we used this characterization to identify differences caused by the culturing process.

## Results

*DRG neurones display distinct responses to sustained depolarising currents*

The responses of acutely-dissociated and short-term cultured DRG neurones to sustained depolarising and hyperpolarizing currents (230 ms, 0.2 Hz) were examined. Five phenotypic responses to depolarising current were identified mirroring those described in dorsal horn neurones (Ruscheweyh and Sandkuhler, 2002). Burst-firing was characterized by a rapid discharge of 2-3 action potentials at the beginning of the pulse but no more despite the increasing magnitude of the pulses. Delayed-firing neurones possessed a slow depolarization towards threshold when current was injected. This delay in

initiation grew shorter as current magnitude increased and firing frequency increased. At suprathreshold currents neurones fired without delay in a manner similar to tonic-firing. Phasic-firing and tonic-firing neurones both increased their frequency of discharge in response to suprathreshold currents. The distinguishing feature that differentiates these two groups is their interspike interval. Tonic-firing neurones fire regularly when depolarized with an even interspike interval. Phasic-firing neurones, however, have an irregular interspike interval until they reach maximum firing frequency at which point the interspike interval is regular like tonic-firing neurones. The last group responded to depolarising current with a solitary primary spike and do not increase their firing frequency when current magnitude is increased. These are transient-firing neurones as their response to sustained depolarising current is brief (Fig. 4.1). The characteristics of each firing phenotype were used to form a logic by which they could be readily classified in a consistent manner (Fig. 4.2).

**Figure 4.1. Responses of DRG neurones to sustained depolarization can be classified as one of five phenotypes.**

Responses to 230 ms depolarising current injections were classified as burst-, delayed-, phasic-, tonic- or transient firing. Burst-firing occurred at the start of depolarization after which the cell remained silent. Delayed-firing were slow to fire from the initiation of the pulse. As pulse magnitude increased the delay in reaching threshold diminished. Tonic-firing neurones discharged with increasing frequency as pulse magnitude increased and maintained a regular interspike interval. Phasic-firing could be distinguished by the irregular interspike interval present at submaximal stimulations. Transient-firing neurones responded quickly with a primary spike in response to depolarization but did not become more excitable when the current was increased.

**Figure 4.1.**

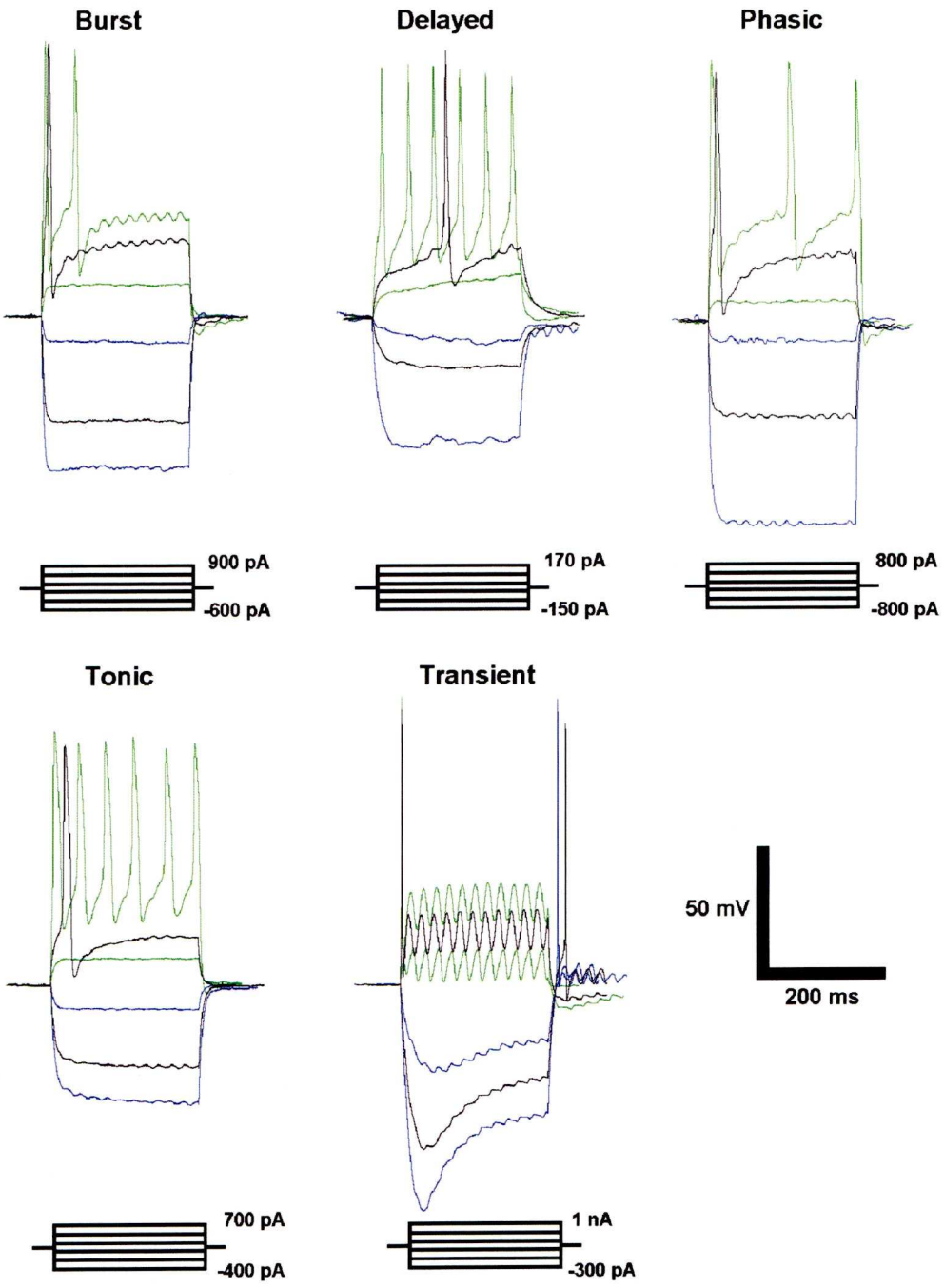
Burst
900 pA
-600 pA
Delayed
170 pA
-150 pA
Phasic
800 pA
-800 pA
Tonic
700 pA
-400 pA
Transient
1 nA
-300 pA
50 mV
200 ms

**Figure 4.2. Classification criteria for firing phenotype**

Neuronal firing patterns could be grouped in to one of five firing phenotypes. This diagram demonstrates the logic followed in the classification of neuronal responses to depolarising current pulses.

**Figure 4.2.**

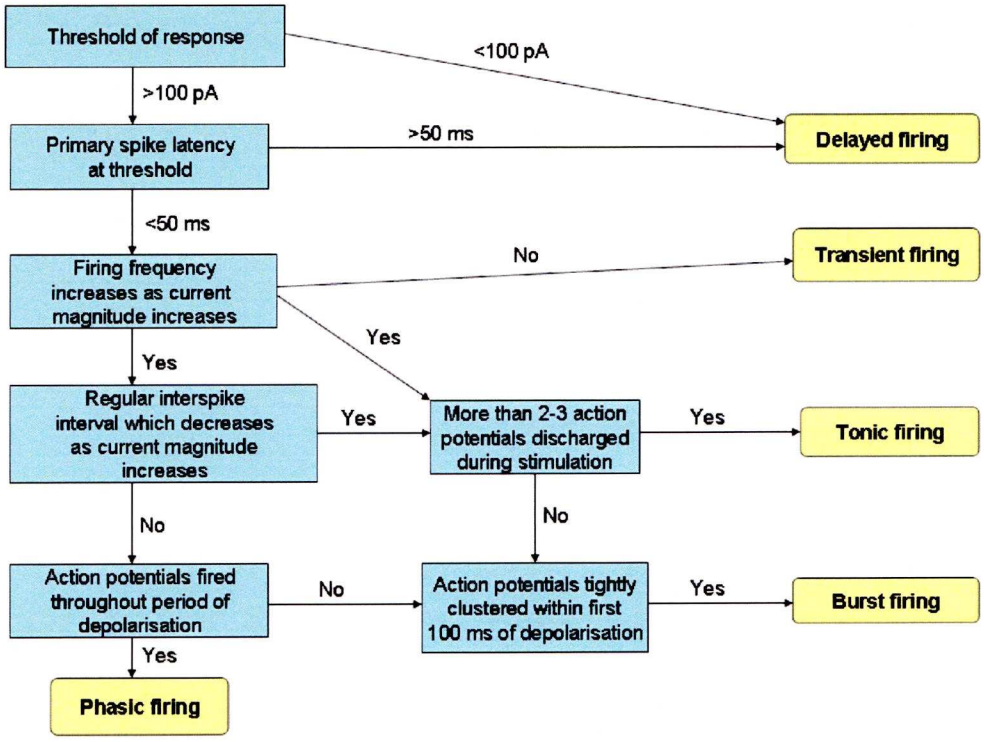
Threshold of response
<100 pA
>100 pA
Primary spike latency at threshold
>50 ms
Delayed firing
<50 ms
Firing frequency increases as current magnitude increases
No
Transient firing
Yes
Yes
Regular interspike interval which decreases as current magnitude increases
Yes
More than 2-3 action potentials discharged during stimulation
Yes
Tonic firing
No
No
Action potentials fired throughout period of depolarisation
No
Action potentials tightly clustered within first 100 ms of depolarisation
Yes
Burst firing
Yes
Phasic firing

*Distribution of responses between eGFP-expressing and eGFP-ve acutely-dissociated DRG neurones*

Responses to depolarising current were recorded from eGFP-ve (n=15) and eGFP+ve (n=30) acutely dissociated DRG neurones. Most eGFP-ve neurones were phenotypically delayed-firing (n=9/15) and eGFP+ve neurones were predominantly transient-firing (Table 4.1A). There was no difference in action potential duration measured at half amplitude but action potentials from eGFP+ve neurones did not overshoot as much as they did in eGFP-ve neurones ($p<0.01$) (Table 4.1B). Neurones expressing eGFP were on average of larger diameter than eGFP-ve neurones ($p<0.0001$) (Table 4.1B).When neurones were hyperpolarized, transient-firing cells (15 of 27 cells tested) showed a delayed rectification indicative of a hyperpolarisation, cyclic nucleotide-gated (HCN) current, $I_h$ (Fig. 4.1 Transient). Although not exclusive to transient-firing neurones this response was rarely observed in other phenotypes and was often accompanied by a rebound action potential (15 of 27 cells tested).

*Redistribution of firing phenotype in cultured eGFP+ve DRG neurones*

Short-term culturing of eGFP+ve DRG neurones led to a redistribution of firing phenotype. Approximately half (50.9%) of cultured neurones were transient-firing but a larger proportion than was seen in the acutely-dissociated cells were now tonic-firing (43.4%). Acutely dissociated eGFP+ve DRG neurones were

primarily transient- (71%) and rarely tonic- firing (6.4%). Tonic-firing neurones had longer duration action potentials which were larger in both amplitude and overshoot than those of transient-firing neurones (Fig. 4.3).

**Table 4.1. Characteristics of acutely dissociated eGFP+ve and eGFP-ve DRG neurones**

A) The predominant phenotype amongst eGFP-ve cells was delayed-firing. The bracketed numbers (n=) are the number of replicates for that group.

B) On average, eGFP+ve neurones (27.23 ± 0.69 μm, n=31) were larger than eGFP-ve neurones (20.67 ± 1.07 μm, n=15, $p<0.0001$). The action potentials of these smaller neurones possessed greater AP overshoot (38.47 ± 3.42 mV, n=15, $p=0.0072$) than the eGFP+ve neurones (27.60 ± 2.12 mV, n=31).

**Table 4.1.**

**A**

| | Burst (n=5) | Delayed (n=10) | Phasic (n=2) | Tonic (n=3) | Transient (n=26) |
|---|---|---|---|---|---|
| eGFP+ve (n=31) | 12.9% (4/31) | 3.2% (1/31) | 6.4% (2/31) | 6.4% (2/31) | 71% (22) |
| eGFP-ve (n=15) | 6.66% (1/15) | 60% (9/15) | 0% (0/15) | 6.66% (1/15) | 26.67% (4/15) |

**B**

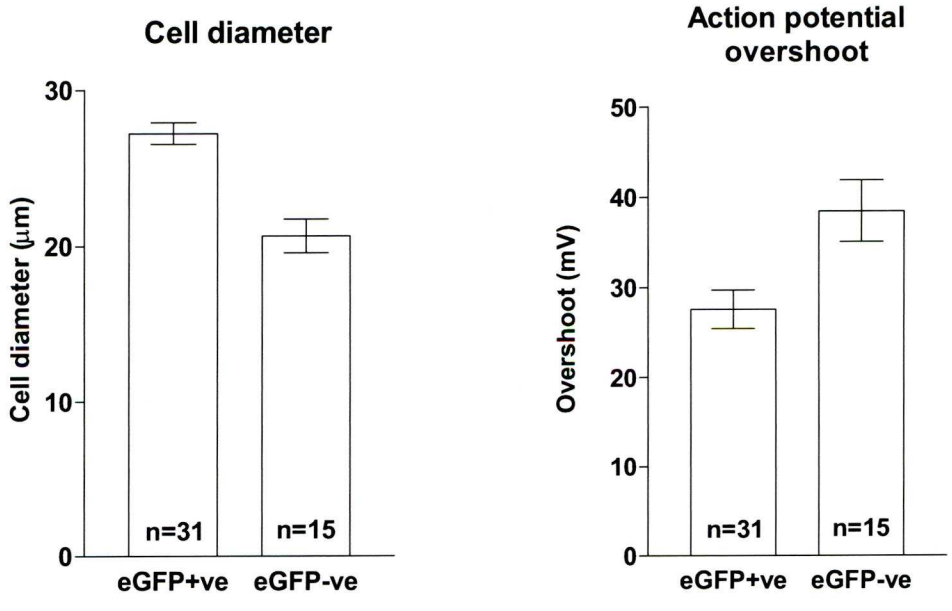

**Figure 4.3. Action potentials in tonic-firing cultured DRG neurones are bigger and longer.**

Action potential duration, measured at half-amplitude, was longer in tonic-firing neurones (top graph, $p<0.05$). Both overshoot and amplitude of action potentials in tonic-firing neurones were larger (middle and bottom graph respectively, $p<0.01$). Results are mean ± SEM, two-tailed t-test.

# Figure 4.3.

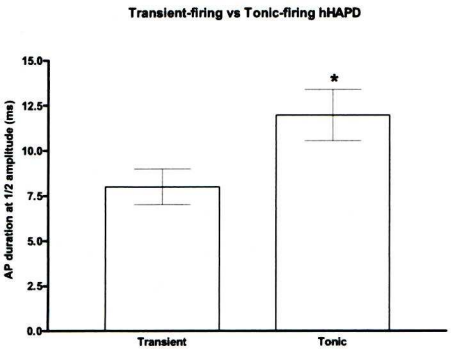
Transient-firing vs Tonic-firing hHAPD
AP duration at 1/2 amplitude (ms)
15.0
12.5
10.0
7.5
5.0
2.5
0.0
*
Transient
Tonic

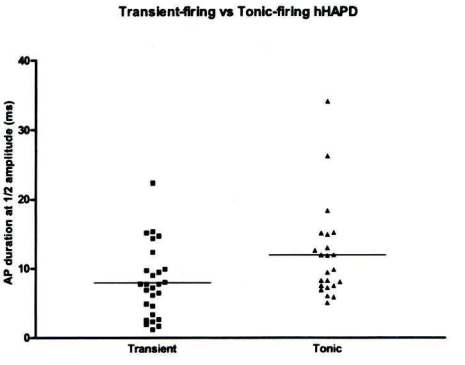
Transient-firing vs Tonic-firing hHAPD
AP duration at 1/2 amplitude (ms)
40
30
20
10
0
Transient
Tonic

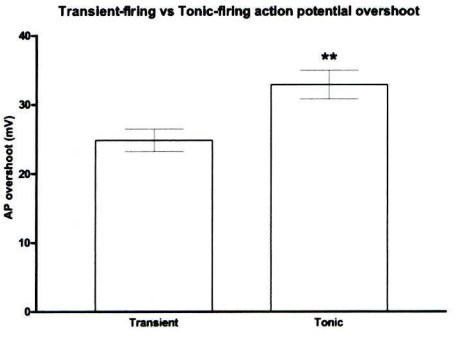
Transient-firing vs Tonic-firing action potential overshoot
AP overshoot (mV)
40
30
20
10
0
**
Transient
Tonic

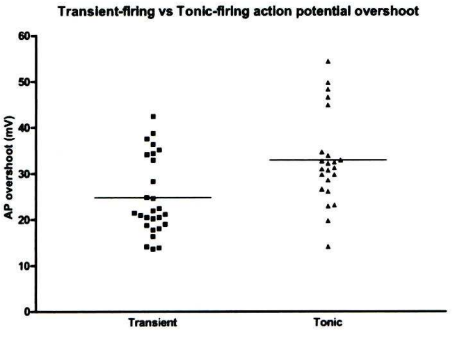
Transient-firing vs Tonic-firing action potential overshoot
AP overshoot (mV)
60
50
40
30
20
10
0
Transient
Tonic

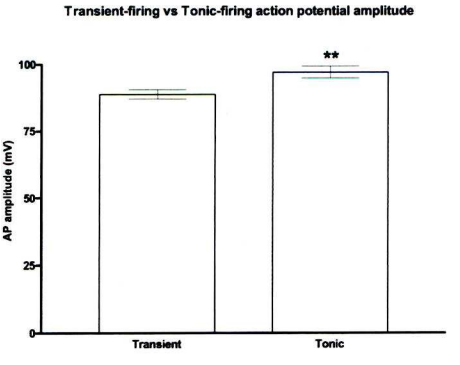
Transient-firing vs Tonic-firing action potential amplitude
AP amplitude (mV)
100
75
50
25
0
**
Transient
Tonic

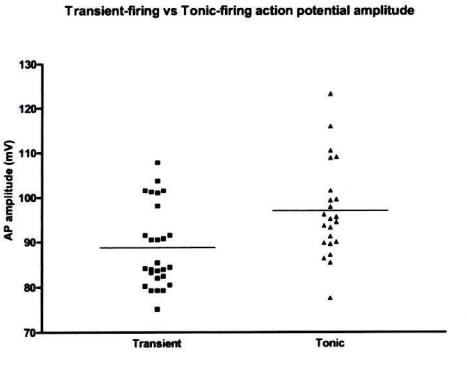
Transient-firing vs Tonic-firing action potential amplitude
AP amplitude (mV)
130
120
110
100
90
80
70
Transient
Tonic

**Chapter summary**

Five phenotypes of firing were identified in acutely dissociated DRG neurones, these were burst-, delayed-, phasic-, tonic- and transient-firing. These firing phenotypes were not evenly distributed within eGFP+ve and eGFP-ve populations of acutely-dissociated DRG neurone. Most (60%) eGFP-ve neurones were delayed-firing, showing a slow depolarising ramp from the depolarisation due to the current pulse to the action potential threshold. This delay decreased as the current magnitude of the pulse increased and responded maximally without delay with sustained repetitive firing. In contrast, eGFP+ve neurones were predominately (~70%) transient-firing. They fired a primary action potential without delay at the start of the current pulse and remained silent throughout the remaining depolarisation. This did not change as current pulse magnitude increased.

When short-term cultured, eGFP+ve neurones remained predominately transient-firing but there was a large increase in the number of tonic-firing neurones. Action potentials in tonic-firing, cultured DRG neurones were of greater amplitude and duration than the remaining transient-firing population.

# Chapter 5

## THE PRESENSCE OF AN M-CURRENT AND ITS ROLE IN DETERMINING THE FIRING PROPERTIES OF TRANSIENT-FIRING NEURONES

## Introduction

The M-current ($I_{K(M)}$) is a non-inactivating potassium current first described in sympathetic ganglion neurones (Brown & Adams, 1980). It is activated by depolarisation to potentials more positive than -60 mV and regulates neuronal excitability (Brown & Adams, 1980). The molecular correlates of the M-current is the $K_v7$ family of voltage-gated potassium channels (VGKC), also referred to by their gene name, KCNQ (Maljevic, Wuttke & Lerche, 2008). Of the 5 members known only $K_v7.2$-5 are found in the central and peripheral nervous systems (Jentsch, 2000). Like all VGKCs, each gene encodes a 6-transmembrane (6TM) spanning subunit which assembles into homomeric or heteromeric tetramers to form a functional channel (Gutamn et al., 2005). Whilst $K_v7.3$ will form heteromeric channels with either $K_v7.2$ or $K_v7.5$, they will not form functional channels with each other (Lerche et al., 2000; Schroeder et al., 2000). Channelopathies due to mutations in one or both genes contributing to a functional channel are associated with pathologies associated with neuronal hyperexcitability (Maljevic, Wuttke & Lerche, 2008). A haploinsufficiency resulting from a single faulty copy of the *kcnq2* gene produces a 25% reduction in the $K_v7.2/3$ current and causes benign familial neonatal seizures (BFNS) (Schroeder et al., 1998; Maljevic, Wuttke & Lerche, 2008).

A novel anticonvulsant, retigabine, shifts the voltage activation curve of $K_v$7.2-5 containing channels in the hyperpolarising direction thus increasing the channel open probability at any given membrane potential (Main et al., 2000; Wickenden et al., 2000; Tatulian et al., 2001). In rat models of neuropathic pain retigabine is hypoalgesic (Passmore et al., 2003; Dost et al., 2004). The M-current was recorded in small, capsaicin sensitive and insensitive rat DRG neurones suggesting it is present in both nociceptive and non-nociceptive cells (Passmore et al., 2003). Single-cell PCR and immunofluoresent staining of cultured rat DRG neurones detected the presence of $K_v$7.2, 7.3 & 7.5 but not $K_v$7.4 subunits in small and large neurones although $K_v$7.4 was detectable by RT-PCR in whole ganglia preparations (Passmore et al., 2003).

The M-current, so called due to its initial characterisation by inhibition through the activation of muscarinic acetylcholine receptors, has been functionally associated with several GPCRs (Adams et a., 1982; Zaika et al., 2007). Recently it was shown that β-alanine inhibits the M-current in small, $IB_4$-labelled rat DRG neurones (Crozier et al., 2007). A GABA analogue, β-alanine is an agonist at the Mrgprd receptor but its effect is not altered by the presence of a $GABA_B$ antagonist (Shinohara et al., 2004; Crozier et al., 2007). This inhibition could also be reproduced in Chinese hamster ovaries (CHO) by coexpressing Mrgprd with $K_v$7.2/3 channels (Crozier et al., 2007). Mrgprd is a GPCR that is exclusively expressed in small diameter, nonpeptidergic mouse DRG neurones (Zylka et al., 2005). These neurones innervate the epidermis as superficially as

the stratum granulosum and are selectively sensitive to ATP (Zylka et al., 2005; Dussor et al., 2008).

Cultured keratinocytes release ATP when mechanically stimulated and in much larger concentrations when damaged (Cook & McCleskey, 2002; Koizumi et al., 2004). Members of the metabotropic ATP receptor family, P2Y, are expressed in both keratinocytes and DRG neurones (Svichar et al., 1997; Tominaga et al., 2001; Greig et al., 2003; Koizumi et al., 2004). In DRG, activation of P2Y receptors inhibits N-type voltage-gated calcium channels (VGCaC) and facilitates desensitisation of $P2X_3$ channels (Gerevich et al., 2004; Gerevich et al., 2007). P2Y receptors are functionally associated with Kv7 channels in other tissues (Brown et al., 1982; Filippov et al., 2006). The P2Y1 agonist, ADP, inhibits the M-current in hippocampal pyramidal neurones and increases neuronal firing (Filippov et al., 2006). Meanwhile it was known that UTP inhibited the M-current before the P2Y family was discovered (Adams et al., 1982; Burnstock & Kennedy, 1985). Murine cutaneous afferents are excited by UTP (Stucky et al., 2004) and the P2Y2 receptor, at which UTP is equally efficacious as ATP (Malin et al., 2008), is required for the normal functioning of $TRPV_1$ (Tominaga et al., 2001).

In light of the preceding literature two questions were raised. Do epidermal primary afferents express $K_v7$ channels and the associated M-current as

suggested by Crozier et al., (2007)? Secondly, is the M-current in epidermal primary afferents modulated by P2Y receptors and if so which ones?

## Results

*Epidermal primary afferents labelled with eGFP possess M-currents*

Medium-diameter DRG neurones (25-30.56 μm) expressing eGFP were selected for investigation of the M-current in epidermal afferents as the signal to noise ratio of smaller cells was insufficient to allow accurate analysis. A voltage clamp protocol which depends on the steady-state inactivation of other voltage gated ion channels to isolate the M-current was used (Passmore et al., 2003). Cells were voltage clamped at -20 mV and hyperpolarised in 10 mV increments for 1 s at 5 s intervals (Fig. 5.1A). The M-current does not inactivate but is deactivated by hyperpolarising-voltage steps from a depolarised holding potential (Brown & Adams, 1980). Hyperpolarisation beyond -60 mV should result in ohmic steps as M-current channels ($K_v7$) are closed (Brown and Adams, 1980). Subpopulations of DRG neurones of all sizes possess a hyperpolarisation-activated current ($I_h$) which is sensitive to $Cs^+$ ions (Scroggs et al., 1994). As the current recorded from -90 to -110 mV was used to calculate the leak subtraction, 1mM CsCl was used to inhibit $I_h$ during voltage clamp recordings (Passmore et al., 2003).

Voltage-clamp recordings were made from 44 cells expressing eGFP. Of these, 56.8% (25/44) possessed currents that resembled the M-current originally described by Brown & Adams (1980). Analysis of these currents resulted in

76% (19/25) being deemed M-current and used for statistical analysis (Fig. 5.1B). Application of the selective $K_v7$ blocker, XE-991 (10 μM), was used to confirm the current observed was indeed the M-current in some cells (n=4) (Fig. 5.1C).

**Figure 5.1. Evidence for an M-current in eGFP-labelled, cultured neurones with epidermal afferents**

A) Whole-cell voltage-clamp was used to isolate the M-current in cultured DRG neurones expressing eGFP. Currents from medium-diameter neurones (n=44) were recorded and 43.2% (n=19/44) fulfilled the requirements to be classed as M-currents (defined by Brown and Adams, 1980).

B) Instantaneous (black) and steady-state (red) currents ($I_{inst}$ and $I_{ss}$ respectively) were measured and plotted. Reversal of $I_{inst}$ near to the potassium equilibrium potential indicates that $K^+$ ions are the primary charge carrier.

C) M-currents diminished with time. Rundown during the drug incubation period was compensated for by using time matched controls. The traces show a control recording and block by XE-991 (10 μM) in the same cell (raw current trace shown in A) with a time matched control (TMC) trace from a different cell superimposed on top. Time matching was performed by repeating the protocol 5 minutes after an initial run of the protocol to mimic the drug incubation period.

**Figure 5.1.**

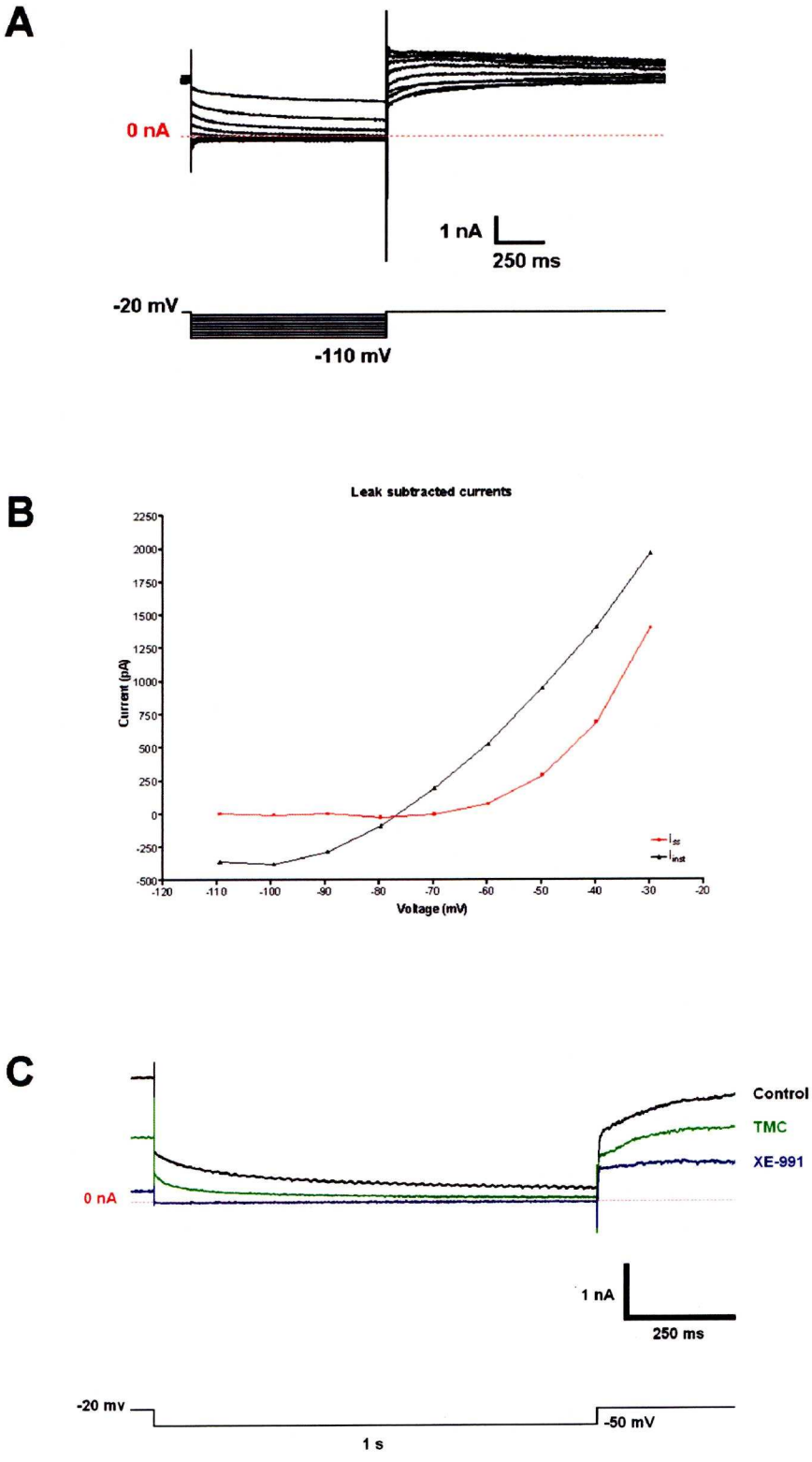
A
0 nA
1 nA
250 ms
-20 mV
-110 mV
B
Leak subtracted currents
Current (pA)
Voltage (mV)
C
Control
TMC
XE-991
0 nA
1 nA
250 ms
-20 mv
-50 mV
1 s

Rundown of the M-current was observed during the 5 min drug wash in period so time-matched controls (TMC) were used for the comparison of agonist effects (Fig. 5.1C). Recordings were performed using the whole-cell configuration and rundown was most likely due to dilution of intracellular second messengers such as ATP and phosphatidylinositol 4,5-bisphosphate ($PIP_2$) (Simmons & Schneider, 1998; Suh & Hille, 2002). During a hyperpolarising pulse, the M-current deactivates slowly after an initial decrease related to the change in command voltage (Brown & Adams, 1980). The instantaneous current ($I_{inst}$) is measured within the first 10 ms of the pulse and the steady-state current ($I_{ss}$) was measured within the last 10 ms of the pulse (Fig. 5.1A, B). The $I_{inst}$ reverses at approximately -78 mV, close to the potassium equilibrium potential ($E_K$) (Fig. 5.1B). Subtraction of the $I_{ss}$ from $I_{inst}$ at a command potential gives the M-current deactivated by the change in voltage. These values will vary between cells depending on the maximum current ($I_{max}$) evoked by the -20 mV holding potential. To normalise the currents measured, the fraction of the maximum conductance ($G_{max}$) activated at each command potential was derived. This is referred to as the relative conductance ($G/G_{max}$).

Application of UTP (10 μM, n=4) significantly reduced the conductance of the M-current ($G_M$) at -30 mV and -40 mV ($p < 0.05$ for both) (Fig. 5.2). In the presence of XE-991 (10 μM, n=4), $G_M$ was significantly reduced at command

potentials of -30 mV ($p < 0.0001$), -40 mV ($p < 0.01$) and -50 mV ($p < 0.05$) (Fig. 5.2). ADP (10 μM, n=4) had no significant effect on $G_M$ (Fig. 5.2). The results were analysed using a MANOVA with a Dunnett t post test.

**Figure 5.2. UTP and XE-991 but not ADP, inhibit M-current conductance in eGFP+ve neurones with epidermal afferents**

This graph plots the M-current $G/G_{max}$ against command potential. Maximal conductance would be time matched control (-20 mV) = 1, if it was shown. The effects of the P2Y agonists UTP, ADP and the selective M-current blocker, XE-991 on $G_M$ are shown in comparison to TMC (n=7, black squares). UTP (10 μM, n=4, blue inverted triangles) inhibited $G_M$ at command potentials of -30 and -40 mV ($p < 0.05$ for both). ADP (10 μM, n=4, red triangles) had no significant effect on $G_M$. The M-current blocker XE-991 (10 μM, n=4, green diamonds) significantly blocked $G_M$ at -30, -40 and -50 mV ($p < 0.0001$, $p < 0.01$ and $p < 0.05$ respectively).

**Figure 5.2.**

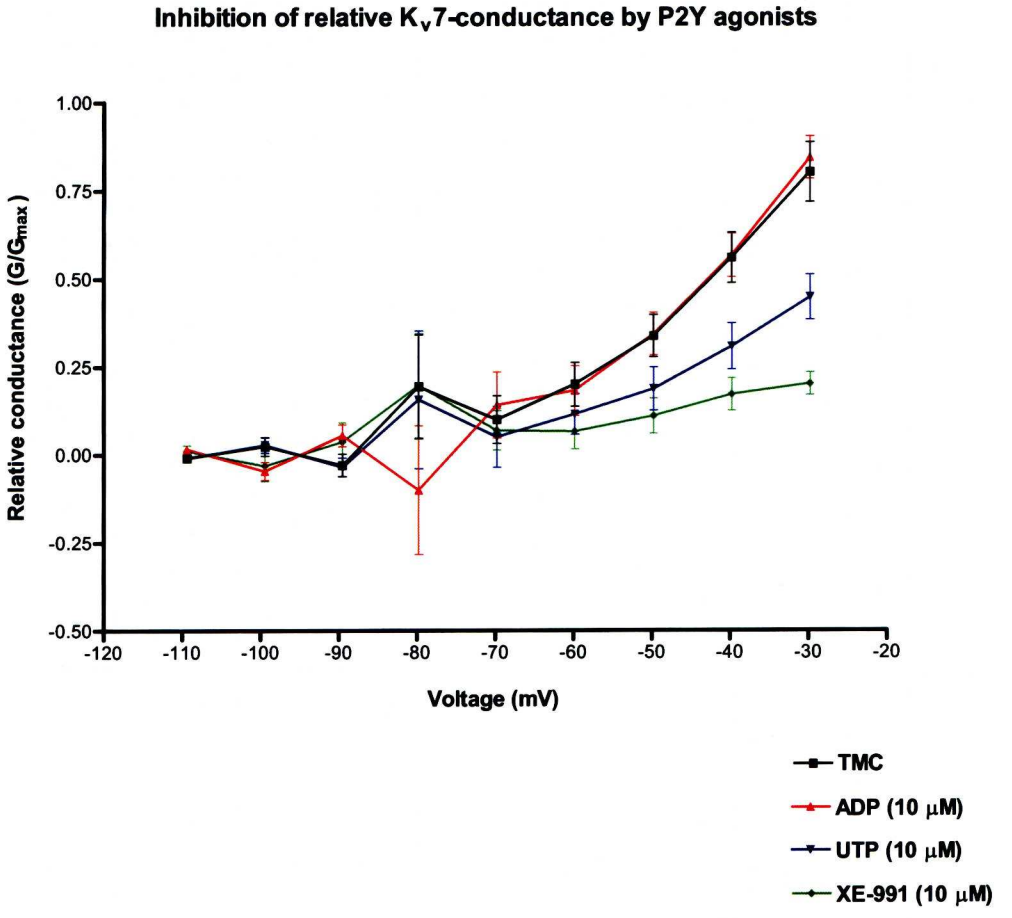
Inhibition of relative $K_V7$-conductance by P2Y agonists
Relative conductance ($G/G_{max}$)
1.00
0.75
0.50
0.25
0.00
-0.25
-0.50
-120
-110
-100
-90
-80
-70
-60
-50
-40
-30
-20
Voltage (mV)
TMC
ADP (10 μM)
UTP (10 μM)
XE-991 (10 μM)

*The effects of P2Y agonists on the excitability of transient-firing, eGFP+ve neurones*

Current-clamp recordings were performed in the absence of 1mM CsCl. Depolarising and hyperpolarising pulses (230 ms, 0.2 Hz) were applied in 100 pA increments (0.1-1 nA) to characterise the firing phenotype before suprathreshold pulses were applied (230 ms, 0.2 Hz). After a stable control period, agonists were bath applied for 5-10 min. The effects of UTP and ADP on transient-firing neurones were examined. Of 20 neurones recorded, 80% (16/20) fired with a transient response to depolarising current pulses. When hyperpolarising current pulses were injected transient-firing cells responded with an $I_h$-like delayed rectification (15/16 cells) and rebound action potential (16/16 cells).

UTP (10 μM) increased afterdepolarisation and secondary spike-firing in 3/5 cells tested (Fig. 5.3A). When ADP (10 μM) was applied the primary spike was blocked in a similar proportion of neurones (2/5 cells) (Fig. 5.3B). The lack of effect in some cells was unexpected so to check if all cells responded to nucleotide agonists or not ATP (10 μM) was bath applied. Spontaneous action potentials were observed in 4/6 cells treated with ATP but increased firing during evoked responses was only observed in 2/6 cells (Fig. 5.3C).

When mean cell diameters for voltage-clamped (n=19) and current-clamped (n=16) neurones were examined no significant difference was observed (27.78 ± 0.48 μm and 28.04 ± 0.51 μm respectively, mean ± SEM, two-tailed, unpaired t-test). Nor was any difference observed in the mean diameters of current-clamped neurones responding (27.38 ± 0.72 μm, n=7) and not responding (28.55 ± 0.70 μm, n=9) to nucleotide agonists. Using a one way ANOVA with Tukey post test, no difference in mean cell diameter was observed between individual experimental groups (voltage-clamp UTP, current-clamp UTP, etc) when compared to each other.

**Figure 5.3. The effects of P2Y agonists on the excitability of transient-firing neurones with epidermal afferents**

A) UTP (10 μM) increases the incidence of afterdepolarisation and secondary spiking in some transient-firing neurones (n=3/5 cells).

B) ADP (10 μM) blocked the primary spike evoked by depolarising current in 2/5 cells tested.

C) Sensitivity of neurones (25-30.56 μm diameter) to nucleotide agonists was tested by bath applying ATP (10 μM). In 4/6 cells, spontaneous action potentials were observed. Increased firing in response to evoked current pulses was detected in 2 of the 4 cells with spontaneous activity.

**Figure 5.3.**

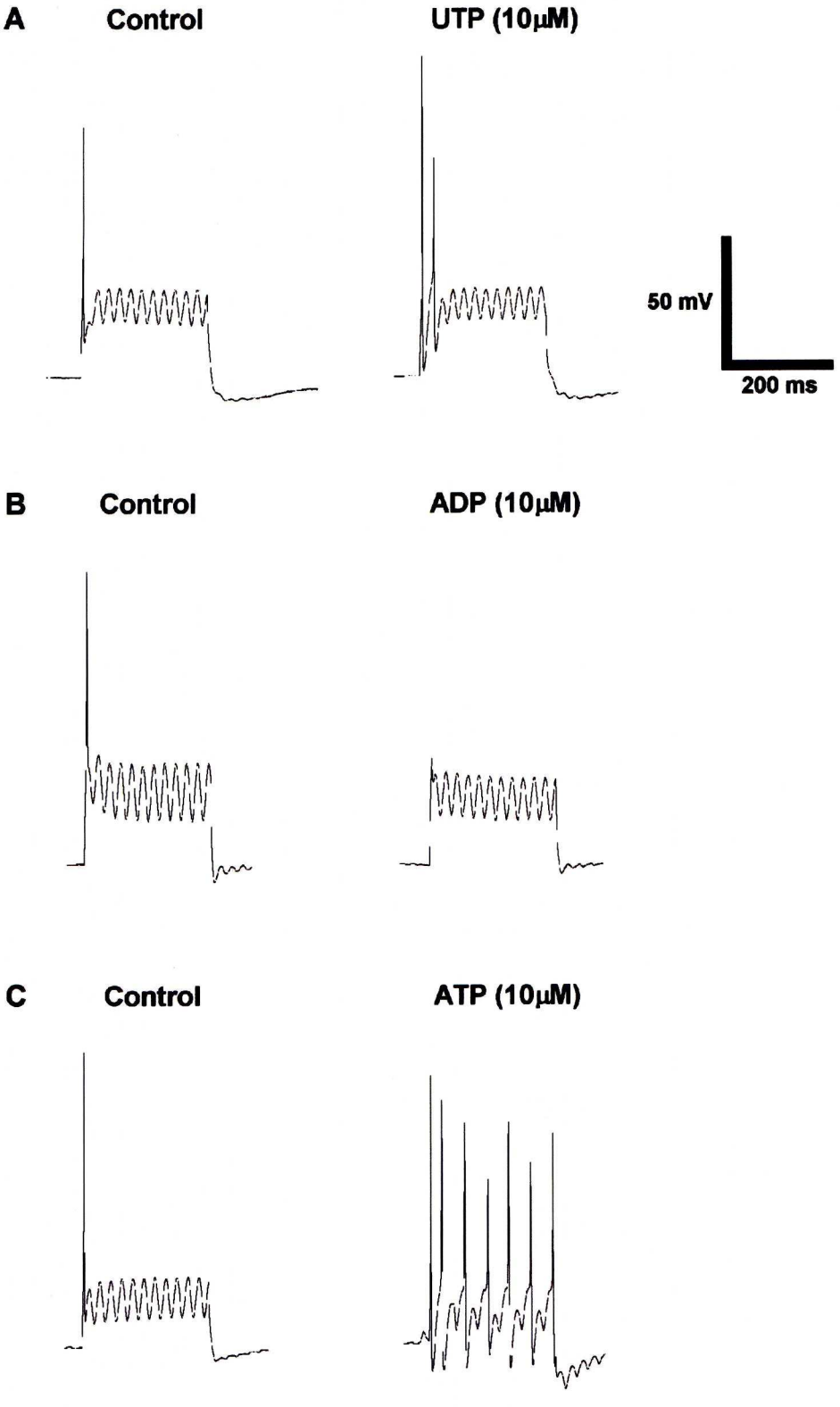
A
Control
UTP (10μM)
50 mV
200 ms
B
Control
ADP (10μM)
C
Control
ATP (10μM)

**Chapter summary**

In a population of cultured eGFP- expressing neurones, whose processes project peripherally to the epidermis in vivo, regulation of excitability by the M-current has been demonstrated. M-current inhibition in rat DRG neurones by β-alanine has previously been reported (Crozier et al., 2007) but whilst it may be implied that these were epidermal afferents from Mrgprd-expression studies in the mouse, it is not certain (Zylka et al., 2005). Inhibition of the M-current by UTP has been demonstrated in bullfrog sympathetic neurones (Adams et al., 1982) and it is known that UTP excites murine cutaneous afferents (Stucky et al., 2004) but a role for the M-current in this action was not speculated. In current-clamp, 10 μM UTP elicits a modest increase in excitability in some neurones.

The $G_M$ was not affected by ADP (10 μM) application but inhibited evoked activity was affected in some cells suggesting it was either acting through a P2Y receptor in a $K_v7$-independent mechanism or that the effects of ADP were P2y/$K_v7$-independent. Due to the high colocalisation of $P2X_3$-ir, ATP was expected to affect the excitability of most eGFP+ve neurones. The higher incidence of spontaneous activity than of increased excitability to evoked responses hints that two mechanisms, probably one P2X3-mediated and one P2Y-mediated, are involved and the robust increase in evoked excitability that was observed may be due to their combined actions.

# Chapter 6

## DISCUSSION AND CONCLUSION

## Discussion

The work collected here outlines a role for a population of transgenically-labelled afferents innervating the epidermis in the monitoring of this tissues status. Although a heterogeneous population of neurones, these cells can be described as predominately small- and medium-sized, ATP-sensitive afferents. There is no colocalisation with either $TRPV_1$ or gastrin-releasing peptide which, in the mouse, are expressed in "peptidergic" neurones (Zwick et al., 2002; Sun & Chen, 2007). The high colocalisation with $P2X_3$ and restricted peripheral terminations would suggest that as a population these neurones are likely to overlap quite considerably with the Mrgprd population described by Zylka et al., (2005). Work on Mrgprd-transgenic mice has revealed that these neurones are not only ATP-sensitive but actually ATP-selective (Dussor et al., 2008). Ablation of this population in adult animals using a directed cytotoxin results in deficits in noxious mechanotransduction but no changes in thermal sensitivity (Cavanaugh et al., 2009). Putatively, these neurones have been classed as nociceptors (Dussor et al., 2008) and are distinguishable from another population of Mrgpr-expressing epidermal tactile afferents by their expression of Runx1 and $P2X_3$ (Liu et al., 2007; Liu et al., 2008; Zylka et al., 2005). Interestingly, oral administration of β-alanine leads to paraesthesia in humans (Harris et al., 2006) but this effect cannot be directly attributed to activation of Mrgprd in the

periphery as β-alanine readily crosses the blood-brain-barrier (Komura et al., 1996) and may have undetermined central effects.

Deinnervation of the epidermis is also observed in the GFRα2-KO mouse (Lindfors et al., 2006). As opposed to the destruction of a population of afferents, "nonpeptidergic" afferents are atrophied and fail to reach the epidermis resulting in a 70% hypoinnervation by "nonpeptidergic" neurones (Lindfors et al., 2006). Despite this, no mechanotransductive deficit was detected but an absence in the persistent phase of the formalin inflammatory pain test was, indicating a role in the second phase of inflammation (Lindfors et al., 2006). The mouse also exhibits similar behaviours in response to formalin-induced inflammatory pain and temperatures above or below thermoneutrality, as the $P2X_3$-KO animal (Lindfors et al., 2006). This is not surprising given the high colocalisation of both GFRα2-ir and $P2X_3$-ir with eGFP-labelled cutaneous afferents in this *thy1.2-eGFP* mouse. $P2X_3$-ir has recently been described in the fine nerve endings of hairy and glabrous skin (Taylor et al., 2009). In mice the separation of "peptide" and "nonpeptide" classes is more distinct than in rat (Price and Flores, 2007). GFRα2 is not expressed alongside CGRP or $TRPV_1$ in mice (Lindfors et al., 2006) making it unlikely that the population of GFRα2-ir/eGFP-ve neurones observed in the thy1.2-eGFP mouse is colocalised with other peptidergic markers. More reasonably, they probably represent a group of "nonpeptidergic" afferents innervating glabrous skin.

The M-current was reported to control the excitability of transient-firing (termed phasic by the authors) DRG neurones in the rat (Crozier et al., 2007). Inhibition of the M-current by activation of Mrgprd with β-alanine led to increased excitability (Crozier et al., 2007). Cutaneous nociceptors are excited by UTP (Stucky et al., 2004) which has been shown to inhibit the M-current in other tissues (Adams et al., 1982). As no source for β-alanine in the epidermis has been suggested (Dussor et al., 2008) and no other endogenous ligands for Mrgprd have been identified (Dussor et al., 2009; Shinohara et al., 2004) we investigated whether the M-current controlled the excitability of transient-firing eGFP+ve neurones in the *thy1.2-eGFP* (SA36) mouse and if it could be modulated through P2Y receptor activation.

Neurones labelled with eGFP expressed $K_V7$ channels leading to a functional M-current which was identified by its unique activation kinetics (Brown and Adams, 1980) and sensitivity to XE-991. UTP blocked the M-current significantly and increased excitability in sensitive cells. Some neurones did not respond to UTP application and did not differ in average soma diameter. This suggests that a population of transient-firing neurones either do not express P2Y or their excitability is not controlled by the M-current. Molliver et al., (2002) showed that 90% of small-sized DRG neurones expressed P2Y2 which has an important role in $TRPV_1$ function (Malin et al., 2008; Moriyama et al., 2003).

Another viable candidate is $P2Y_4$ which is predominately expressed medium-sized DRG neurones and colocalises with $P2X_3$-ir and NF200-ir in 25% and 30% of rat DRG neurones respectively (Ruan and Burnstock, 2003).

Unlike a previous report (Filippov et al., 2006), ADP application did not inhibit the M-current. In current clamp, it blocked the primary spike in a similar proportion of neurones as responded to UTP. In DRG, $P2Y_1$ is highly colocalised with $P2X_3$ (Ruan and Burnstock, 2003) and its activation inhibits both N-type voltage-gated calcium channel- and $P2X_3$-mediated currents (Gerevich et al., 2004; Gerevich et al., 2007). To check if this apparent insensitivity was due to a lack of P2 receptors ATP was bath applied at the same concentration. Spontaneous activity was observed in a greater proportion of neurones but still not all of them responded. This may be due to the range of cell sizes correlating with medium-sized neurones not all of which were P2X3-ir. Amongst the spontaneously active neurones only half showed an increase in excitability during evoked responses but fired with an increased frequency when compared to neurones which responded to UTP. The increased excitability during evoked responses may be a collective effect of $P2X_3$ and $P2Y_{2/4}$ activation whereas $P2X_3$ activation was sufficient to induce the spontaneous activity but not increase excitability during sustained depolarisation.

An $I_h$-like response to hyperpolarisation is frequently observed in transient-firing eGFP+ve DRG neurones. A mechanism of interaction between Ih and the M-current recently reported (George et al., 2009) would enhance low threshold and inhibit high threshold depolarisations of the nerve ending if it were applicable to this system. In "peptidergic" DRG neurones the potentiation of mechanosensitive rapidly-adapting currents by UTP and ATP acting through $P2Y_2$ receptors was recently described (Lechner and Lewin, 2009). They ascribed this effect to an undetermined G-protein-dependent mechanism (Lechner and Lewin, 2009). Keratinocytes may not be the sole source of ATP in the epidermis as under sustained depolarisation DRG neurones are capable of its release (Zeng et al., 2008). Through autoreception P2Y receptors are then activated and leads to oscillations in intracellular calcium concentration (Zeng et al., 2008).

## Conclusions

In a mouse which expresses eGFP in a heterogeneous population of epidermal primary afferents the molecular and physiological characteristics of these cells was investigated. This study found that afferents with small- and medium-sized soma expressed the $P2X_3$ receptor which would confer upon them sensitivity to extracellular ATP. Immunoreactivity for GFRα2 was also observed further supporting the trophic role of neurturin in epidermal innervation. In agreement with the observations of Belle et al., (2007) that these neurones are "nonpeptidergic", no expression of TRPV1 or GRP was found as these are strongly associated with CGRP expression in the mouse.

Physiologically, these neurones can be distinguished from eGFP-ve neurones by their responses to sustained depolarisation. Neurones devoid of eGFP had a lower threshold of activation with a slow ramp of depolarisation until the action potential threshold was reached. This "delay" in firing was a defining characteristic and became reduced as depolarisation magnitude increased finally resulting in a fully tonic firing response without delay. In contrast, eGFP+ve neurones had a higher threshold of activation but responded transiently with a single primary spike at the start of the current pulse. This transient-firing response remained unaffected by increases in the magnitude of depolarising

current. When transient-firing neurones were hyperpolarised responses were frequently observed to have a delayed rectification which is indicative of $I_h$ and were accompanied by a rebound action potential. When these neurones were cultured the transient-firing response remained the predominant phenotype but a marked increase in tonic-firing neurones was observed. Although the modality of transient-firing neurones was not determined, their rapidly adapting response to sustained depolarisation would suggest a role the detection of novel stimuli. Inference from studies in a population of neurones with an almost identical pattern of innervations and similar expression of immunohistochemical markers would suggest that transient-firing, eGFP+ve afferents are mechanosensitive, if not directly then through ATP released from stimulated keratinocytes.

The regulation of cellular excitability in transient-firing neurones was investigated as a potential mechanism of sensitisation. Voltage-clamp experiments identified the $K_v7$-mediated M-current in eGFP+ve neurones. This was inhibited by application of ADP and XE-991 but not ADP suggesting the presence of $P2Y_{2/4}$ coupling to $K_v7$ channels. When the effects of these agonists on cellular excitability were examined it was observed that not all neurones responded to their application. This may have been because the population being used was predominately-medium sized and may have contained less neurones expressing the P2 receptors we were interested in. As expected, UTP increased neuronal excitability through the inhibition of the M-current. The

inhibition of the primary spike by ADP was probably mediated by P2Y1 receptors which are highly colocalised with $P2X_3$ and exert an inhibitory action on excitatory channels. The application of ATP produced an effect from which two responses could be extrapolated, one mediated by $P2X_3$ channels and one mediated by $P2Y_{2/4}$. The spontaneous activity observed during bath application of ATP was not a continuous effect suggesting some form of adaptation and could be explained by tachyphylaxsis of $P2X_3$ ion channels. The increased excitability during sustained depolarisation was observed in a subset of spontaneously active neurones indicating an alternative underlying mechanism. When the excitability of evoked responses was increased the response was greater than observed for UTP alone and may represent the combined effects of $P2X_3$ and $P2Y_{2/4}$ activation. It may be possible to mimic this by coapplication of UTPγS and α,β-methylene ATP, specific agonists of $P2Y_{2/4}$ and $P2X_3$ respectively. Tentatively, from these three populations of transient-firing neurone can be defined: 1) a population without P2 receptors, 2) a population with $P2X_3$ but not $P2Y_{2/4}$, and 3) a population expressing both $P2X_3$ and $P2Y_{2/4}$.

In this scenario, normal ATP release from non-noxious stimulation of a keratinocyte would cause a transient response in the neurone. The M-current would prevent repetitive firing in response to prolonged stimulation. Should a noxious stimulus occur then more ATP would be released and be present for longer leading to recurrent firing of the afferent at a rate determined by tachyphylaxsis of the $P2X_3$ channels present. Coactivation of $P2Y_2$ would inhibit the M-current which would increase the excitability of the neurone if a

second sustained stimulus was applied regardless of whether it was a noxious or innocuous stimulus (Fig. 6.1).

To conclude, eGFP+ve neurones innervating the epidermis detect novel stimuli transduced by keratinocytes through the release of ATP. Under normal conditions they produce a rapidly adapting response to sustained stimulation. Through a process of sensitisation whereby the M-current is inhibited by the activation of $P2Y_{2/4}$ receptors the same previously innocuous stimulation would no longer result in a transient response but a tonic firing of action potentials. This mechanism potentially describes a role for this population of neurones in mechanical hypersensitivity.

**Figure 6.1. Proposed mechanism of sensitisation for eGFP expressing epidermal primary afferents**

This diagram outlines the basic hypothesis for a mechanism of sensitisation through $P2Y_{2/4}$ inhibition of the M-current in transient-firing, eGFP-labelled epidermal afferents in the *thy1.2-egfp* (SA36) mouse.

Under normal conditions innocuous stimulation (e.g. mechanical) of the keratinocytes induces the release of ATP. This causes a brief depolarisation of the nerve-ending sufficient to initiate an action potential. Should the stimulus be sustained then activation of Kv7 channels inhibits further action potentials giving a "transient" response.

If a sufficiently noxious stimulus is applied, then ATP and UTP may be released. ATP activates $P2X_3$ channels causing recurrent depolarisations dependent on the rate of recovery of $P2X_3$ from tachyphylaxis. Coactivation of the $P2Y_{2/4}$ receptor inhibits the $K_v7$-mediated M-current and the cell becomes hyperexcitable. Assuming that the $P2X_3$ channels are inactivated due to tachyphylaxis then a second sustained stimulus would be required to depolarise the nerve ending which would fire tonically without a functional M-current.

**Figure 6.1.**

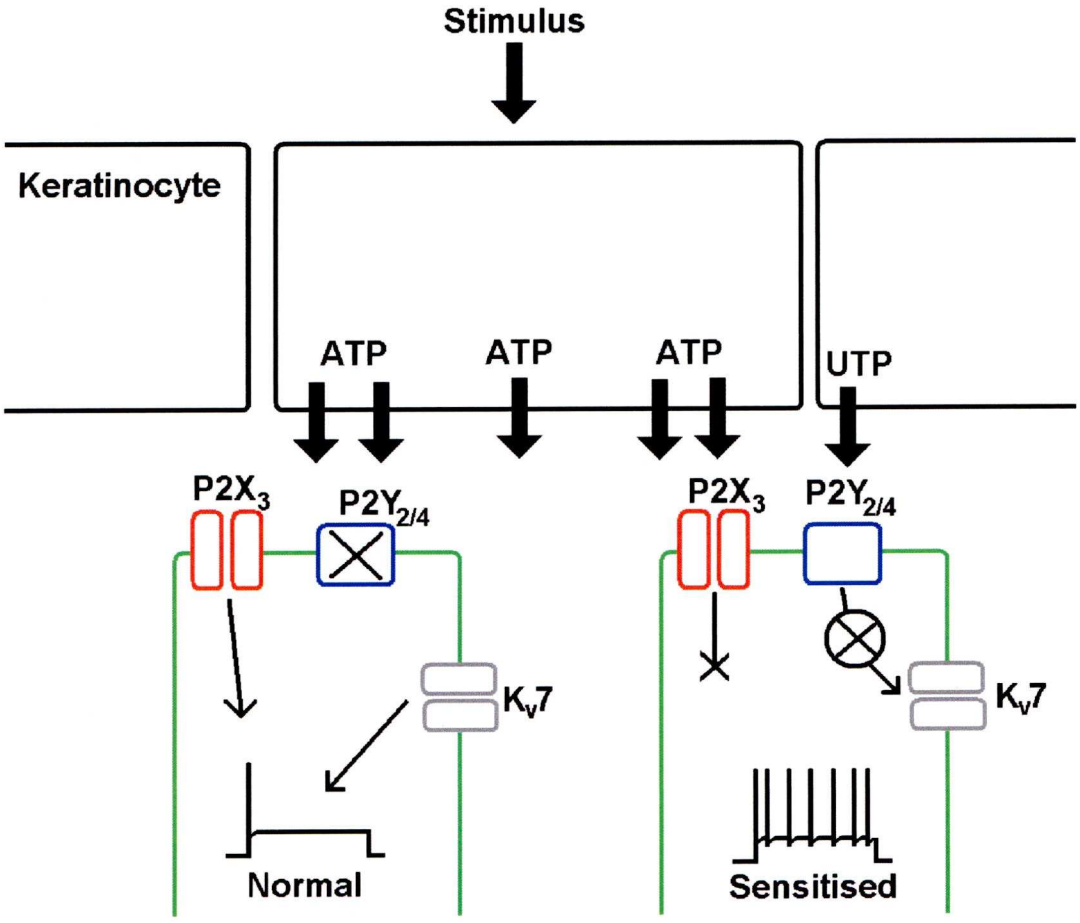
Stimulus
Keratinocyte
ATP
ATP
ATP
UTP
P2X3
P2Y2/4
P2X3
P2Y2/4
Kv7
Kv7
Normal
Sensitised

# References


Adams, P.R., Brown, D.A., and Constanti, A. (1982). Pharmacological inhibition of the M-current. J Physiol *332*, 223-262.

Airaksinen, M.S., and Saarma, M. (2002). The GDNF family: signalling, biological functions and therapeutic value. Nat Rev Neurosci *3*, 383-394.
Albers, K.M., and Davis, B.M. (2007). The skin as a neurotrophic organ. Neuroscientist *13*, 371-382.

Amaral, D. (2001). The Functional Organization of Perception and Movement. In Principles of Neural Science, E. Kandel, J. Schwartz, and T. Jessell, eds. (New York, McGraw-Hill), pp. 337-348.

Atanassoff, P.G., Brull, S.J., Zhang, J., Greenquist, K., Silverman, D.G., and Lamotte, R.H. (1999). Enhancement of experimental pruritus and mechanically evoked dysesthesiae with local anesthesia. Somatosens Mot Res *16*, 291-298.
Babes, A., Zorzon, D., and Reid, G. (2004). Two populations of cold-sensitive neurons in rat dorsal root ganglia and their modulation by nerve growth factor. Eur J Neurosci *20*, 2276-2282.

Bandell, M., Macpherson, L.J., and Patapoutian, A. (2007). From chills to chilis: mechanisms for thermosensation and chemesthesis via thermoTRPs. Curr Opin Neurobiol *17*, 490-497.

Barrandon, Y., and Green, H. (1987). Three clonal types of keratinocyte with different capacities for multiplication. Proc Natl Acad Sci U S A *84*, 2302-2306.
Bautista, D.M., Jordt, S.E., Nikai, T., Tsuruda, P.R., Read, A.J., Poblete, J., Yamoah, E.N., Basbaum, A.I., and Julius, D. (2006). TRPA1 mediates the inflammatory actions of environmental irritants and proalgesic agents. Cell *124*, 1269-1282.

Belle, M.D., Pattison, E.F., Cheunsuang, O., Stewart, A., Kramer, I., Sigrist, M., Arber, S., and Morris, R. (2007). Characterization of a thy1.2 GFP transgenic mouse reveals a tissue-specific organization of the spinal dorsal horn. Genesis *45*, 679-688.

Belmonte, C., and Viana, F. (2008). Molecular and cellular limits to somatosensory specificity. Mol Pain *4*, 14.

Bessou, P., and Perl, E.R. (1969). Response of cutaneous sensory units with unmyelinated fibers to noxious stimuli. J Neurophysiol *32*, 1025-1043.

Bobker, D.H., and Williams, J.T. (1989). Serotonin augments the cationic current Ih in central neurons. Neuron *2*, 1535-1540.

Boulais, N., and Misery, L. (2008). The epidermis: a sensory tissue. Eur J Dermatol *18*, 119-127.

Bradbury, E.J., Burnstock, G., and McMahon, S.B. (1998). The expression of P2X3 purinoreceptors in sensory neurons: effects of axotomy and glial-derived neurotrophic factor. Mol Cell Neurosci *12*, 256-268.

Brauchi, S., Orta, G., Salazar, M., Rosenmann, E., and Latorre, R. (2006). A hot-sensing cold receptor: C-terminal domain determines thermosensation in transient receptor potential channels. J Neurosci *26*, 4835-4840.

Brewer, G.J., Torricelli, J.R., Evege, E.K., and Price, P.J. (1993). Optimized survival of hippocampal neurons in B27-supplemented Neurobasal, a new serum-free medium combination. J Neurosci Res *35*, 567-576.

Brown, A.G., and Iggo, A. (1967). A quantitative study of cutaneous receptors and afferent fibres in the cat and rabbit. J Physiol *193*, 707-733.

Brown, D.A., and Adams, P.R. (1980). Muscarinic suppression of a novel voltage-sensitive K+ current in a vertebrate neurone. Nature *283*, 673-676.

Buj-Bello, A., Adu, J., Pinon, L.G., Horton, A., Thompson, J., Rosenthal, A., Chinchetru, M., Buchman, V.L., and Davies, A.M. (1997). Neurturin responsiveness requires a GPI-linked receptor and the Ret receptor tyrosine kinase. Nature *387*, 721-724.

Burnstock, G., and Kennedy, C. (1985). Is there a basis for distinguishing two types of P2-purinoceptor? Gen Pharmacol *16*, 433-440.

Calixto, J.B., Kassuya, C.A., Andre, E., and Ferreira, J. (2005). Contribution of natural products to the discovery of the transient receptor potential (TRP) channels family and their functions. Pharmacol Ther *106*, 179-208.

Caroni, P. (1997). Overexpression of growth-associated proteins in the neurons of adult transgenic mice. J Neurosci Methods *71*, 3-9.

Caterina, M.J., Schumacher, M.A., Tominaga, M., Rosen, T.A., Levine, J.D., and Julius, D. (1997). The capsaicin receptor: a heat-activated ion channel in the pain pathway. Nature *389*, 816-824.

Cavanaugh, D.J., Lee, H., Lo, L., Shields, S.D., Zylka, M.J., Basbaum, A.I., and Anderson, D.J. (2009). Distinct subsets of unmyelinated primary sensory fibers

mediate behavioral responses to noxious thermal and mechanical stimuli. Proc Natl Acad Sci U S A *106*, 9075-9080.

Chateau, Y., and Misery, L. (2004). Connections between nerve endings and epidermal cells: are they synapses? Exp Dermatol *13*, 2-4.

Chen, C.C., Akopian, A.N., Sivilotti, L., Colquhoun, D., Burnstock, G., and Wood, J.N. (1995). A P2X purinoceptor expressed by a subset of sensory neurons. Nature *377*, 428-431.

Chen, C.L., Broom, D.C., Liu, Y., de Nooij, J.C., Li, Z., Cen, C., Samad, O.A., Jessell, T.M., Woolf, C.J., and Ma, Q. (2006). Runx1 determines nociceptive sensory neuron phenotype and is required for thermal and neuropathic pain. Neuron *49*, 365-377.

Church, D., Elsayed, S., Reid, O., Winston, B., and Lindsay, R. (2006). Burn wound infections. Clin Microbiol Rev *19*, 403-434.

Cook, S.P., and McCleskey, E.W. (2002). Cell damage excites nociceptors through release of cytosolic ATP. Pain *95*, 41-47.

Crozier, R.A., Ajit, S.K., Kaftan, E.J., and Pausch, M.H. (2007). MrgD activation inhibits KCNQ/M-currents and contributes to enhanced neuronal excitability. J Neurosci *27*, 4492-4496.

Cuello, A.C., Priestley, J.V., and Sofroniew, M.V. (1983). Immunocytochemistry and neurobiology. Q J Exp Physiol *68*, 545-578.

De Paola, V., Arber, S., and Caroni, P. (2003). AMPA receptors regulate dynamic equilibrium of presynaptic terminals in mature hippocampal networks. Nat Neurosci *6*, 491-500.

Denda, M., Nakatani, M., Ikeyama, K., Tsutsumi, M., and Denda, S. (2007). Epidermal keratinocytes as the forefront of the sensory system. Exp Dermatol *16*, 157-161.

Dhaka, A., Murray, A.N., Mathur, J., Earley, T.J., Petrus, M.J., and Patapoutian, A. (2007). TRPM8 is required for cold sensation in mice. Neuron *54*, 371-378.
Dhaka, A., Uzzell, V., Dubin, A.E., Mathur, J., Petrus, M., Bandell, M., and Patapoutian, A. (2009). TRPV1 is activated by both acidic and basic pH. J Neurosci *29*, 153-158.

Dixon, C.J., Bowler, W.B., Littlewood-Evans, A., Dillon, J.P., Bilbe, G., Sharpe, G.R., and Gallagher, J.A. (1999). Regulation of epidermal homeostasis through P2Y2 receptors. Br J Pharmacol *127*, 1680-1686.

Dong, X., Han, S., Zylka, M.J., Simon, M.I., and Anderson, D.J. (2001). A diverse family of GPCRs expressed in specific subsets of nociceptive sensory neurons. Cell *106*, 619-632.

Dost, R., Rostock, A., and Rundfeldt, C. (2004). The anti-hyperalgesic activity of retigabine is mediated by KCNQ potassium channel activation. Naunyn Schmiedebergs Arch Pharmacol *369*, 382-390.

Durbec, P., Marcos-Gutierrez, C.V., Kilkenny, C., Grigoriou, M., Wartiowaara, K., Suvanto, P., Smith, D., Ponder, B., Costantini, F., Saarma, M., *et al.* (1996). GDNF signalling through the Ret receptor tyrosine kinase. Nature *381*, 789-793.

Dussor, G., Koerber, H.R., Oaklander, A.L., Rice, F.L., and Molliver, D.C. (2009). Nucleotide signaling and cutaneous mechanisms of pain transduction. Brain Res Rev *60*, 24-35.

Dussor, G., Zylka, M.J., Anderson, D.J., and McCleskey, E.W. (2008). Cutaneous sensory neurons expressing the Mrgprd receptor sense extracellular ATP and are putative nociceptors. J Neurophysiol *99*, 1581-1589.

Filippov, A.K., Choi, R.C., Simon, J., Barnard, E.A., and Brown, D.A. (2006). Activation of P2Y1 nucleotide receptors induces inhibition of the M-type K+ current in rat hippocampal pyramidal neurons. J Neurosci *26*, 9340-9348.

Fuchs, E., and Raghavan, S. (2002). Getting under the skin of epidermal morphogenesis. Nat Rev Genet *3*, 199-209.

Fundin, B.T., Arvidsson, J., Aldskogius, H., Johansson, O., Rice, S.N., and Rice, F.L. (1997). Comprehensive immunofluorescence and lectin binding analysis of intervibrissal fur innervation in the mystacial pad of the rat. J Comp Neurol *385*, 185-206.

Furuse, M., Hata, M., Furuse, K., Yoshida, Y., Haratake, A., Sugitani, Y., Noda, T., Kubo, A., and Tsukita, S. (2002). Claudin-based tight junctions are crucial for the mammalian epidermal barrier: a lesson from claudin-1-deficient mice. J Cell Biol *156*, 1099-1111.

Gallego, R., and Eyzaguirre, C. (1978). Membrane and action potential characteristics of A and C nodose ganglion cells studied in whole ganglia and in tissue slices. J Neurophysiol *41*, 1217-1232.

Gardner, E., Martin, J., and Jessell, T. (2000). The Bodily Senses. In Principles of Neural Science, E. Kandel, J. Schwartz, and T. Jessell, eds. (New York, McGraw-Hill), pp. 430-450.

George, M.S., Abbott, L.F., and Siegelbaum, S.A. (2009). HCN hyperpolarization-activated cation channels inhibit EPSPs by interactions with M-type K(+) channels. Nat Neurosci *12*, 577-584.

Gerevich, Z., Borvendeg, S.J., Schroder, W., Franke, H., Wirkner, K., Norenberg, W., Furst, S., Gillen, C., and Illes, P. (2004). Inhibition of N-type voltage-activated calcium channels in rat dorsal root ganglion neurons by P2Y receptors is a possible mechanism of ADP-induced analgesia. J Neurosci *24*, 797-807.

Gerevich, Z., Zadori, Z., Muller, C., Wirkner, K., Schroder, W., Rubini, P., and Illes, P. (2007). Metabotropic P2Y receptors inhibit P2X3 receptor-channels via G protein-dependent facilitation of their desensitization. Br J Pharmacol *151*, 226-236.

Gold, M.S., Levine, J.D., and Correa, A.M. (1998). Modulation of TTX-R INa by PKC and PKA and their role in PGE2-induced sensitization of rat sensory neurons in vitro. J Neurosci *18*, 10345-10355.

Goldstein, M.E., House, S.B., and Gainer, H. (1991). NF-L and peripherin immunoreactivities define distinct classes of rat sensory ganglion cells. J Neurosci Res *30*, 92-104.

Greig, A.V., Linge, C., Terenghi, G., McGrouther, D.A., and Burnstock, G. (2003). Purinergic receptors are part of a functional signaling system for proliferation and differentiation of human epidermal keratinocytes. J Invest Dermatol *120*, 1007-1015.

Gu, J.G., and MacDermott, A.B. (1997). Activation of ATP P2X receptors elicits glutamate release from sensory neuron synapses. Nature *389*, 749-753.
Guo, A., Vulchanova, L., Wang, J., Li, X., and Elde, R. (1999).

Immunocytochemical localization of the vanilloid receptor 1 (VR1): relationship to neuropeptides, the P2X3 purinoceptor and IB4 binding sites. Eur J Neurosci *11*, 946-958.

Gutman, G.A., Chandy, K.G., Grissmer, S., Lazdunski, M., McKinnon, D., Pardo, L.A., Robertson, G.A., Rudy, B., Sanguinetti, M.C., Stuhmer, W., *et al.* (2005). International Union of Pharmacology. LIII. Nomenclature and molecular relationships of voltage-gated potassium channels. Pharmacol Rev *57*, 473-508.

Haake, A., Scott, G., and Holbrook, K. (2001). Structure and function of the skin: overview of the epidermis and dermis. In The Biology of the Skin, R. Freinkel, and D. Woodley, eds. (New York, Parthenon), pp. 19-46.

Hamann, W. (1995). Mammalian cutaneous mechanoreceptors. Prog Biophys Mol Biol *64*, 81-104.

Hamill, O.P., Marty, A., Neher, E., Sakmann, B., and Sigworth, F.J. (1981). Improved patch-clamp techniques for high-resolution current recording from cells and cell-free membrane patches. Pflugers Arch *391*, 85-100.

Harlan, D.M., Graff, J.M., Stumpo, D.J., Eddy, R.L., Jr., Shows, T.B., Boyle, J.M., and Blackshear, P.J. (1991). The human myristoylated alanine-rich C kinase substrate (MARCKS) gene (MACS). Analysis of its gene product, promoter, and chromosomal localization. J Biol Chem *266*, 14399-14405.

Harris, R.C., Tallon, M.J., Dunnett, M., Boobis, L., Coakley, J., Kim, H.J., Fallowfield, J.L., Hill, C.A., Sale, C., and Wise, J.A. (2006). The absorption of orally supplied beta-alanine and its effect on muscle carnosine synthesis in human vastus lateralis. Amino Acids *30*, 279-289.

Heisig, M., Lieckfeldt, R., Wittum, G., Mazurkevich, G., and Lee, G. (1996). Non steady-state descriptions of drug permeation through stratum corneum. I. The biphasic brick-and-mortar model. Pharm Res *13*, 421-426.

Herzog, R.I., Cummins, T.R., and Waxman, S.G. (2001). Persistent TTX-resistant Na+ current affects resting potential and response to depolarization in simulated spinal sensory neurons. J Neurophysiol *86*, 1351-1364.

Hjerling-Leffler, J., Alqatari, M., Ernfors, P., and Koltzenburg, M. (2007). Emergence of functional sensory subtypes as defined by transient receptor potential channel expression. J Neurosci *27*, 2435-2443.

Houben, E., De Paepe, K., and Rogiers, V. (2007). A keratinocyte's course of life. Skin Pharmacol Physiol *20*, 122-132.

Huang, J., Zhang, X., and McNaughton, P.A. (2006). Inflammatory pain: the cellular basis of heat hyperalgesia. Curr Neuropharmacol *4*, 197-206.

Huang, S.M., Lee, H., Chung, M.K., Park, U., Yu, Y.Y., Bradshaw, H.B., Coulombe, P.A., Walker, J.M., and Caterina, M.J. (2008). Overexpressed transient receptor potential vanilloid 3 ion channels in skin keratinocytes modulate pain sensitivity via prostaglandin E2. J Neurosci *28*, 13727-13737.

Huguenard, J.R. (1996). Low-threshold calcium currents in central nervous system neurons. Annu Rev Physiol *58*, 329-348.

Hunt, S.P., and Rossi, J. (1985). Peptide- and non-peptide-containing unmyelinated primary afferents: the parallel processing of nociceptive information. Philos Trans R Soc Lond B Biol Sci *308*, 283-289.

Ibrahim, M.M., Porreca, F., Lai, J., Albrecht, P.J., Rice, F.L., Khodorova, A., Davar, G., Makriyannis, A., Vanderah, T.W., Mata, H.P., *et al.* (2005). CB2 cannabinoid receptor activation produces antinociception by stimulating peripheral release of endogenous opioids. Proc Natl Acad Sci U S A *102*, 3093-3098.

Ichikawa, H., Jacobowitz, D.M., and Sugimoto, T. (1997). Coexpression of calretinin and parvalbumin in Ruffini-like endings in the rat incisor periodontal ligament. Brain Res *770*, 294-297.

Ichikawa, H., and Sugimoto, T. (1997). Parvalbumin- and calbindin D-28k-immunoreactive innervation of orofacial tissues in the rat. Exp Neurol *146*, 414-418.

Iggo, A. (1960). Cutaneous mechanoreceptors with afferent C fibres. J Physiol *152*, 337-353.

Ikoma, A., Steinhoff, M., Stander, S., Yosipovitch, G., and Schmelz, M. (2006). The neurobiology of itch. Nat Rev Neurosci *7*, 535-547.

Janeke, G., Siefken, W., Carstensen, S., Springmann, G., Bleck, O., Steinhart, H., Hoger, P., Wittern, K.P., Wenck, H., Stab, F., *et al.* (2003). Role of taurine accumulation in keratinocyte hydration. J Invest Dermatol *121*, 354-361.

Jentsch, T.J. (2000). Neuronal KCNQ potassium channels: physiology and role in disease. Nat Rev Neurosci *1*, 21-30.

Jessell, T.M., and Dodd, J. (1985). Structure and expression of differentiation antigens on functional subclasses of primary sensory neurons. Philos Trans R Soc Lond B Biol Sci *308*, 271-281.

Ji, R.R., Kohno, T., Moore, K.A., and Woolf, C.J. (2003). Central sensitization and LTP: do pain and memory share similar mechanisms? Trends Neurosci *26*, 696-705.

Jing, S., Wen, D., Yu, Y., Holst, P.L., Luo, Y., Fang, M., Tamir, R., Antonio, L., Hu, Z., Cupples, R., *et al.* (1996). GDNF-induced activation of the ret protein tyrosine kinase is mediated by GDNFR-alpha, a novel receptor for GDNF. Cell *85*, 1113-1124.

Johnson, E.M., Jr., Gorin, P.D., Brandeis, L.D., and Pearson, J. (1980). Dorsal root ganglion neurons are destroyed by exposure in utero to maternal antibody to nerve growth factor. Science *210*, 916-918.

Johnson, K.O. (2001). The roles and functions of cutaneous mechanoreceptors. Curr Opin Neurobiol *11*, 455-461.
Jones, P.H., and Watt, F.M. (1993). Separation of human epidermal stem cells from transit amplifying cells on the basis of differences in integrin function and expression. Cell *73*, 713-724.

Jordt, S.E., McKemy, D.D., and Julius, D. (2003). Lessons from peppers and peppermint: the molecular logic of thermosensation. Curr Opin Neurobiol *13*, 487-492.

Khodorova, A., Fareed, M.U., Gokin, A., Strichartz, G.R., and Davar, G. (2002). Local injection of a selective endothelin-B receptor agonist inhibits endothelin-1-induced pain-like behavior and excitation of nociceptors in a naloxone-sensitive manner. J Neurosci *22*, 7788-7796.

Khodorova, A., Navarro, B., Jouaville, L.S., Murphy, J.E., Rice, F.L., Mazurkiewicz, J.E., Long-Woodward, D., Stoffel, M., Strichartz, G.R., Yukhananov, R., *et al.* (2003). Endothelin-B receptor activation triggers an endogenous analgesic cascade at sites of peripheral injury. Nat Med *9*, 1055-1061.

Klein, R.D., Sherman, D., Ho, W.H., Stone, D., Bennett, G.L., Moffat, B., Vandlen, R., Simmons, L., Gu, Q., Hongo, J.A., *et al.* (1997). A GPI-linked protein that interacts with Ret to form a candidate neurturin receptor. Nature *387*, 717-721.

Ko, M.C., Song, M.S., Edwards, T., Lee, H., and Naughton, N.N. (2004). The role of central mu opioid receptors in opioid-induced itch in primates. J Pharmacol Exp Ther *310*, 169-176.

Koerber, H.R., Druzinsky, R.E., and Mendell, L.M. (1988). Properties of somata of spinal dorsal root ganglion cells differ according to peripheral receptor innervated. J Neurophysiol *60*, 1584-1596.

Koizumi, S., Fujishita, K., Inoue, K., Shigemoto-Mogami, Y., and Tsuda, M. (2004). Ca2+ waves in keratinocytes are transmitted to sensory neurons: the involvement of extracellular ATP and P2Y2 receptor activation. Biochem J *380*, 329-338.

Koltzenburg, M., Stucky, C.L., and Lewin, G.R. (1997). Receptive properties of mouse sensory neurons innervating hairy skin. J Neurophysiol *78*, 1841-1850.

Komura, J., Tamai, I., Senmaru, M., Terasaki, T., Sai, Y., and Tsuji, A. (1996). Sodium and chloride ion-dependent transport of beta-alanine across the blood-brain barrier. J Neurochem *67*, 330-335.

Kwan, K.Y., Allchorne, A.J., Vollrath, M.A., Christensen, A.P., Zhang, D.S., Woolf, C.J., and Corey, D.P. (2006). TRPA1 contributes to cold, mechanical, and chemical nociception but is not essential for hair-cell transduction. Neuron *50*, 277-289.

Lawson, S.N. (1979). The postnatal development of large light and small dark neurons in mouse dorsal root ganglia: a statistical analysis of cell numbers and size. J Neurocytol *8*, 275-294.

Lechner, S.G., and Lewin, G.R. (2009). Peripheral sensitisation of nociceptors via G-protein-dependent potentiation of mechanotransduction currents. J Physiol *587*, 3493-3503.

Lerche, C., Scherer, C.R., Seebohm, G., Derst, C., Wei, A.D., Busch, A.E., and Steinmeyer, K. (2000). Molecular cloning and functional expression of KCNQ5, a potassium channel subunit that may contribute to neuronal M-current diversity. J Biol Chem *275*, 22395-22400.

Lewin, G.R., and Moshourab, R. (2004). Mechanosensation and pain. J Neurobiol *61*, 30-44.

Lindfors, P.H., Voikar, V., Rossi, J., and Airaksinen, M.S. (2006). Deficient nonpeptidergic epidermis innervation and reduced inflammatory pain in glial cell line-derived neurotrophic factor family receptor alpha2 knock-out mice. J Neurosci *26*, 1953-1960.

Liu, Q., Vrontou, S., Rice, F.L., Zylka, M.J., Dong, X., and Anderson, D.J. (2007). Molecular genetic visualization of a rare subset of unmyelinated sensory neurons that may detect gentle touch. Nat Neurosci *10*, 946-948.

Liu, Y., Yang, F.C., Okuda, T., Dong, X., Zylka, M.J., Chen, C.L., Anderson, D.J., Kuner, R., and Ma, Q. (2008). Mechanisms of compartmentalized expression of Mrg class G-protein-coupled sensory receptors. J Neurosci *28*, 125-132.

Livet, J., Sigrist, M., Stroebel, S., De Paola, V., Price, S.R., Henderson, C.E., Jessell, T.M., and Arber, S. (2002). ETS gene Pea3 controls the central position and terminal arborization of specific motor neuron pools. Neuron *35*, 877-892.

Loken, L.S., Wessberg, J., Morrison, I., McGlone, F., and Olausson, H. (2009). Coding of pleasant touch by unmyelinated afferents in humans. Nat Neurosci *12*, 547-548.

Lumpkin, E.A., and Caterina, M.J. (2007). Mechanisms of sensory transduction in the skin. Nature *445*, 858-865.

Luo, W., Wickramasinghe, S.R., Savitt, J.M., Griffin, J.W., Dawson, T.M., and Ginty, D.D. (2007). A hierarchical NGF signaling cascade controls Ret-dependent and Ret-independent events during development of nonpeptidergic DRG neurons. Neuron *54*, 739-754.

Macpherson, L.J., Dubin, A.E., Evans, M.J., Marr, F., Schultz, P.G., Cravatt, B.F., and Patapoutian, A. (2007). Noxious compounds activate TRPA1 ion channels through covalent modification of cysteines. Nature *445*, 541-545.

Macpherson, L.J., Hwang, S.W., Miyamoto, T., Dubin, A.E., Patapoutian, A., and Story, G.M. (2006). More than cool: promiscuous relationships of menthol and other sensory compounds. Mol Cell Neurosci *32*, 335-343.

Madison, K.C. (2003). Barrier function of the skin: "la raison d'etre" of the epidermis. J Invest Dermatol *121*, 231-241.

Madison, K.C., Swartzendruber, D.C., Wertz, P.W., and Downing, D.T. (1987). Presence of intact intercellular lipid lamellae in the upper layers of the stratum corneum. J Invest Dermatol *88*, 714-718.

Main, M.J., Cryan, J.E., Dupere, J.R., Cox, B., Clare, J.J., and Burbidge, S.A. (2000). Modulation of KCNQ2/3 potassium channels by the novel anticonvulsant retigabine. Mol Pharmacol *58*, 253-262.

Malin, S.A., Davis, B.M., Koerber, H.R., Reynolds, I.J., Albers, K.M., and Molliver, D.C. (2008). Thermal nociception and TRPV1 function are attenuated in mice lacking the nucleotide receptor P2Y2. Pain *138*, 484-496.

Maljevic, S., Wuttke, T.V., and Lerche, H. (2008). Nervous system KV7 disorders: breakdown of a subthreshold brake. J Physiol *586*, 1791-1801.

McKemy, D.D., Neuhausser, W.M., and Julius, D. (2002). Identification of a cold receptor reveals a general role for TRP channels in thermosensation. Nature *416*, 52-58.

Merad, M., Ginhoux, F., and Collin, M. (2008). Origin, homeostasis and function of Langerhans cells and other langerin-expressing dendritic cells. Nat Rev Immunol *8*, 935-947.

Metze, D. (2001). Neurophysiology of the skin--functional anatomy of the skin nervous system. Exp Dermatol *10*, 365-366.

Millan, M.J. (1999). The induction of pain: an integrative review. Prog Neurobiol *57*, 1-164.

Molliver, D.C., Cook, S.P., Carlsten, J.A., Wright, D.E., and McCleskey, E.W. (2002). ATP and UTP excite sensory neurons and induce CREB phosphorylation through the metabotropic receptor, P2Y2. Eur J Neurosci *16*, 1850-1860.

Molliver, D.C., and Snider, W.D. (1997). Nerve growth factor receptor TrkA is down-regulated during postnatal development by a subset of dorsal root ganglion neurons. J Comp Neurol *381*, 428-438.

Molliver, D.C., Wright, D.E., Leitner, M.L., Parsadanian, A.S., Doster, K., Wen, D., Yan, Q., and Snider, W.D. (1997). IB4-binding DRG neurons switch from NGF to GDNF dependence in early postnatal life. Neuron *19*, 849-861.

Momin, A., and McNaughton, P.A. (2009). Regulation of firing frequency in nociceptive neurons by pro-inflammatory mediators. Exp Brain Res *196*, 45-52.

Moriyama, T., Iida, T., Kobayashi, K., Higashi, T., Fukuoka, T., Tsumura, H., Leon, C., Suzuki, N., Inoue, K., Gachet, C., *et al.* (2003). Possible involvement of P2Y2 metabotropic receptors in ATP-induced transient receptor potential vanilloid receptor 1-mediated thermal hypersensitivity. J Neurosci *23*, 6058-6062.

Mullen, R.J., Buck, C.R., and Smith, A.M. (1992). NeuN, a neuronal specific nuclear protein in vertebrates. Development *116*, 201-211.

Munger, B.L., and Ide, C. (1988). The structure and function of cutaneous sensory receptors. Arch Histol Cytol *51*, 1-34.

Nagy, J.I., and Hunt, S.P. (1982). Fluoride-resistant acid phosphatase-containing neurones in dorsal root ganglia are separate from those containing substance P or somatostatin. Neuroscience *7*, 89-97.

Navarro, X., Verdu, E., Wendelscafer-Crabb, G., and Kennedy, W.R. (1995). Innervation of cutaneous structures in the mouse hind paw: a confocal microscopy immunohistochemical study. J Neurosci Res *41*, 111-120.

Neumann, S., Braz, J.M., Skinner, K., Llewellyn-Smith, I.J., and Basbaum, A.I. (2008). Innocuous, not noxious, input activates PKCgamma interneurons of the spinal dorsal horn via myelinated afferent fibers. J Neurosci *28*, 7936-7944.

Noel, J., Zimmermann, K., Busserolles, J., Deval, E., Alloui, A., Diochot, S., Guy, N., Borsotto, M., Reeh, P., Eschalier, A., *et al.* (2009). The mechano-activated K+ channels TRAAK and TREK-1 control both warm and cold perception. EMBO J *28*, 1308-1318.

Norrsell, U., Finger, S., and Lajonchere, C. (1999). Cutaneous sensory spots and the "law of specific nerve energies": history and development of ideas. Brain Res Bull *48*, 457-465.

Passmore, G.M., Selyanko, A.A., Mistry, M., Al-Qatari, M., Marsh, S.J., Matthews, E.A., Dickenson, A.H., Brown, T.A., Burbidge, S.A., Main, M., *et al.* (2003). KCNQ/M currents in sensory neurons: significance for pain therapy. J Neurosci *23*, 7227-7236.

Patapoutian, A., Peier, A.M., Story, G.M., and Viswanath, V. (2003). ThermoTRP channels and beyond: mechanisms of temperature sensation. Nat Rev Neurosci *4*, 529-539.

Pearson, K., and Gordon, J. (2001). Spinal Reflexes. In Principles of Neural Science, E. Kandel, J. Schwartz, and T. Jessell, eds. (New York, McGraw-Hill), pp. 713-7737.

Peier, A.M., Moqrich, A., Hergarden, A.C., Reeve, A.J., Andersson, D.A., Story, G.M., Earley, T.J., Dragoni, I., McIntyre, P., Bevan, S., *et al.* (2002a). A TRP channel that senses cold stimuli and menthol. Cell *108*, 705-715.

Peier, A.M., Reeve, A.J., Andersson, D.A., Moqrich, A., Earley, T.J., Hergarden, A.C., Story, G.M., Colley, S., Hogenesch, J.B., McIntyre, P., *et al.* (2002b). A heat-sensitive TRP channel expressed in keratinocytes. Science *296*, 2046-2049.

Price, T.J., and Flores, C.M. (2007). Critical evaluation of the colocalization between calcitonin gene-related peptide, substance P, transient receptor potential vanilloid subfamily type 1 immunoreactivities, and isolectin B4 binding in primary afferent neurons of the rat and mouse. J Pain *8*, 263-272.

Proksch, E., Brandner, J.M., and Jensen, J.M. (2008). The skin: an indispensable barrier. Exp Dermatol *17*, 1063-1072.

Ramsey, I.S., Delling, M., and Clapham, D.E. (2006). An introduction to TRP channels. Annu Rev Physiol *68*, 619-647.

Rau, K.K., Johnson, R.D., and Cooper, B.Y. (2005). Nicotinic AChR in subclassified capsaicin-sensitive and -insensitive nociceptors of the rat DRG. J Neurophysiol *93*, 1358-1371.

Reid, G., and Flonta, M. (2001). Cold transduction by inhibition of a background potassium conductance in rat primary sensory neurones. Neurosci Lett *297*, 171-174.

Reinisch, C.M., and Tschachler, E. (2005). The touch dome in human skin is supplied by different types of nerve fibers. Ann Neurol *58*, 88-95.

Renganathan, M., Cummins, T.R., and Waxman, S.G. (2001). Contribution of Na(v)1.8 sodium channels to action potential electrogenesis in DRG neurons. J Neurophysiol *86*, 629-640.

Rexed, B. (1952). The cytoarchitectonic organization of the spinal cord in the cat. J Comp Neurol *96*, 414-495.

Ruan, H.Z., and Burnstock, G. (2003). Localisation of P2Y1 and P2Y4 receptors in dorsal root, nodose and trigeminal ganglia of the rat. Histochem Cell Biol *120*, 415-426.

Ruscheweyh, R., and Sandkuhler, J. (2002). Lamina-specific membrane and discharge properties of rat spinal dorsal horn neurones in vitro. J Physiol *541*, 231-244.

Schepers, R.J., and Ringkamp, M. (2009). Thermoreceptors and thermosensitive afferents. Neurosci Biobehav Rev *33*, 205-212.

Schmechel, D., Marangos, P.J., and Brightman, M. (1978). Neurone-specific enolase is a molecular marker for peripheral and central neuroendocrine cells. Nature *276*, 834-836.

Schmelz, M., Hilliges, M., Schmidt, R., Orstavik, K., Vahlquist, C., Weidner, C., Handwerker, H.O., and Torebjork, H.E. (2003). Active "itch fibers" in chronic pruritus. Neurology *61*, 564-566.

Schmelz, M., Schmidt, R., Bickel, A., Handwerker, H.O., and Torebjork, H.E. (1997). Specific C-receptors for itch in human skin. J Neurosci *17*, 8003-8008.

Schoenen, J., Delree, P., Leprince, P., and Moonen, G. (1989). Neurotransmitter phenotype plasticity in cultured dissociated adult rat dorsal root ganglia: an immunocytochemical study. J Neurosci Res *22*, 473-487.

Schroeder, B.C., Hechenberger, M., Weinreich, F., Kubisch, C., and Jentsch, T.J. (2000). KCNQ5, a novel potassium channel broadly expressed in brain, mediates M-type currents. J Biol Chem *275*, 24089-24095.

Schroeder, B.C., Kubisch, C., Stein, V., and Jentsch, T.J. (1998). Moderate loss of function of cyclic-AMP-modulated KCNQ2/KCNQ3 K+ channels causes epilepsy. Nature *396*, 687-690.

Scroggs, R.S., and Fox, A.P. (1992). Calcium current variation between acutely isolated adult rat dorsal root ganglion neurons of different size. J Physiol *445*, 639-658.

Scroggs, R.S., Todorovic, S.M., Anderson, E.G., and Fox, A.P. (1994). Variation in IH, IIR, and ILEAK between acutely isolated adult rat dorsal root ganglion neurons of different size. J Neurophysiol *71*, 271-279.

Shinohara, T., Harada, M., Ogi, K., Maruyama, M., Fujii, R., Tanaka, H., Fukusumi, S., Komatsu, H., Hosoya, M., Noguchi, Y., *et al.* (2004). Identification of a G protein-coupled receptor specifically responsive to beta-alanine. J Biol Chem *279*, 23559-23564.

Silverman, J.D., and Kruger, L. (1990). Selective neuronal glycoconjugate expression in sensory and autonomic ganglia: relation of lectin reactivity to peptide and enzyme markers. J Neurocytol *19*, 789-801.

Simmons, M.A., and Schneider, C.R. (1998). Regulation of M-type potassium current by intracellular nucleotide phosphates. J Neurosci *18*, 6254-6260.

Smack, D.P., Korge, B.P., and James, W.D. (1994). Keratin and keratinization. J Am Acad Dermatol *30*, 85-102.

Southall, M.D., Li, T., Gharibova, L.S., Pei, Y., Nicol, G.D., and Travers, J.B. (2003). Activation of epidermal vanilloid receptor-1 induces release of proinflammatory mediators in human keratinocytes. J Pharmacol Exp Ther *304*, 217-222.

Story, G.M., Peier, A.M., Reeve, A.J., Eid, S.R., Mosbacher, J., Hricik, T.R., Earley, T.J., Hergarden, A.C., Andersson, D.A., Hwang, S.W., *et al.* (2003). ANKTM1, a TRP-like channel expressed in nociceptive neurons, is activated by cold temperatures. Cell *112*, 819-829.

Strachan, L.R., and Ghadially, R. (2008). Tiers of clonal organization in the epidermis: the epidermal proliferation unit revisited. Stem Cell Rev *4*, 149-157.

Streit, W.J., Schulte, B.A., Balentine, D.J., and Spicer, S.S. (1985). Histochemical localization of galactose-containing glycoconjugates in sensory neurons and their processes in the central and peripheral nervous system of the rat. J Histochem Cytochem *33*, 1042-1052.

Stucky, C.L., and Lewin, G.R. (1999). Isolectin B(4)-positive and -negative nociceptors are functionally distinct. J Neurosci *19*, 6497-6505.

Stucky, C.L., Medler, K.A., and Molliver, D.C. (2004). The P2Y agonist UTP activates cutaneous afferent fibers. Pain *109*, 36-44.

Suh, B.C., and Hille, B. (2002). Recovery from muscarinic modulation of M current channels requires phosphatidylinositol 4,5-bisphosphate synthesis. Neuron *35*, 507-520.

Sun, Y.G., and Chen, Z.F. (2007). A gastrin-releasing peptide receptor mediates the itch sensation in the spinal cord. Nature *448*, 700-703.
Svichar, N., Shmigol, A., Verkhratsky, A., and Kostyuk, P. (1997). ATP induces Ca2+ release from IP3-sensitive Ca2+ stores exclusively in large DRG neurones. Neuroreport *8*, 1555-1559.

Talavera, K., Nilius, B., and Voets, T. (2008a). Neuronal TRP channels: thermometers, pathfinders and life-savers. Trends Neurosci *31*, 287-295.
Talavera, K., Voets, T., and Nilius, B. (2008b). Mechanisms of Thermosensation in TRP channels. In Sensing with Ion Channels, B. Martinac, ed. (Berlin, Springer), pp. 101-120.

Tarpley, J.W., Kohler, M.G., and Martin, W.J. (2004). The behavioral and neuroanatomical effects of IB4-saporin treatment in rat models of nociceptive and neuropathic pain. Brain Res *1029*, 65-76.

Tatulian, L., Delmas, P., Abogadie, F.C., and Brown, D.A. (2001). Activation of expressed KCNQ potassium currents and native neuronal M-type potassium currents by the anti-convulsant drug retigabine. J Neurosci *21*, 5535-5545.

Taylor, A.M., Peleshok, J.C., and Ribeiro-da-Silva, A. (2009). Distribution of P2X(3)-immunoreactive fibers in hairy and glabrous skin of the rat. J Comp Neurol *514*, 555-566.

Thompson, R.J., Doran, J.F., Jackson, P., Dhillon, A.P., and Rode, J. (1983). PGP 9.5--a new marker for vertebrate neurons and neuroendocrine cells. Brain Res *278*, 224-228.

Tominaga, M., Wada, M., and Masu, M. (2001). Potentiation of capsaicin receptor activity by metabotropic ATP receptors as a possible mechanism for ATP-evoked pain and hyperalgesia. Proc Natl Acad Sci U S A *98*, 6951-6956.

Trupp, M., Arenas, E., Fainzilber, M., Nilsson, A.S., Sieber, B.A., Grigoriou, M., Kilkenny, C., Salazar-Grueso, E., Pachnis, V., and Arumae, U. (1996). Functional receptor for GDNF encoded by the c-ret proto-oncogene. Nature *381*, 785-789.

Tunggal, J.A., Helfrich, I., Schmitz, A., Schwarz, H., Gunzel, D., Fromm, M., Kemler, R., Krieg, T., and Niessen, C.M. (2005). E-cadherin is essential for in vivo epidermal barrier function by regulating tight junctions. EMBO J *24*, 1146-1156.

Viana, F., de la Pena, E., and Belmonte, C. (2002). Specificity of cold thermotransduction is determined by differential ionic channel expression. Nat Neurosci *5*, 254-260.

Vidal, M., Morris, R., Grosveld, F., and Spanopoulou, E. (1990). Tissue-specific control elements of the Thy-1 gene. EMBO J *9*, 833-840.

Voets, T., Talavera, K., Owsianik, G., and Nilius, B. (2005). Sensing with TRP channels. Nat Chem Biol *1*, 85-92.

Volonte, C., Amadio, S., D'Ambrosi, N., Colpi, M., and Burnstock, G. (2006). P2 receptor web: complexity and fine-tuning. Pharmacol Ther *112*, 264-280.

Vulchanova, L., Olson, T.H., Stone, L.S., Riedl, M.S., Elde, R., and Honda, C.N. (2001). Cytotoxic targeting of isolectin IB4-binding sensory neurons. Neuroscience *108*, 143-155.

Wang, L., Hilliges, M., Jernberg, T., Wiegleb-Edstrom, D., and Johansson, O. (1990). Protein gene product 9.5-immunoreactive nerve fibres and cells in human skin. Cell Tissue Res *261*, 25-33.

Wickenden, A.D., Yu, W., Zou, A., Jegla, T., and Wagoner, P.K. (2000). Retigabine, a novel anti-convulsant, enhances activation of KCNQ2/Q3 potassium channels. Mol Pharmacol *58*, 591-600.

Wiederkehr, A., Staple, J., and Caroni, P. (1997). The motility-associated proteins GAP-43, MARCKS, and CAP-23 share unique targeting and surface activity-inducing properties. Exp Cell Res *236*, 103-116.

Wilmer, J.L., Burleson, F.G., Kayama, F., Kanno, J., and Luster, M.I. (1994). Cytokine induction in human epidermal keratinocytes exposed to contact irritants and its relation to chemical-induced inflammation in mouse skin. J Invest Dermatol *102*, 915-922.

Wohlrab, D., Wohlrab, J., and Markwardt, F. (2000). Electrophysiological characterization of human keratinocytes using the patch-clamp technique. Exp Dermatol *9*, 219-223.

Woodbury, C.J., Zwick, M., Wang, S., Lawson, J.J., Caterina, M.J., Koltzenburg, M., Albers, K.M., Koerber, H.R., and Davis, B.M. (2004). Nociceptors lacking TRPV1 and TRPV2 have normal heat responses. J Neurosci *24*, 6410-6415.

Xu, H., Delling, M., Jun, J.C., and Clapham, D.E. (2006). Oregano, thyme and clove-derived flavors and skin sensitizers activate specific TRP channels. Nat Neurosci *9*, 628-635.

Xu, H., Ramsey, I.S., Kotecha, S.A., Moran, M.M., Chong, J.A., Lawson, D., Ge, P., Lilly, J., Silos-Santiago, I., Xie, Y., *et al.* (2002). TRPV3 is a calcium-permeable temperature-sensitive cation channel. Nature *418*, 181-186.

Yoshida, S., and Matsuda, Y. (1979). Studies on sensory neurons of the mouse with intracellular-recording and horseradish peroxidase-injection techniques. J Neurophysiol *42*, 1134-1145.

Zaika, O., Tolstykh, G.P., Jaffe, D.B., and Shapiro, M.S. (2007). Inositol triphosphate-mediated Ca2+ signals direct purinergic P2Y receptor regulation of neuronal ion channels. J Neurosci *27*, 8914-8926.

Zeng, Y., Lv, X.H., Zeng, S.Q., Tian, S.L., Li, M., and Shi, J. (2008). Sustained depolarization-induced propagation of [Ca(2+)](i) oscillations in cultured DRG neurons: The involvement of extracellular ATP and P2Y receptor activation. Brain Res.

Zhang, X., Huang, J., and McNaughton, P.A. (2005). NGF rapidly increases membrane expression of TRPV1 heat-gated ion channels. EMBO J *24*, 4211-4223.

Zhu, W., Galoyan, S.M., Petruska, J.C., Oxford, G.S., and Mendell, L.M. (2004). A developmental switch in acute sensitization of small dorsal root ganglion (DRG) neurons to capsaicin or noxious heating by NGF. J Neurophysiol *92*, 3148-3152.

Zimmermann, K., Leffler, A., Babes, A., Cendan, C.M., Carr, R.W., Kobayashi, J., Nau, C., Wood, J.N., and Reeh, P.W. (2007). Sensory neuron sodium channel Nav1.8 is essential for pain at low temperatures. Nature *447*, 855-858.

Zwick, M., Davis, B.M., Woodbury, C.J., Burkett, J.N., Koerber, H.R., Simpson, J.F., and Albers, K.M. (2002). Glial cell line-derived neurotrophic factor is a survival factor for isolectin B4-positive, but not vanilloid receptor 1-positive, neurons in the mouse. J Neurosci *22*, 4057-4065.

Zylka, M.J., Rice, F.L., and Anderson, D.J. (2005). Topographically distinct epidermal nociceptive circuits revealed by axonal tracers targeted to Mrgprd. Neuron *45*, 17-25.

# Appendix I:

**Immunohistochemistry for tissue sections prepared using a cryostat.**

1. Using a cryostat, cut DRG sections 12μm thick, skin and spinal cord sections 30μm thick and collect sections onto CAG-coated slides (0.5% w/v gelatine, 0.1% w/v chrome alum, 0.5% w/v sodium azide, in distilled water). Slides are stored at -20°C until needed.
2. Wash slides with 0.1M PBS for 10min. Repeat 3x.
3. Remove PBS and dry edges/ rear of slide. Cover sections in Triton 100X solution for 10-20min. For thin sections (<15μm) use 0.4% solution and for thicker sections (>30 μm) use 2% solution.
4. Wash slides with 0.1M PBS for 10 min. Repeat 3x.
5. Incubate sections in 5% NDS (normal donkey serum in 0.1M PBS) for 30-60 min.
6. Dilute primary antibody in antibody diluent (0.25% sodium azide, 2.5% NDS, in 0.1M PBS) and add 200μl to each slide. Store slides in a humidified environment overnight at 4°C.
7. Wash slides with 0.1M PBS for 10 min. Repeat 6x.
8. Dilute secondary antibody in antibody diluent and add 200μl to each slide. Store slides in a humidified environment overnight at 4°C.
9. Wash slides with 0.1M PBS for 10min. Repeat 6x.
10. To stain nuclei, incubate with 300nM DAPI (in PBS) for 5 min and wash a further 3x.

11. Remove PBS and immerse slide in distilled water for 5 min to remove salt residues.
12. Wipe edges/rear of slide with a tissue and allow water to evaporate from surface without letting the sections dry. Mount coverslip using Vectashield mounting medium (Vector Laboratories, USA).

# Appendix II:

**Immunohistochemistry for tissue sections prepared using a freezing knife microtome.**

1. Skin and spinal cord sections (40μm) thick are collected into tubes half filled with 0.1M PBS.
2. Sections are washed for 10min with 0.1M PBS three times.
3. PBS is aspirated off and replaced with 1ml 2% Triton 100X solution for 10-20min.
4. Sections are washed for 10min with 0.1M PBS three times.
5. Sections are incubated with 1ml 5% NDS for 30-60min.
6. Tubes are aspirated and 200μl of primary antibody (in antibody diluent) is added to each. To aid tissue penetration, 0.4% Triton 100X solution can be used instead of antibody diluent. Tubes are covered with parafilm and stored at 4°C overnight.
7. Primary antibody is aspirated off and tubes are washed with 0.1M PBS, 6 x 10min.
8. Tubes are aspirated and 200μl secondary antibody is added to sections. Tubes are covered and incubated overnight at 4°C.
9. Tubes are aspirated and sections are washed for 10min with 0.1M PBS six times.

10. To stain nuclei, incubate with 200µl DAPI (300nM in PBS) for 5 min and wash a further 3x.
11. Mount sections onto CAG-coated slides. Avoid letting mounted sections dry out whilst doing this. Once sections are mounted allow them to partially dry before gently dipping the slide in to distilled water a few times.
12. Remove excess water and allow sections to dry a little before mounting the coverslip with Vectashield. Mount coverslip using Vectashield mounting medium (Vector Laboratories, USA).

# Appendix III:

**Immunohistochemistry for cultured DRG neurones.**

1. Coat 2 eight-well culture slides (BD Falcon) with 100μg/ml poly-D-lysine (350μl/well) per culture. Leave for 1 hour then rinse with distilled water (1 hour) and leave to dry in a sterile environment.
2. Culture DRG neurones as described for electrophysiology but after dissociating the cells suspend in 8ml of plating media instead of 10ml.
3. Pipette 500μl into each well of the culture slide and incubate neurones at 37°C for 48 hours (5% $CO_2$).
4. Carefully pipette off 400μl and replace with 4% PFA. Leave for 10 min.
5. Wash with 0.1M PBS 5x always leaving at least 100μl in the well.
6. Slides can be stored in a humidified environment at 4°C so that multiple culture slides can be processed together. Leave at least 500μl in each well and check weekly to ensure they do not dry out.
7. When ready to use for immunohistochemistry, aspirate off the old PBS and replace with 400μl fresh PBS. Wells were washed gently by replacing half the volume (200μl) with fresh PBS each time. Wash wells 3 x 10min with 0.1M PBS.
8. Aspirate wells and incubate cells in 0.4% Triton 100X solution for 15 minutes.
9. Aspirate off the Triton solution and wash gently with PBS 5 x 10min.

10. Aspirate the PBS and replace with 5% NDS. Incubate for 30-60min.
11. Aspirate the wells and add 200µl of primary antibody to each. Incubate at 4°C overnight in a humidified environment.
12. Aspirate the primary antibody and replace with 400µl of PBS. Wash gently 8 x 10min with PBS.
13. Remove the PBS and add 200µl of secondary antibody to each well. Incubate at 4°C overnight in a humidified environment.
14. Aspirate the secondary antibody and replace with 400µl of PBS. Wash gently 8 x 10min with PBS.
15. Whilst the wells are still full, remove the plastic wells from the slide using the separator provided. Ensuring to keep the slide covered with PBS, carefully remove the remaining adhesive from the slide with a scalpel. Use a dissecting microscope.
16. Place slide into distilled water for 5-10min to remove salt residue. Remove excess water from the back and sides of the slide. Do not allow the cells to dry out. Mount a coverslip using Vectashield mounting medium (Vector Laboratories, USA). You may need to use a little more than normal to avoid air bubbles then blot off the excess with a tissue.

# Appendix IV:

## Antibody concentration and incubation times

| Tissue | 1° Antibody | Company | Concentration | Duration | 2° Antibody | 2° Company | 2° Concentration | 2° Duration |
|---|---|---|---|---|---|---|---|---|
| DRG | Rb Polyclonal αP2X3 | Abcam (USA) | 1:10,000 | >12 hours | Donkey αRb Cy3 | Jackson (USA) | 1:200 | >12 hours |
| DRG | Rb Polyclonal αTRPV1 | Abcam (USA) | 1:1,000 | >36 hours | Donkey αRb Cy3 | Jackson (USA) | 1:200 | >12 hours |
| DRG | Gt Polyclonal αGFRα2 | R&D Systems(USA) | 1:500 | >12 hours | Donkey αGt Cy3 | Jackson (USA) | 1:500 | >12 hours |
| DRG | Rb Polyclonal αCalbindin D-28K | Paul Emson (gift) | 1:1,000 | >12 hours | Donkey αRb Cy3 | Jackson (USA) | 1:500 | >12 hours |
| DRG | Rb Polyclonal αCalbindin D-28K | Paul Emson (gift) | 1:1,000 | >12 hours | Donkey αRb Cy5 | Jackson (USA) | 1:500 | >12 hours |
| DRG | Rb Polyclonal αGRP | Immunostar (USA) | 1:500 | >12 hours | Donkey αRb Cy3 | Jackson (USA) | 1:500 | >12 hours |
| SC | Rb Polyclonal αP2X3 | Abcam (USA) | 1:5,000 | >12 hours | Donkey αRb Cy3 | Jackson (USA) | 1:500 | >12 hours |
| SC | Rb Polyclonal αTRPV1 | Abcam (USA) | 1:1,000 | >36 hours | Donkey αRb Cy3 | Jackson (USA) | 1:500 | >12 hours |
| SC | Gt Polyclonal αGFRα2 | R&D Systems(USA) | 1:500 | >12 hours | Donkey αGt Cy3 | Jackson (USA) | 1:500 | >12 hours |
| SC | Rb Polyclonal αCalbindin D-28K | Paul Emson (gift) | 1:1,1000 | >12 hours | Donkey αRb Cy5 | Jackson (USA) | 1:500 | >12 hours |
| Skin | Gt Polyclonal αGFRα2 | R&D Systems(USA) | 1:500 | >12 hours | Donkey αGt Cy3 | Jackson (USA) | 1:500 | >12 hours |

# Appendix V:

**Fluophore excitation-emission spectra**

| Fluophore | Excitation λ (nm) | Emission λ (nm) |
|---|---|---|
| Cy3 | 550 | 570 |
| Cy5 (Far Red) | 649 | 670 |
| DAPI | 358 | 461 |
| FITC (and eGFP) | 494 | 518 |

# Appendix VI:

**Output from this research:**

Bruce G, Belle MDC & Morris R (2007) Characteristics of epidermal primary afferents expressing GFP under the control of thy1.2 in the mouse. British Neurosci. Assoc. Abstr., Vol 19, P59.01

Bruce G, Barrett-Jolley R & Morris R (2008) Characterisation of epidermal primary afferents in the mouse. J Physiol, Proc Physiol Soc 11, C73

Bruce G, Barrett-Jolley R & Morris R (2009) Nucleotide modulation of Kv7/M-current in epidermal primary afferent cell bodies in the mouse. British Neurosci. Assoc. Abstr., Vol 20, P32.04

Bruce G, Barrett-Jolley R & Morris R (2009) P2Y activation affects the excitability of murine epidermal primary afferents through modulation of the Kv7-mediated M-current. J Physiol, Proc Physiol Soc 15, C44

UNIVERSITY OF LIVERPOOL

FACULTY of VETERINARY SCIENCE

Pain Relief Foundation

# Characteristics of epidermal primary afferents expressing GFP under the control of *thy1.2* in the mouse

Gareth Bruce[1], Mino D C Belle[2], Richard Barrett-Jolley[1] and Richard Morris[1].

[1]Department of Veterinary Preclinical Sciences, Faculty of Veterinary Sciences, Brownlow Hill and Crown Street, Liverpool, L69 7ZJ.
[2]Faculty of Life Sciences, University of Manchester, 1.124 Stopford Building, Oxford Road, Manchester, M13 9PT.

## Introduction

In a transgenic mouse line, expressing enhanced green fluorescent protein (eGFP) under the control of the promoter for a glycosylphosphatidylinositol (GPI) linked glycoprotein, thy1.2, a population of epidermal primary afferents were found to express the reporter. Neurones expressing the thy1.2-eGFP transgene have free endings in the epidermis of hairy skin and project onto lamina II of the dorsal horn. Fluorescence is ubiquitous throughout the neurone enabling anatomical and electrophysiological characterisation.
Previous work by our group (unpublished) has shown small and medium dorsal root ganglion (DRG) neurones express eGFP in these mice. Most (74%) of these also bind isolectin $B_4$ ($IB_4$) from *Griffonia simplicifolia*, but do not express calcitonin gene-related peptide (CGRP) or substance P. A small population of medium sized neurones were eGFP positive, $IB_4$ negative but contained calbindin. In the skin this correlated with the eGFP staining of club-shaped endings in hair follicles. The work presented here continues the characterisation of these transgenically labelled neurones by starting to examine their receptor/channel expression and physiology.

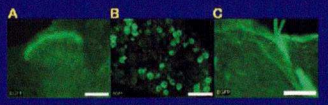


Fig. 1. eGFP expression in the peripheral nervous system of the *thy1.2*-eGFP mouse. A. Lamina II can be clearly identified by eGFP expression (x100mag, scale bar 200μm). B. Nonpeptidergic neurones in the DRG express eGFP (x200mag, scale 100μm). C. Nonpeptidergic, eGFP positive fibres innervate the epidermis of hairy skin (x200mag, scale bar 100μm).

## Materials and Methods

All procedures were approved by The University of Liverpool Animal Ethics committee and were carried out under the provisions of the UK Animal (Scientific Procedures) Act 1986. Transgenic mice were genotyped using basic PCR to confirm presence of the eGFP transgene. Immunohistochemical staining was performed on the spinal cord and DRG from adult transgenic mice (SA36 strain) that had been 'fixed' by perfusion with 4% paraformaldehyde. Sections of DRG (12μm) and spinal cord (40μm) were cut on a cryostat and freezing knife microtome respectively. Sections were washed with PBS and non-specific binding blocked with normal donkey serum before the antibodies to P2X$_3$ and TRPV1 receptors (both Abcam, USA) were incubated individually with the section for 12 and 36 hours respectively. Thorough washing with phosphate buffered saline (PBS) preceded incubation with Donkey anti-Rabbit Cy3 for 12 hours. Sections were again washed with PBS before coverslipping using Vectorshield (Vector Laboratories, USA). Fluorescent microscopy was used to visualise sections for acquisition by Metavue software. Data was analysed using Metamorph and statistical analysis applied with Prism 3 Graphpad.
Electrophysiological recordings were performed using the whole cell patch clamp technique on dissociated DRG neurones. Adult transgenic mice (SA36 strain) were deeply anaesthetised with halothane before being rapidly decapitated. DRG from all levels were microsurgically removed and digested with collagenase (2mgml$^{-1}$) and dispase (5mgml$^{-1}$) for 70min at 35°C in a water-bath. Cells were dissociated by mechanical trituration and plated on poly-D-lysine coated, 35mm glass bottom microwell tissue culture dishes. Recordings were performed 2-24 hours after plating on an epifluorescence equipped, inverted microscope and logged using Spike2v5.14.

## Results

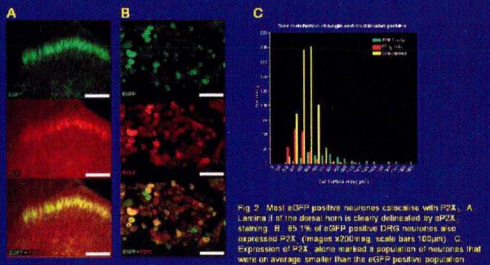


Fig 2. Most eGFP positive neurones colocalise with P2X$_3$. A. Lamina II of the dorsal horn is clearly delineated by eP2X$_3$ staining. B. 85.1% of eGFP positive DRG neurones also expressed P2X$_3$ (images x200mag, scale bars 100μm). C. Expression of P2X$_3$ alone marked a population of neurones that were on average smaller than the eGFP positive population

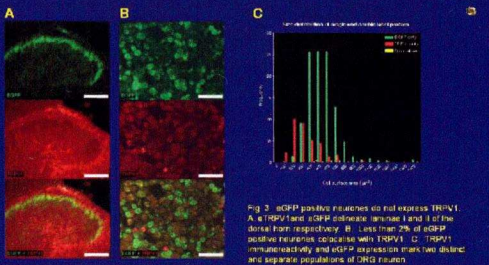


Fig 3. eGFP positive neurones do not express TRPV1. A. eTRPV1and eGFP delineate laminae I and II of the dorsal horn respectively. B. Less than 2% of eGFP positive neurones colocalise with TRPV1. C. TRPV1 immunoreactivity and eGFP expression mark two distinct and separate populations of DRG neuron

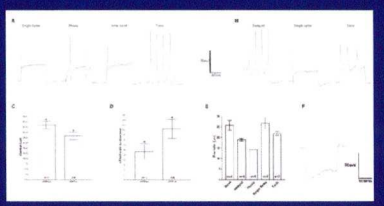

Fig 4. Small eGFP positive DRG neurones are a heterogeneous population. A. eGFP positive DRG neurones can be classified by their response to depolarising current injections (230ms, 0.14-1nA, 0.2Hz, n=12). B. Small DRG neurones that didn't express eGFP also produced a varied response to the same pulse protocol including a delayed response not seen in eGFP positive neurones (230ms, 0.05-1nA, 0.2Hz, n=9). C. Consistent with the immunohistochemical data, eGFP negative DRG (29.79 ± 1.79pF, n=9) cells were generally smaller than the transgenically labelled neurones (25.97 ± 1.78pF, n=11, p=0.6258). D. Primary action potentials in response to 20ms depolarising current injections (0.02-1nA) were shorter in duration at half-maximal amplitude for eGFP positive neurones (5.668 ± 1.573ms, n=12; p=0.0353) than for eGFP negative neurones (10.24 ± 1.921ms, n=9). E. Responses to current injections showed some correlation to size. Delayed firing was only observed in eGFP negative neurones. F. A single rebound spike was observed in response to hyperpolarising current pulses (730ms, 0.1-1.3nA, 0.2Hz) in some eGFP positive neurones (n=5). These neurones responded to depolarising pulses with either a single spike (n=4) or burst firing (n=1).

## Discussion

The present data suggests that most of DRG neurones expressing eGFP in this mouse innervate the epidermis, express P2X$_3$ receptors and bind $IB_4$ lectin and have central terminations in LII of the dorsal horn. These neurones did not express TRPV1, however in the mouse small DRG neurones that don't express TRPV1 or TRPV2 have been shown to respond to noxious heat suggesting that another channel/receptor mediates these responses (Woodbury et al. 2004). Preliminary electrophysiological characterisation of acutely dissociated small DRG neurones expressing eGFP from these animals has been carried out. The most consistent characteristic of the neurones was the production of a single spike to depolarising pulses and the presence of a rebound spike following hyperpolarising current pulses. It has been shown that low doses of the K-channel blocker 4-AP will convert single responses to depolarising stimuli to tonic responses revealing the importance of a potassium channel (Raschowsyh & Sandkuhler, 2002). The rebound spike is probably mediated by a T-type Calcium channel (McRory *et al.*, 2001; Hildebrand & Snutch, 2006), however this needs pharmacological characterisation. This transgenic animal should permit the physiological properties of this population of epidermal afferents to be characterised in detail.

## References

Hildebrand ME & Snutch TP (2006) Drug Disc. Today: Dis. Mech. 3(3):335-341
McRory JE *et al.* (2001) J Biol Chem 276(6):3999-4011
Ruscheweyh R & Sandkuhler J (2002) J Physiol 541.1:231-244
Woodbury CJ *et al.*, (2004) J Neurosci 24:6410-6415.

## Characterisation of epidermal primary afferents in the mouse.

G. Bruce[1], R. Barrett-Jolley[1], R. Morris[1]

1. Veterinary Preclinical Sciences, University of Liverpool, Liverpool, United Kingdom.

The epidermis is richly innervated with sensory afferents most of which are of the "non-peptidergic" group (Zylka *et al.*, 2005; Belle *et al.*, 2007) and in the present study some of the characteristics of these afferents have been determined. Studies were conducted on C57/Bl6 mice (SA36 strain) carrying the *thy1.2-egfp* gene expressed in non-peptide epidermal afferents (Belle *et al.*, 2007). For anatomy, animals were terminally anaesthetised with sodium pentobarbitone i.p. (80mg/kg) prior to whole body perfusion fixation with 4% paraformaldehyde and for electrophysiology they were anaesthetised with halothane and killed by decapitation. Dorsal root ganglion (DRG) neurones were either studied shortly following acute dissociation (AD) within 2-9 hours of plating or after maintaining in short-term culture (SC) between 1-3 days post-plating. The responses of eGFP positive neurones recorded in whole-cell current-clamp mode to depolarising and hyperpolarising current pulses were investigated. All results given are mean ± S.E.M and statistical analysis between cell types was done by one-way ANOVA with Tukey post test unless otherwise stated. Immunoreactivity for $P2X_3$ (mean surface area (m.s.a.) 444.3 ± 4.43μm$^2$, $n$=800) was observed in 85.1% of eGFP-positive neurones (m.s.a. 509.9 ± 7.32μm$^2$, $n$=737), whilst $TRPV_1$ immunoreactivity (m.s.a. 358.1 ± 15.7μm$^2$, $n$=179) marked a separate, smaller population of neurones only 5.02% of which expressed eGFP (1.62% of eGFP population). The mean size of the AD eGFP-positive neurones ($n$=32) (mean soma diameter 26.1 ± 0.76μm) was larger than those in SC ($n$=52) (mean soma diameter 21.31 ± 0.42μm, $p < 0.001$). This could be due to shrinkage following loss of axonal arborisation or be due to selective loss of small neurones that may not have settled in the acutely dissociated preparations. Their firing patterns to depolarising pulses could also be separated into five distinct groups burst (AD 12.5%, SC 3.8%), delayed (AD 3.1%, SC 0%), phasic (AD 9.3%, SC 1.9%), transient (AD 68.7%, SC 50%) and tonic firing (AD 6.2%, SC 44.2%). Action potential overshoot magnitudes were similar under the two conditions (AD 28.14 ± 2.12mV, SC 28.96 ± 1.39mV, $p > 0.05$) but action potentials were broader in SC neurones (AD 6.59 ± 1.1ms, SC 9.88 ± 0.85ms, $p < 0.05$) and more frequently had inflections on their repolarising slope. Approximately half of the AD neurones (53.13%) displayed delayed rectification and a rebound spike when hyperpolarised suggesting the HCN mediated current, $I_h$, is present. These results are consistent with the literature, showing that non-peptidergic primary afferents innervating the epidermis in the mouse are sensitive to ATP but not to capsaicin. Whilst some display characteristics of nociceptors (broad, inflected action potentials) others share properties that have been reported in cold sensitive neurones ($I_h$).

Supported by the Pain Relief Foundation.

Belle M.D. *et al.* (2007). *Genesis* **45**, 679-688
Zylka M.J. *et al.* (2005). *Neuron* **45**, 17-25

UNIVERSITY OF LIVERPOOL

FACULTY of VETERINARY SCIENCE

Pain Relief Foundation

# Nucleotide modulation of $K_v7$/M-current in epidermal primary afferent cell bodies in the mouse

Gareth Bruce[1], Richard Barrett-Jolley[1] and Richard Morris[1].

[1]Department of Veterinary Preclinical Sciences, Faculty of Veterinary Sciences, Brownlow Hill and Crown Street, Liverpool, L69 7ZJ.

## Introduction

The epidermis is densely innervated by "non-peptidergic" primary afferent neurones in the mouse (Zylka et al., 2005; Delle et al., 2007). Two separate populations have thus far been identified by their expression of mas-related G-protein-coupled receptors (Mrgprs) and show differences in their innervation of the epidermis as well as the cytochemical markers they express (Zylka et al., 2005; Liu et al., 2007). Neurones expressing MrgprD4 are found solely in hairy skin where they terminate around the necks of hair follicles and the surrounding epidermis (Liu et al., 2007). Whilst they bind the "non-peptidergic" marker, IB4, they don't express the P2X$_3$ subunit (Liu et al., 2007). In contrast, neurones expressing MrgprD innervate the epidermis of both hairy and glabrous skin, are IB$_4$-binding/P2X$_3$-immunoreactive and in electrophysiological studies are selectively sensitive to ATP (Zylka et al., 2005; Dussor et al., 2008).

Activation of MrgprD in IB$_4$-labelled rat dorsal root ganglion (DRG) neurones leads to an increase in neuronal excitability through inhibition of the $K_v7$ mediated M-current (Crozier et al., 2007). The P2Y$_1$ agonist UTP is a known inhibitor of the M-current in bullfrog sympathetic neurones (Adams et al., 1982). Previously we reported that "non-peptidergic" DRG neurones from a mouse that expressed green fluorescent protein (GFP) in cutaneous primary afferents were P2X$_3$-immunoreactive and fired in a predominantly transient manner (Bruce et al., 2008). We investigated whether this firing pattern was due to the presence of an M-current and, if so, how it was modulated by endogenous P2Y agonists.

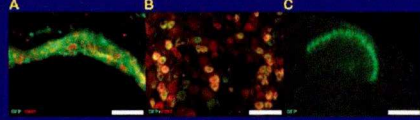


Fig. 1. eGFP expression in the peripheral nervous system of the *thy1* 2-eGFP mouse. A) Non-peptidergic, eGFP positive fibres innervate the epidermis of hairy skin (x400mag, scale bar 50μm). B) Most (85.1%) eGFP expressing DRG neurones are also P2X3-immunoreactive. (Bruce et al., 2008, x200mag, scale 100μm). C) Lamina II can be clearly identified by eGFP expression (x100mag, scale bar 200μm).

## Materials and Methods

All procedures were approved by The University of Liverpool Animal Ethics committee and were carried out under the provisions of the UK Animal (Scientific Procedures) Act 1986.

Transgenic mice (SA36 strain) expressing enhanced green fluorescent protein (eGFP) under the control of the thy1.2 gene promoter shows selective expression of eGFP in the epidermal primary afferents of hairy skin (Delle et al., 2007). Adult mice were deeply anaesthetised with halothane and killed by decapitation. DRG from all levels were enzymatically digested and mechanically dissociated for short term culture (1-3 days) using a protocol based upon the methods of Rau et al., 2005. Cultured DRG neurones (25-31μm) were perfused with an extracellular recording solution (in mM: 142 NaCl, 2.8 KCl, 2 CaCl$_2$, 1 MgCl$_2$,6 CsCl, 5 HEPES, 10 D-glucose, pH 7.4 with 1M NaOH). Whole cell recordings were made using borosilicate glass pipettes filled with a potassium gluconate intracellular recording solution (in mM: 142 potassium gluconate, 1 CaCl$_2$, 2 MgCl2,5H2O, 10 HEPES, 11 EGTA, pH 7.4 with 1M KOH) and a final resistance of 4-7MΩ. Recordings were made in voltage and current clamp using WinWCP (John Dempster, University of Strathclyde, UK) and Spike2 (CED, UK) respectively through a Cairn Optopatch amplifier (Cairn Research, UK). Data was digitised at 10-20 KHz, filtered at 5KHz and logged to PC via a Micro1401 (CED, UK).

In voltage clamp mode, the M-current ($I_{KM}$) was isolated using a voltage deactivation protocol and 1mM CsCl (Brown and Adams, 1980; Passmore et al., 2003). Current measurements from DRG neurones were leak subtracted before normalising through division of the steady state current ($I_{ss}$) by the instantaneous current ($I_{inst}$) to give the relative conductance for each voltage command.

## Results

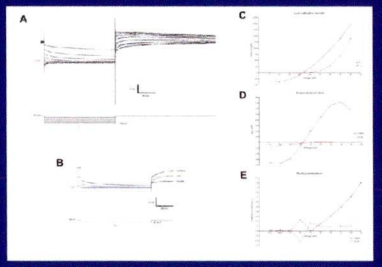


Fig. 2. The M-current is present in eGFP DRG neurones. A) Superimposed current traces recorded from an eGFP-expressing DRG neurone. Cells were held at -20mV and hyperpolarised in 10mV steps (1s duration). B) Time-matched controls (TMC) were used to compensate for rundown between control and drug voltages swings. C) Leak subtracted currents from (A). Measurements for $I_{ss}$ and $I_{inst}$ were taken in the initial and final 10ms of the voltage step respectively. D) The difference between $I_{ss}$ and $I_{inst}$ varied with command potential. XE-991 (10μM) blocked the M-current (red line). E) Currents were normalised by converting them into relative conductances.

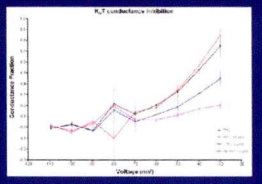


Fig. 3. UTP but not ADP inhibits $K_v7$ conductance in epidermal primary afferent neurones. ADP (10μM) had no significant effect on channel conductance after 5 minutes exposure. UTP (10μM) inhibited channel conductance at -30 to -40mV whilst inhibition by XE-991 (10μM) was significant at -30mV to -50mV (P<0.05, MANOVA with Dunnetts *T*).

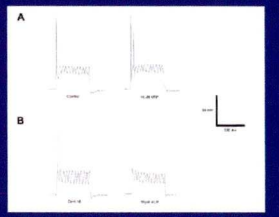


Fig. 4. UTP and ADP affect the firing of transient DRG neurones differently. Under current clamp conditions most (10/13) DRG neurones fired transients in response to depolarising current injection (500-600pA, 200ms, 0.2Hz). Of those that fired transiently, many (5/10) also exhibited responses to hyperpolarisation indicative of HCN channels. A) UTP (10μM) increased afterdepolarisation amplitude and secondary spike frequency (2/5 cells). B) ADP (10μM) reduced or blocked the primary spike in some transiently firing neurones (2/5 cells).

## Discussion

We have previously shown that the majority of eGFP expressing DRG neurones fired a primary spike and then remained silent when depolarised, a response we described as transient (Bruce et al., 2008). Whilst the stimulus transduced by these neurones remains unclear we surmised that they may be involved in the transduction of novel stimulus.

Inhibition of the M-current in rat DRG neurones caused tonic firing in previously transient cells (Crozier et al., 2007). UTP and ADP have both been shown to inhibit the M-current in neurones and UTP activates cutaneous afferents (Brown, 1982; Stucky, 2004; Filippov, 2005). The discrepancy between the effect of ADP in the literature and the results shown here may be explained by its degradation and action through an alternative pathway. DRG neurones which bind IB$_4$ express a fluoride-resistant acid phosphatase (FRAP) recently identified as a transmembrane isoform of prostatic acid phosphatase (TM-PAP) (Zylka et al., 2008). TM-PAP has ectonucleotidase activity and can dephosphorylate AMP, and to a lesser extent ADP, to produce adenosine which then acts through the A1-adenosine receptor to suppress pain (Zylka et al., 2008).

Kobzuni et al., (2004) demonstrated that keratinocytes could stimulate DRG neurones through the release of ATP in a P2Y-dependent manner. The discovery that a group of epidermal primary afferents are selectively sensitive to ATP and growing evidence that keratinocytes may be the primary transducer of some stimuli provides compelling reasons to look further at the possible mechanisms that may regulate this signalling pathway (Dussor et al., 2008; reviewed in Dussor et al., 2009).

This data demonstrates nucleotide modulation of cellular excitability in neurones anatomically positioned to receive input from keratinocytes.

## References

Adams PR et al., (1982) J Physiol 332 223-262
Bello MO et al., (2003) Genesis 45 674-683
Brown DA, Adams PR (1980) Nature 283 673-676
Bruce G et al., (2008) Proc Physiol Soc 11 C73
Crozier RA et al., (2007) J Neurosci 27 4492-4496
Dussor G et al., (2008) J Neurophysiol 99 1581-1589
Dussor G et al., (2009) Brain Res Rev 60 24-35
Filippov AK et al., (2006) J Neurosci 26 9340-9348
Kobzuni S et al., (2004) Biochem J 380 329-338
Liu Q et al., (2007) Nat Neurosci 10 946-948
Passmore GM et al., (2003) J Neurosci 23 7227-7236
Rau KK et al., (2005) J Neurophysiol 93 1358-1371
Stucky CL et al., (2004) Pain 109 36-44
Zylka MJ et al., (2005) Neuron 45 17-25
Zylka MJ et al., (2008) Neuron 60 111-122

## P2Y activation affects the excitability of murine epidermal primary afferents through modulation of the $K_v7$-mediated M-current

G. Bruce[1], R. Barrett-Jolley[1], R. Morris[1]

1. Veterinary Preclinical Sciences, University of Liverpool, Liverpool, United Kingdom.

Koizumi *et al.*, (2004) demonstrated the importance of ATP and $P2Y_2$ receptors in signalling between keratinocytes and sensory neurones. A population of neurones innervating the epidermis are selectively sensitive to ATP in mice (Dussor *et al.*, 2008). They also express mas-related G protein-coupled receptor D (MrgprD), activation of which inhibits the M-current in $IB_4$-labelled rat dorsal root ganglion (DRG) neurones (Dussor *et al.*, 2008; Crozier *et al.*, 2007). The $P2Y_2$ agonist, uridine triphosphate (UTP), has long been known to inhibit the M-current in bullfrog sympathetic neurones (Adams *et al.*, 1982). Previously we reported that "non-peptidergic" DRG neurones from a mouse that expressed green fluorescent protein (GFP) in epidermal primary afferents fired in a predominantly transient manner (Bruce *et al.*, 2008). We investigated whether this firing pattern was due to the presence of an M-current and, if so, how it was modulated by endogenous P2Y agonists. Transgenic mice carrying the *thy1.2-egfp* gene on a C57/Bl6 template (SA36 strain) were deeply anaesthetised with halothane and killed by decapitation. Dissociated DRG neurones were short-term cultured (1-3) days and used for whole-cell voltage or current clamp recording. The M-current was isolated in voltage-clamped DRG neurones (25-31 µm diameter) using an inactivation protocol and 1mM CsCl. XE-991 (10µM) and UTP (10µM) significantly reduced the conductance through $K_v7$ channels at -30 to -50 mV and -30 to -40 mV respectively ($P<0.05$, Dunnetts T). ADP (10µM) had no significant effect on M-current conductance. Under current clamp conditions, DRG neurones produced predominately transient responses to depolarising current injections (16/20 cells). UTP (10µM) increased afterdepolarisation amplitude and secondary spike frequency (3/5 cells). ADP (10µM) reduced or blocked the primary spike in some transiently firing neurones (2/5 cells). Bath applied ATP (10µM) elicited spontaneous activity (4/6 cells) and tonic firing in response to current injection (2/6 cells). This data demonstrates that the excitability of neurones anatomically positioned to receive input from keratinocytes can be modulated by nucleotides through P2Y/$K_v7$ signalling.

Supported by the Pain Relief Foundation.

Adams PR *et al.* (1982). *J Physiol* **332**, 223-262.
Bruce G *et al.* (2008). *Proc Physiol Soc* **11**, C73
Crozier RA *et al.* (2007). *J Neurosci* **27(16)**, 4492-4496
Dussor G *et al.* (2008). *J Neurophysiol* **99(4)**, 1581-1589
Koizumi S *et al.* (2004). *Biochem J* **380**, 329-338